National Library of Canada
Bibliothèque nationale du Canada

Canadian Theses Service
Service des thèses canadiennes

Ottawa, Canada
K1A 0N4

NOTICE

The quality of this microform is heavily dependent upon the quality of the original thesis submitted for microfilming. Every effort has been made to ensure the highest quality of reproduction possible.

If pages are missing, contact the university which granted the degree.

Some pages may have indistinct print especially if the original pages were typed with a poor typewriter ribbon or if the university sent us an inferior photocopy.

Previously copyrighted materials (journal articles, published tests, etc.) are not filmed.

Reproduction in full or in part of this microform is governed by the Canadian Copyright Act, R.S.C. 1970, c. C-30.

AVIS

La qualité de cette microforme dépend grandement de la qualité de la thèse soumise au microfilmage. Nous avons tout fait pour assurer une qualité supérieure de reproduction.

S'il manque des pages, veuillez communiquer avec l'université qui a conféré le grade.

La qualité d'impression de certaines pages peut laisser à désirer, surtout si les pages originales ont été dactylographiées à l'aide d'un ruban usé ou si l'université nous a fait parvenir une photocopie de qualité inférieure.

Les documents qui font déjà l'objet d'un droit d'auteur (articles de revue, tests publiés, etc.) ne sont pas microfilmés.

La reproduction, même partielle, de cette microforme est soumise à la Loi canadienne sur le droit d'auteur, SRC 1970, c. C-30.

NL-339 (r. 88/04)

Canada

THE UNIVERSITY OF ALBERTA

FIBRONECTIN DISTRIBUTION DURING NEWT LENS REGENERATION

BY

KAREN L. ELGERT

A THESIS

SUBMITTED TO THE FACULTY OF GRADUATE STUDIES AND RESEARCH

IN PARTIAL FULFILLMENT OF THE REQUIREMENTS FOR THE DEGREE

OF MASTER OF SCIENCE

IN

CELL BIOLOGY

DEPARTMENT OF ZOOLOGY

EDMONTON, ALBERTA

FALL, 1987

Permission has been granted to the National Library of Canada to microfilm this thesis and to lend or sell copies of the film.

The author (copyright owner) has reserved other publication rights, and neither the thesis nor extensive extracts from it may be printed or otherwise reproduced without his/her written permission.

L'autorisation a été accordée à la Bibliothèque nationale du Canada de microfilmer cette thèse et de prêter ou de vendre des exemplaires du film.

L'auteur (titulaire du droit d'auteur) se réserve les autres droits de publication; ni la thèse ni de longs extraits de celle-ci ne doivent être imprimés ou autrement reproduits sans son autorisation écrite.

ISBN 0-315-40925-8

THE UNIVERSITY OF ALBERTA

RELEASE FORM

NAME OF AUTHOR: Karen Louise Elgert

TITLE OF THESIS: Fibronectin Distribution during Newt Lens Regeneration

DEGREE FOR WHICH THESIS WAS PRESENTED: Master of Science

YEAR THIS DEGREE GRANTED: 1987

Permission is hereby granted to THE UNIVERSITY OF ALBERTA LIBRARY to reproduce single copies of this thesis and to lend or sell such copies for private, scholarly or scientific research purposes only.

The author reserves other publication rights, and neither the thesis nor extensive extracts from it may be printed or otherwise reproduced without the author's written permission.

(Signed) Karen Elgert

10655 - 84 Avenue

Edmonton, Alberta

Dated May 19/ 1987

THE UNIVERSITY OF ALBERTA

FACULTY OF GRADUATE STUDIES AND RESEARCH

The undersigned certify that they have read, and recommend to the Faculty of Graduate Studies and Research for acceptance, a thesis entitled FIBRONECTIN DISTRIBUTION DURING NEWT LENS REGENERATION submitted by KAREN L. ELGERT in partial fulfillment of the requirements for the degree of MASTER OF SCIENCE IN ZOOLOGY, FIELD OF STUDY: CELL BIOLOGY.

Supervisor

Date May 19 1987

DEDICATION

This thesis is dedicated to my husband, Larry, and my children, Lisa and David, whose patience and support have allowed me the privilege of pursuing my academic interests.

ABSTRACT

Lens regeneration in newts represents an example of cell type conversion in which the pigmented iris epithelial cells (IECs) dedifferentiate and then redifferentiate into lens cells. During the process of dedifferentiation, alterations in cell morphology are associated temporarily with alternations in cell surface macromolecules (Zalik and Scott, 1972 & 1973) and an increased synthesis of glycosaminoglycans (Kulyk and Zalik, 1982). These results suggest that the extracellular matrix undergoes changes during dedifferentiation. The objective of this study was to examine the distribution of fibronectin, a component of the extracellular matrix, within the iris during the process of lens regeneration. In addition, it was of interest to correlate any changes in fibronectin distribution associated with the morphological changes which accompany the cellular processes of dedifferentiation and redifferentiation.

Prior to or at various intervals after lentectomy, iris tissue from newt, Notophthalmus viridescens, was removed and cryostat sections were prepared for immunofluorescent staining. An indirect immunofluorescent labeling technique was employed to examine fibronectin within the newt iris tissue sections. Commercial antiserum raised to human plasma fibronectin proved to be less reactive with newt fibronectin when compared to an antiserum raised to affinity purified Xenopus plasma fibronectin. The anti-Xenopus Fn antiserum, when allowed to react against protein blots of solubilized newt tissue proteins, interacted with protein bands with a molecular weight similar to that of fibronectin. The bands of lower molecular weight that were observed

with this antiserum likely corresponded to proteolytic fragments of fibronectin.

Indirect immunofluorescent staining of fibronectin within the normal and lens regenerating iris reveal that during IEC dedifferentiation fibronectin deposition at lateral and apical cell surfaces occurs concomitantly with the formation of intercellular spaces. As depigmenting IECs adopt a pleomorphic cell shape, extracellular fibronectin accumulates at the cellular projections of the basolateral cell surface. In the completely dedifferentiated IEC fibronectin is homogeneously distributed around the entire cell surface. As completely dedifferentiated IECs begin to redifferentiate and elongate into lens fibers, fibronectin progressively disappears from the cell surface. As partially dedifferentiated IECs begin to redifferentiate into their former melanocyte phenotype, fibronectin is lost from their lateral cell surfaces, but is maintained at the basal cell surface. It is possible that fibronectin of the extracellular matrix surrounding the dedifferentiating IEC may be part of a micro-environment which facilitates the dedifferentiation process. The removal of fibronectin from the extracellular matrix may be necessary in order to create a micro-environment which supports the redifferentiation of cells.

ACKNOWLEDGEMENTS

I am very grateful to my supervisor, Dr. Sara E. Zalik, for her guidance, encouragement and support during the course of this work. I would also like to thank Irene Ledsham for her technical assistance in histological procedures and especially for her photographic expertise in the reproduction of the color fluorescent micrographs. I greatly appreciate the assistance of Eva Dimitrov in microdissection techniques. I am fortunate to have had the opportunity to work with Dr. Nadine Milos, Geraldine Mbamalu, Dr. Harriet Harris, Dr. Bill Kulyk and Anne Darragh.

I would like to acknowledge my financial support from the Department of Zoology of the University of Alberta. This research was also supported by grants to Dr. S.E. Zalik from the Natural Sciences and Engineering Research Council of Canada.

TABLE OF CONTENTS

	Page
DEDICATION	iv
ABSTRACT	v
ACKNOWLEDGEMENTS	vii
LIST OF FIGURES	xi
INTRODUCTION	1
LITERATURE REVIEW	4
1. ANATOMY OF THE NEWT EYE	4
2. LENS REGENERATION: MORPHOLOGICAL AND CELLULAR-BIOCHEMICAL EVENTS	12
2.1 Stage 0: Normal Iris	13
2.2 Stage I: 3 to 6 days post-lentectomy	17
2.3 Stage II: 6 to 10 days post-lentectomy	21
2.4 Stage III: 8 to 10 days post-lentectomy	24
2.5 Stage IV: 9 to 15 days post-lentectomy	25
2.6 Stage V: 12 to 15 days post-lentectomy	26
2.7 Stage VI: 12 to 16 days post-lentectomy	27
2.8 Stage VII: 15 to 18 days post-lentectomy	27
2.9 Stage VIII: 15 to 19 days post-lentectomy	29
2.10 Stage IX: 18 to 20 days post-lentectomy	30
2.11 Stage X: 18 to 25 days post-lentectomy	31
2.12 Stage XI: 21 to 30 days post-lentectomy	32
3. CELL SURFACE ALTERATIONS	32
4. GLYCOSAMINOGLYCAN SYNTHESIS	34
5. CONTROL OF LENS REGENERATION	36

Page

6. THE EXTRACELLULAR MATRIX 38

6.1 Collagens 39

6.2 Laminin 41

6.3 Glycosaminoglycans 44

a. Hyaluronic Acid 44

b. Proteoglycans 46

6.4 Fibronectin 50

MATERIALS AND METHODS 60

1. COLLECTION OF XENOPUS PLASMA 60

2. ISOLATION OF XENOPUS PLASMA FIBRONECTIN BY AFFINITY CHROMATOGRAPHY 60

3. PROTEIN DETERMINATION AND SODIUM DODECYL SULFATE-POLYACRYLAMIDE GEL ELECTOPHORESIS 62

4. PREPARATION OF RABBIT ANTI-XENOPUS PLASMA FIBRONECTIN ANTISERUM 66

5. PROTEIN BLOTTING AND IMMUNOBLOTTING 66

6. LOCALIZATION OF FIBRONECTIN IN THE NEWT IRIS DURING LENS REGENERATION BY IMMUNOFLUORESCENCE 71

6.1 Maintenance and Lentectomy of Newts 71

6.2 Histological Preparation of Newt Iris Tissue 72

6.3 Immunofluorescent Staining of Newt Iris Tissue 73

RESULTS 76

1. ISOLATION OF XENOPUS PLASMA FIBRONECTIN 76

2. IMMUNOBLOT ANALYSIS 84

3. IMMUNOFLUORESCENT LOCALIZATION OF FIBRONECTIN WITHIN THE NORMAL AND LENS REGENERATING NEWT IRIS 90

3.1 Anti-Xenopus Fibronectin (Fn) Antiserum 96

a. Stage 0: Normal Iris Epithelium 96

Page

b. Stages I through III: Iris Epithelial Cell Dedifferentiation 103

c. Stages IV through IX: Redifferentiation and Establishment of the Lens Vesicle 120

3.2 Anti-Human Fibronectin (Fn) Antiserum 141

DISCUSSION 149

REFERENCES 161

LIST OF FIGURES

FIGURE		Page
1.	Schematic illustration of the eye of the newt, Notophthalamus viridescens	6
2.	Schematic illustration of the development of the tunica interna of the vertebrate eye	10
3.	Schematic illustration of the dorsal iris at various stages of lens regeneration	15
4.	Schematic diagram of fibronectin	53
5.	A. Preabsorption of Xenopus plasma on a Sepharose 4B column	78
	B. Affinity chromatography of Xenopus plasma fibronectin	79
6.	SDS-PAGE analysis of affinity purified Xenopus plasma fibronectin sample	
	A. Silver and coomassie blue staining	82
	B. Coomassie blue staining	82
7.	A. Immunoblots of newt tissue proteins probed with Anti-Xenopus Fn antiserum	86
	B. Immunoblots of newt tissue proteins probed with Anti-Xenopus Fn antiserum obtained from Dr. Hynes	89
8.	A. Immunoblots of Newt plasma proteins probed with commercial Anti-Human Fn antiserum	92
	B. Immunoblots of Newt tissue proteins probed with commercial Anti-Human Fn antiserum	92
9.	Control: Dorsal iris of stage II regenerate	98
10.	Stage 0: Normal dorsal iris	100
11.	Stage 0: Normal dorsal iris	102
12.	Stage I Regenerate: Dorsal iris (5 days post-lentectomy)	106
13.	Stage II Regenerates:	
	A. Dorsal Iris (10 days post-lentectomy)	109
	B. Ventral Iris (10 days post-lentectomy)	110

Page

14. Stage III Regenerate: Dorsal Iris (15 days post-lentectomy) . 112

15. Stage III Regenerate: Dorsal Iris (15 days post-lentectomy) . 114

16. Late Stage III Regenerates:

A. Dorsal iris (18 days post-lentectomy) 116

B. Dorsal iris (18 days post-lentectomy) 117

17. Stage IV to V Regenerate: Lens vesicle (20 days post-lentectomy) 122

18. Stage IV Regenerates:

A. Dorsal iris (20 days post-lentectomy) 125

B. Ventral iris (20 days post-lentectomy) 126

19. Stage V to VI: Lens vesicle (30 days post-lentectomy) 129

20. Stage VII: Lens rudiment (36 days post-lentectomy) 131

21. Stage VIII to IX Regenerate:

A. Lens rudiment (40 days post-lentectomy) 134

B. Mature lens of an adult, normal newt eye 135

22. Stage VIII to IX Regenerate: Dorsal iris lateral to lens rudiment (40 days post-lentectomy) 137

23. Ventral iris: 40 days post-lentectomy 140

24. Immunostaining with Anti-human Fn antiserum:

A. Stage I Regenerate: Dorsal iris (5 days post-lentectomy) 143

B. Stage II Regenerate: Dorsal iris (10 days post-lentectomy) 144

25. Immunostaining with Anti-human Fn antiserum:

A. Stage VI: Lens vesicle (30 days post-lentectomy) 147

B. Stage VII to VIII: Lens rudiment (40 days post-lentectomy) 148

INTRODUCTION

In most developmental systems differentiation along a specific pathway implies an irrevocable commitment to a specialized cell phenotype. Lens regeneration in the adult newt however provides a unique developmental system in which developmentally committed cells of a stable somatic cell population are released from the differentiated state and pursue an alternate pathway of differentiation. The process whereby a switch in cell-type occurs after cells have attained a fully differentiated state is referred to as "cell-type conversion" (Yamada, 1977).

Lens regeneration from the dorsal margin of the iris has been observed in several species of newts and salamanders (Stone, 1967). Following removal of the ocular lens, dedifferentiation of iris epithelial cells (IECs) takes place via an ordered sequence of biochemical and morphological changes. RNA (Reese et al., 1969; Reese, 1973) and protein (Yamada and Takata, 1963) synthesis is enhanced, and DNA synthesis and mitotic proliferation is initiated (Eisenberg and Yamada, 1966; Yamada and Roesel, 1969). Increased nuclear volume and alterations in nuclear ultrastructure accompany the enhanced nucleic acid synthesis (Dumont, 1970; Karasaki, 1964). Concomitant alterations in the morphology of IECs include an increase in cell size, an irregular cell surface topography coupled with a decrease in intercellular contacts (Dumont and Yamada, 1972) and Ca^{+2}-mediated exocytosis of cytoplasmic pigment granules (Patmore and Yamada, 1982). During the initial stages of lens regeneration the cytological events associated with dedifferentiation involve IECs in both the dorsal and ventral

regions of the iris. Subsequently, cytological events become more topographically distinct as divergent pathways of redifferentiation are pursued by cells in different regions of the iris. At the mid-dorsal pupillary margin, IECs follow a pathway of cell-type conversion where they continue to proliferate, complete their depigmentation, elongate and synthesize lens-specific proteins. While in the ventral iris and non-marginal regions of the dorsal iris, partially dedifferentiated IECs follow the retrieval pathway. In this case the cells stop proliferating, resynthesize pigment granules and re-establish the former epithelial morphology of the iris epithelium.

During the process of dedifferentiation, alterations in cell morphology are associated temporally with the disappearance of cell surface macromolecules which are sensitive to hyaluronidase and chondroitinase (Zalik and Scott, 1973; Zalik et al., 1976). Further, the synthesis of several types of sulfated glycosaminoglycans progressively increases during IEC dedifferentiation (Kulyk and Zalik, 1982). These results suggest that the extracellular matrix of the IEC undergoes changes during dedifferentiation.

Fibronectin, a prominent component of the extracellular matrix, has been implicated in the control of various cellular process including cell adhesion (Yamada et al., 1978; Pearlstein, 1976), cell migration <u>in vitro</u> (Ali and Hynes, 1978; Greenberg et al., 1981), <u>in vivo</u> morphogenic movements during development (Critchley et al., 1979; Boucaut et al., 1984a, b), cytoskeletal organization (Sugrue and Hay, 1981; Chen et al., 1985; Duband et al., 1986) and cellular differentiation (Podleski et al., 1979; Pennypacker et al., 1979; West et al., 1979; Kosher et al.,

1982 and Tomasek et al., 1982). Furthermore, during newt limb regeneration extracellular fibronectin increases in dedifferentiating limb tissues destined to form the regenerating blastema. As blastema cells subsequently undergo chondrogenic and myogenic redifferentiation, extracellular Fn decreases (Gulati et al., 1983 and Repesh et al., 1982).

The purpose of this study was to examine the distribution pattern of fibronectin within the iris epithelium during the course of lens regeneration. Another aim of this thesis was to attempt to determine if any correlation could be found between changes in fibronectin distribution and the cellular events of dedifferentiation and redifferentiation. This study has employed immunofluorescence histochemistry to determine the localization of fibronectin within the iris epithelial tissue and to study it's changes in distribution during lens regeneration.

LITERATURE REVIEW

1. ANATOMY OF THE NEWT EYE

Before discussing the phenomena of lens regeneration a brief description of the ocular anatomy of the newt eye is necessary. Reyer (1977) reviews the structure of the amphibian eye, with particular emphasis on the newt Notophthalmus viridescens. Anatomically the amphibian eye is quite typical of vertebrates in general, consisting of the three layers; tunica fibrosa, tunica vasculosa and tunica interna.

A median sagittal section through the eye of the adult newt, Notophthalmus viridescens, is illustrated in Figure 1. The most external tunica fibrosa consists of the fibrous sclera posteriorly which extends anteriorly into the corneal stroma. A multilayered external corneal epithelium rests upon an amorphous basement membrane, homologous to the Bowman's membrane of the human eye. Beneath this basement membrane is the corneal stroma, a thick layer of connective tissue composed of numerous lamellae of parallel collagen bundles embedded within an amorphous ground substance. Descemet's membrane, a corneal endothelium is not present in the newt eye.

The tunica vasculosa consists of the vascularized choroid or choricapillaris just interior to the sclera. This network of blood vessels provides for the major vascular blood supply of the eye. At the limbus or sclerocorneal junction, Schlemn's canal and associated trabecular mesh are responsible for drainage of aqueous humour from the anterior eye chamber. More anteriorly the tunica vasculosa transforms gradually into the stromal tissue of the ciliary and iris epithelium.

Figure 1.

Schematic illustration of the eye of the newt, Notophthalmus viridescens, as seen in a medial sagittal section.

Abbreviations:

AC = anterior chamber

C = cornea

CH = choroid

CS = ciliary stroma

dCE = dorsal ciliary epithelium

dIE = dorsal iris epithelium

IS = iris stroma

L = lens

LC = lens capsule

NR = neural retina

ONT = optic nerve tract

OS = ora serrata

PC = posterior chamber

PR = pigmented retina

SC = sclera

VC = vitreous chamber

vCB = ventral ciliary body

vCE = ventral ciliary epithelium

vIE = ventral iris epithelium

ZF = zonular fibers

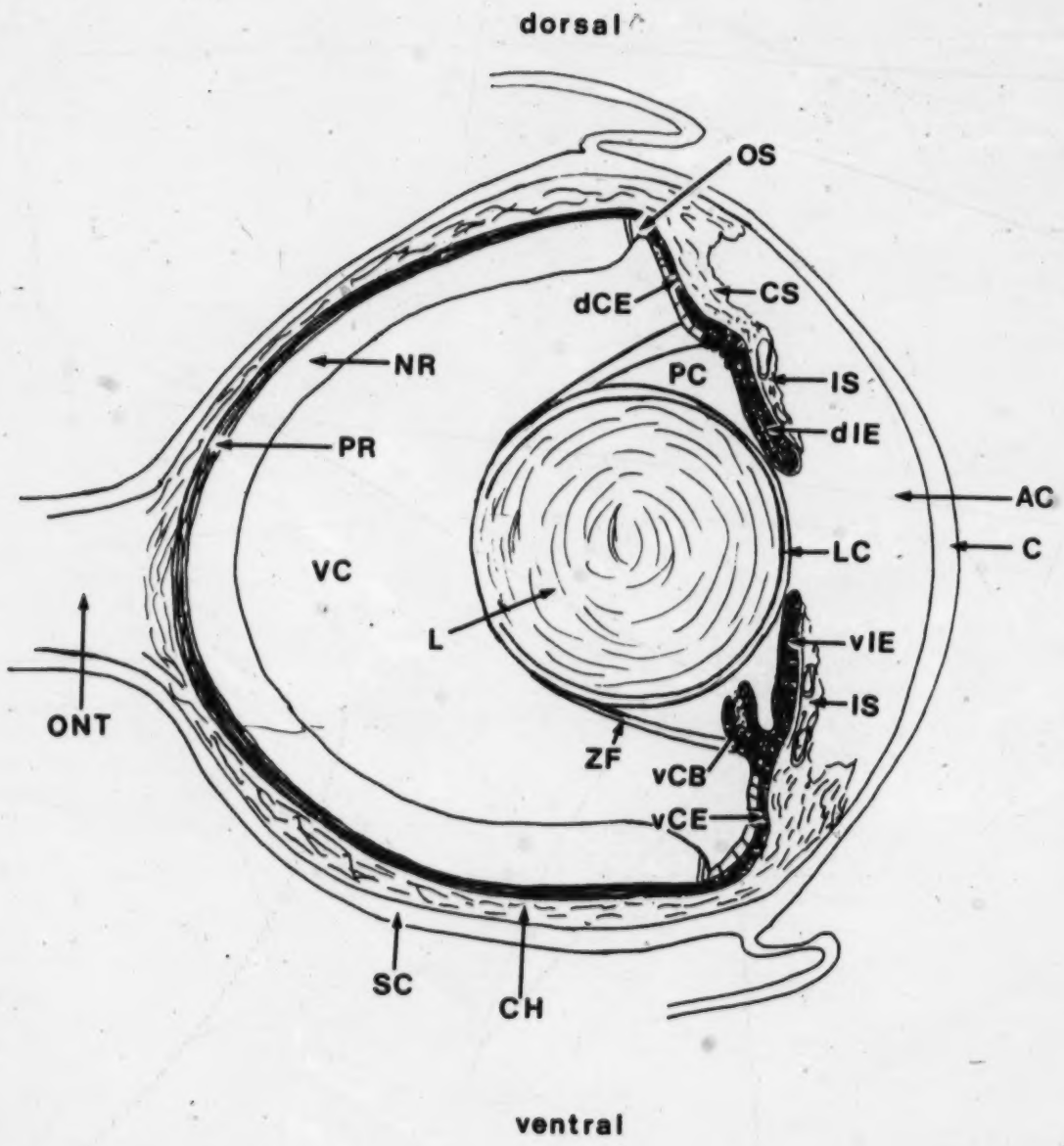
dorsal
OS
dCE
CS
NR
PC
IS
dIE
PR
AC
C
LC
VC
L
vIE
IS
ONT
ZF
vCB
vCE
SC
CH
ventral

This stroma is composed of a meshwork of stromal fibroblasts, green iridophores, yellow or red xanthophores, melanophores, and iridal blood vessels supported in a mesh of loose connective tissue. Pupillary constriction and dilation are controlled by circumferentially oriented sphincter and radially oriented dilator smooth muscle bundles supported within the stroma. A single mid-ventral ciliary body (the remnant of the choroid fissure) is present in the ventral region of the newt eye. The ventral protractor lentis muscle, responsible for pulling the lens into a forward position, originates at the sclerocorneal junction and terminates at the ventral ciliary body. Dorsal and ventral smooth muscle of the tensor chorideae extend from the sclera in a meridianal direction, inserting on the choroid close to the ora serrata.

In order to orient the reader as to the apico-basal polarity of the iris a brief overview of the development of the eye is necessary. As the neural plate is formed a basal lamina is observed at the inner (lower) surface of this plate; the outer (upper) surface of the neural plate is not associated with a basal lamina and therefore this surface is considered as apical. With invagination of the neural plate a hollow neural tube is formed with the basal surface of the neuroepithelium being the outer surface of the neural tube while the apical surface of the neural plate faces the lumen of the neural tube. Arising as a vesicular outpocketing of the forebrain, the neuroepithelium of the optic vesicle is continuous with the neuroepithelium of the diencephalon and the original apico-basal polarity is maintained in the optic vesicle. With further development the optic vesicle invaginates, obliterating the vesicle and giving rise to the double-layered

neuroepithelium of the optic cup. This invagination brings the neuroepithelia into direct apposition along their apical surfaces. The basal surface of the internal epithelium faces the vitreous and aqueous chambers of the eye, while the basal surface of the external epithelial layer faces the tunica vasculosa of the eye. Figure 2 represents a schematic illustration of the development of the optic cup, which in the adult eye constitutes the tunica interna. Posterior to the ora serrata the double-layered tunica interna undergoes a series of developmental transformations to give rise to the external pigmented retina and the internal neural retina.

Anterior to the ora serrata, the tunica interna consists of the external and internal ciliary and iris epithelium. At the pupillary margin the external and internal iris epithelium are continuous. A basement membrane is observed at the basal cell surface of both external and internal ciliary and iris epithelia (Dumont and Yamada, 1972; Fine and Yanoff, 1979). The external epithelium is in contact with the ciliary and iris stroma which is part of the tunica vasculosa. Within the stroma the endothelium-lined capillaries (iridal blood vessels) supply nutrition to the epithelial layers. The stroma, perforated by many lacunae allows the aqueous humour of the anterior chamber to bathe the underlying external epithelium. The internal epithelium is directly exposed to the aqueous humour of the posterior chamber. Except for cells of the internal ciliary epithelium, which are normally underpigmented, the ciliary and iris epithelial cells are heavily pigmented due to a high melanosome content.

Figure 2.

A schematic illustration depicting the development of the tunica interna of the vertebrate eye as observed in a cross-section through the embryo. The apico-basal polarity of the neuroepithelium is indicated by dots (....) representing the apical surface of the epithelium and crosses (x x x) representing the basal surface. In diagram 1 the neural plate (NP) forms within the embryonic ectoderm (Ec) layer. Diagram 2 illustrates formation of the neural tube (NT). In diagram 3 paired optic vesicles (OV) evaginate from the diencephalon (D). Diagram 4 illustrates invagination of the optic vesicle to form the double-layered optic cup (OC). Diagram 5 represents the adult tunica interna, which consists of an external pigmented retina (PR) and internal neural retina (NR) posterior to the ora serrata (OS). Anterior to the ora serrata the tunica interna consists of external and internal ciliary (C) and Iris (I) epithelia.

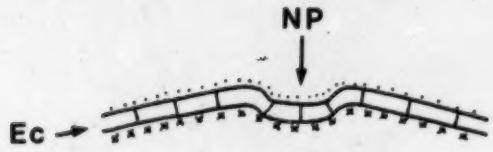

1

2

3

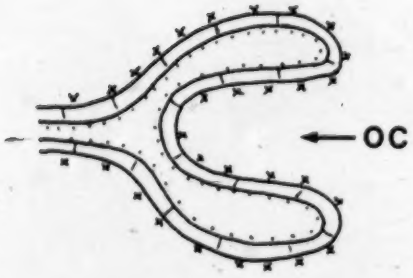

4

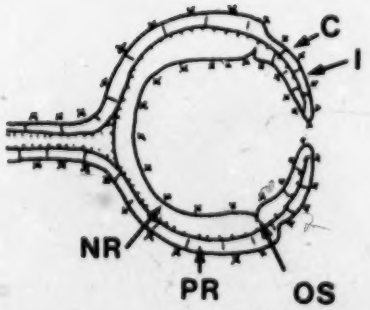

5

The ocular chamber of the eye is subdivided into three separate chambers; the anterior, posterior and vitreous chambers. The anterior chamber occupies that space posterior to the corneal stroma and anterior to the iridal stroma and lens. Aqueous humour, the fluid portion of the blood that is forced through fenestrations in the capillary wall of iridal blood vessels, is transported by the external and internal epithelial layers into the posterior chamber. Via the pupil, aqueous humour circulates into the anterior chamber where drainage is maintained by Schlemn's canal. The posterior chamber extends from the inner surface of the iris to the anterior surface of the zonular fiber apparatus. The vitreous chamber is that space posterior to the lens and zonular fiber apparatus and bordered by the neural retina. Within the vitreous chamber is an acellular matrix composed primarily of glycosaminoglycans and type II collagen. These are synthesized and secreted by cells of the neural retina, the ciliary epithelium and iris epithelium (Fine and Yanoff 1979). Additionally, an ultrafiltrate of blood serum from the choroid, is taken up by pinocytosis into the pigmented retinal cells and then secreted by these cells into the vitreous chamber (Chylack and Bellows, 1978).

The spherical lens of the adult newt eye occupies much of the ocular chamber posterior to the iris. Zonular fibers extend from the iris and ciliary epithelium and attach to the equatorial region of the lens, holding the lens in place. Zonular fibers are derived from the vitreous matrix as well as secretions from cells of the ciliary body and iris epithelium. Zonular fiber attachments enable sphincter and dilator

smooth muscles to hold the lens against the iris surface thus separating anterior and posterior eye chambers.

The newt lens is primarily composed of lens fiber cells concentrically layered around a central core. Primary lens fibers in the central core are derived from the lens vesicle during development, whereas the secondary lens fibers of the outer layers are derived from epithelium present at the equatorial region of the lens. Except for the most superficial layer, lens fiber cells are devoid of nuclei with sparse intracellular organelles and high content of intracellular α, β and γ crystallin protein which are responsible for the transparent optical properties of the lens.

2. LENS REGENERATION: MORPHOLOGICAL AND CELLULAR-BIOCHEMICAL EVENTS

Lens regeneration from the iris has been observed in eighteen species of urodeles. Many factors including; ambient temperature, species variation, developmental age and individual variability, are known to influence the rate at which lens regeneration occurs. (Yamada,1977) In light of such variability Sato (as cited by Yamada,1977) devised a scheme in which the temporal sequence of morphological and cellular changes occurring during lens regeneration are categorized into thirteen separate stages. Yamada (1977) adapted the staging proposed by Sato to the average time course of regenerative events as they are observed to occur in Notophthalmus viridescens. Lens regeneration does not proceed by discrete steps, but rather by a continuous series of cellular events, therefore staging of the regenerative process is somewhat arbitrary. Within a regenerate

population the time course associated with each stage is somewhat variable and therefore considerable overlapping of days is recognized between successive stages. The following review of stages I through XI will discuss the morphological and cellular-biochemical events of lens regeneration. The reader is also referred to Figure 3, which provides an illustrative summary of the morphological changes occurring in the dorsal iris during lens regeneration.

2.1 Stage 0: Normal Iris

The normal iris consists of an internal and external epithelium which is continuous at the pupillary margin. The two epithelial layers are closely apposed at their apical surfaces. Likewise, within the epithelium, the cuboidal pigmented iris epithelial cells (IECs) are closely apposed along their lateral cell surfaces. Desmosomes (Dumont and Yamada, 1972) and terminal bars (Karasaki, 1964) are evident at regions of cell apposition. The basal surface of the external and internal epithelium rests on an amorphous extracellular basement membrane approximately 0.03 μm in thickness. The plasmalemma at the basal region of internal IECs is relatively flat with very few infoldings, in contrast to that of the external IECs where convolutions and tubular invaginations a few microns in length are observed (Karasaki, 1964). Cells of the internal ciliary epithelium (see Figure 1 for reference purposes) are underpigmented relative to iris epithelial cells and are further distinguished from internal IECs by extensions and infoldings of their basal plasmalemma (Eguchi, 1963).

Figure 3.

Schematic illustrations of the dorsal iris at various stages of lens regeneration in the adult newt, Notophthalmus viridescens, depict the overt morphological changes associated with each stage. Diagrams represent a median sagittal section through the eye. Of the original staging system proposed by Sato (1940; as cited by Yamada, 1977) and adapted to Notophthalmus viridescens by Yamada (1977) only some of the stages are represented here.

The abbreviated labeling in the stage 0 (normal) iris corresponds to the following structures; S = stroma, SB = stroma band, EIE = external iris epithelium and IIE = internal iris epithelium. The apical-basal polarity of the iris epithelium is indicated. In the stage III illustration macrophages are labeled as M and partially depigmented iris epithelial cells are portrayed as stippled. In the stage V illustration LV corresponds to lens vesicle and completely depigmented cells are unshaded. The abbreviated labels in the stage VII and stage IX illustrations correspond to the following structures; 1°LFC = primary lens fiber core, 2°LF = secondary lens fibers, LVS = lens vesicle stalk and LE = lens epithelium.

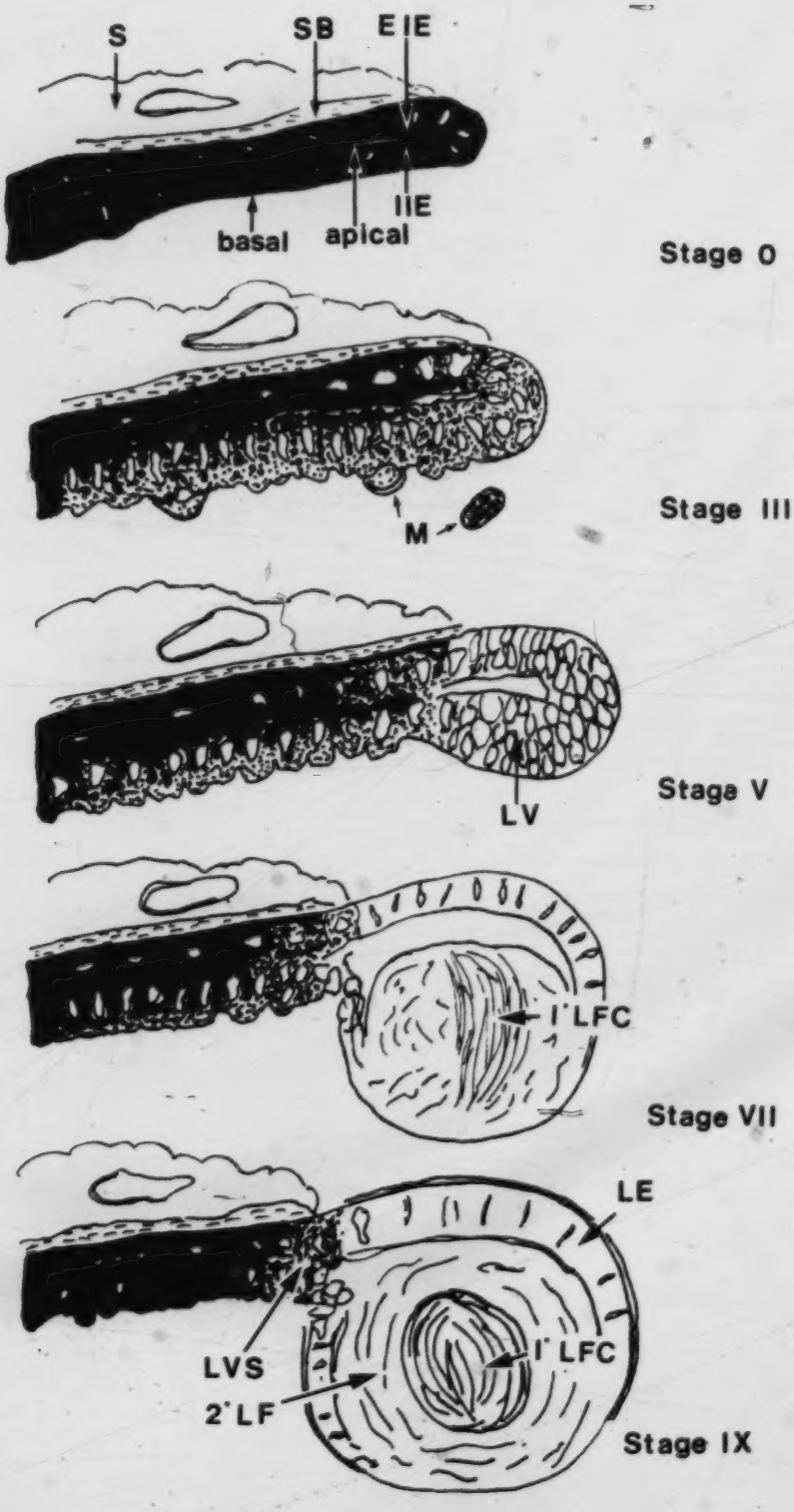
S
SB
E
IE
basal
apical
IIE
Stage 0
M
Stage III
LV
Stage V
1°LFC
Stage VII
LE
LVS
2°LF
1°LFC
Stage IX

Within the external and internal iris epithelial cells randomly dispersed pigment granules (melanosomes) occupy 30-60% of the cytoplasm. The pigment granules of the internal IECs are spherical and are present in relatively lower abundance compared to the ellipsoidal pigment granules of the external IECs. The pigment granules are surrounded by a limiting membrane (Karasaki, 1964). In addition to pigment, IECs possess various intracellular organelles. Smooth endoplasmic reticulum and ribosomes are present. These latter are sparsely distributed in clusters of 5 to 10 and only occasionally do they appear attached to membranous elements. Stacks of lamellar vesicles, characteristic of Golgi complexes, are not prominent. Mitochondria are not abundant and are observed primarily within the basal region of the cell (Karasaki, 1964). It has been reported that mitochondrial number is greater in IECs of the dorsal pupillary margin relative to the ventral (Eguchi, 1963).

The nuclei of iris epithelial cells are characterized by an irregular shape owing to numerous infoldings and indentations of the nuclear envelope. The nucleoplasm, consisting of fine fibrils intermingled with granular material, is quite uniform except for occasional clumping of chromatin subjacent to the nuclear envelope (Karasaki, 1964). Each nucleus contains at least a single nucleolus, which, in the normal IEC, appears as a small, compact structure composed primarily of aggregated fibers 20-50 Å in diameter plus a small contribution of granular elements 100 to 500 Å in diameter (Dumont et al., 1970). Incorporation of ^{3}H-thymidine into nuclear DNA, as demonstrated by autoradiography, is not observed in IECs of the normal

iris (Eisenberg and Yamada, 1966; Yamada and Roesel, 1969; Eguchi and Shingai, 1971). Further, the rate of incorporation of radioactively-labeled RNA and protein precursors reveals that RNA and protein synthesis occurs at a very low level in normal iris epithelial cells (Thorpe et al., 1974). It would appear that the mitotically quiescent iris epithelial cells can be described as a fully differentiated, stable somatic cell population.

2.2 Stage I: 3 to 6 days post-lentectomy

Shortly after lentectomy IECs elongate slightly along their apicobasal axis. Although intercellular spaces become evident at discrete locations along surfaces of cell apposition, desmosomal junctions between adjacent cells remain intact. Similar to normal IECs the paucity of cytoplasmic organelles and the appearance and distribution of pigment granules remains unchanged during stage I (Dumont and Yamada, 1972). During stage I macrophages may be observed in the vicinity of the iris epithelium (Eguchi, 1963).

Occurring at the same time or shortly after the above mentioned events, nuclear changes become evident. The indentations of the nuclear envelope begin to disappear as nuclear volume increases (Karasaki, 1964) and chromatin becomes progressively more dispersed (Dumont et al., 1970). Within the first two days following lentectomy, the number of nuclei containing more than one nucleolus increases three-fold and a further increase in nucleolar number is evident by 4 days post-lentectomy (Dumont et al., 1970). Nucleoli not only increase in number but also in size and a fibro-granular cortex containing putative ribosomes is acquired surrounding the fibrous nucleolar core (Karasaki,

1964; Dumont et al., 1970). The increased nucleolar number and altered nucleolar morphology is accompanied by an increase in cytoplasmic ribosomes (Karasaki, 1964). An increased incorporation of ^{3}H-uridine into RNA of IEC nuclei can be detected by autoradiography within 1 day of lentectomy. Initially 90% of the uridine label is localized within the nucleus, but subsequently the proportion of label present in the cytoplasm increases (Yamada and Karasaki, 1963). Presumably this increase in label is associated with the increase in cytoplasmic ribosomes.

Isolation and fractionation of RNA from the regenerating iris reveals that 2 days after lentectomy there is a significant increase in the incorporation of ^{3}H-uridine into ribosomal and heterogenous nuclear RNA, compared to that of the normal iris tissue. By 4 days post-lentectomy incorporation of labeled precursor into rRNA species is three- to four-fold greater than that of normal IECs (Reese et al., 1969; Reese, 1973). Collins (1972) has shown that enhanced rRNA production results from amplification of rRNA cistrons and an increased rate of transcription of DNA sequences coding for the 40S rRNA precursor.

Because mitosis in IECs is not evident prior to DNA synthesis, it is believed that IECs are arrested in the G_1 phase of the cell cycle. Yamada (1977) has designated this arrested G_1 phase as G_0. The structural and synthetic alterations associated with enhanced RNA synthesis precedes the replication of nuclear DNA, and it is suggested that these events are related to the transition from the stationary G_0 phase to the active G_1 phase. During this transition nucleolar

activation results in an increased capacity for protein synthesis. Indeed, between day 2 to 8 post-lentectomy the level of ^{3}H-leucine incorporation into proteins, as demonstrated by autoradiography, shows a progressive eight-fold increase relative to normal, non-lentectomized levels (Yamada and Takata, 1963).

Also of interest during the G_0 to G_1 transition period are changes in the intracellular levels of adenosine 3', 5' cyclic monophosphate (cAMP) and various enzymatic activities. Within the first two days after lentectomy the level of cAMP in dorsal IECs has decreased to 40% of it's normal (pre-lentectomized) level. This decrease corresponds temporally to a four-fold increase in RNA synthesis. Between day 2 to 4 post-lentectomy, just prior to enhanced DNA synthesis, cAMP levels increase to reach 80% of the normal level (Thorpe et al., 1974). Glutamine synthetase, whose product glutamine is required for a number of biosynthetic reactions including synthesis of nucleotide precursors of RNA and DNA, exhibits a significant increase in activity as IECs leave the G_0 phase and enter the active G_1 phase of the cell cycle. In dorsal IECs glutamine synthetase activity increases slightly within the first 2 days after lentectomy, followed by a marked seven-fold increase between day 2 to 4. This enzyme activity plateaus at day 4 just prior to the enhanced DNA synthesis (Thorpe et al., 1974). Also associated with the initiation of nucleic acid synthesis are alterations in phosphate metabolism. Within the normal iris the activity of alkaline phosphatase, as measured by enzymatic assay of homogenized tissue extracts, is 46% higher in the dorsal relative to ventral iris. Following lentectomy in both the dorsal and ventral iris alkaline

phosphatase activity increases, peaking at day 2 post-lentectomy and returning to normal levels by day 4. In the dorsal iris this transitory increase is followed by a second, more significant increase in alkaline phosphatase activity (Eguchi and Ishikawa, 1963).

The transition from a G_0 to G_1 state, taking place prior to DNA synthesis, appears to be associated with structural changes in the chromosomal DNA of IECs. At various times after lentectomy DNA from dorsal irises was isolated and characterized using hydroxyapatite chromatography, buoyant density in CsCl and $CsSO_4$(Hg), thermal denaturation and sedimentation in neutral and alkaline sucrose gradients (Collins, 1974). It was concluded that compared to the DNA of stationary IECs at G_0 phase, the DNA of cells in early G_1 phase contains a significant number of "nicks". And by late G_1 gaps or missing runs of nucleotides are evident in the chromosomal DNA. These structural changes in chromosomal DNA precede the extended single-stranded configuration of S phase DNA (Collins, 1974).

DNA synthesis as shown by ^3H thymidine incorporation is first evident in a small percentage of dorsal IECs. The number of cells undergoing DNA synthesis increases gradually in the dorsal and ventral iris, although, in the ventral iris the proportion of cells undergoing this event is smaller. Most of the cells incorporating ^3H-thymidine are present within the internal iris epithelium. By day 5 post-lentectomy 20% of IECs in the dorsal and ventral iris epithelium possess nuclear labeling, with 75% of the labeled cells being within the internal epithelium (Yamada and Roesel, 1969).

2.3 Stage II: 6 to 10 days post-lentectomy

During stage II mitotic proliferation and depigmentation events are prominent along the internal iris epithelium. Calculations of cell volume at the mid-dorsal pupillary margin reveal that between day 0 to 8 post-lentectomy cytoplasmic volume increases three-fold and nuclear volume increases five-fold (Dumont and Yamada, 1972). Separation of external and internal epithelia at the apical region of IECs becomes pronounced. IECs progressively elongate along their apico-basal axis and intercellular spaces at laterally apposed cell surfaces become more evident. Macrophages are frequently observed within the lateral intercellular spaces of the internal epithelium and localized disruption of the epithelial basal lamina may accompany the invasive activity (Yamada and Dumont, 1972). Pseudopod-like extensions of the plasmalemma containing mitochondria and numerous melanosomes are evident at the basal surface of IECs. The iris epithelial cell processes are often encircled by pseudopodial extensions of investing macrophages. Phagosomes of the macrophages contain melanosomes as well as dense concretions, these latter may be seen also associated with the IEC plasmalemma surface. These observations are interpreted to suggest that IEC melanosomes are transferred to macrophages by engulfment and phagocytosis of the melanosome-containing cell processes of the IEC by macrophages (Dumont and Yamada, 1972). The coincident presence of melanosome-containing macrophages is not necessarily indicative of their causal involvement in the process of IEC depigmentation. In the absence of macrophages, cultured IECs have an inherent capacity for melanosome discharge (Ortiz et al., 1973).

Electron microscopic evaluation of melanosome discharge by IECs *in situ* or in organ culture has been described to take place in the following manner. In the perinuclear region of the cell melanosomes plus various cytoplasmic organelles are localized in areas of cytoplasmic disintegration. These lytic areas become invested by lysosomal membrane and subsequently these complexes are discharged or externalized from the cell (Dumont and Yamada, unpublished; as cited by Yamada, 1977; Yamada et al., 1978). That IEC depigmentation coincides with lysosomal activation is further evidenced by the increasing levels of N-acetylglucosaminidase (a lysosomal glycosidase). In both dorsal and ventral iris tissue the activity of this enzyme increases slightly by day 8 post-lentectomy, followed by a significant increase after day 8 post-lentectomy. The increase in activity of this enzyme is slightly greater in the dorsal iris relative to the ventral iris. Following lentectomy glucosaminidase activity in the ocular fluid also shows a progressive increase, suggesting a release of the enzyme and possibly an extracellular function during the dedifferentiation phase of lens regeneration. Macrophages possess a high level of lysosomal glycosidase activity and therefore the observed increase in activity may be due in part to the infiltration of macrophages which occurs during IEC depigmentation (Idoyaga-Vargas and Yamada, 1974).

In addition to the active process of melanosome discharge by IECs, melanosome content of IECs is also reduced as a result of successive cell divisions in the absence of melanosome synthesis. Premelanosomes are rarely observed in the proliferating, stage II IECs (Dumont and Yamada, 1972). Further, incorporation of ^{3}H-dopa, an indicator of

melanocyte differentiation, occurs at very low levels during active proliferation of IECs (Stroeva and Mitashov, 1981; as cited by Yamada and McDevitt, 1984). These results suggest that melanosome synthesis is negligible during IEC dedifferentiation. Therefore pre-existing melanosomes should become dilute during IEC proliferation.

During stage II cytoplasmic organelles become more abundant. Mitochondria located primarily in the cell periphery are present in greater number and Golgi complexes are now observed (Dumont and Yamada, 1972). Rough endoplasmic reticulum has apparently replaced the earlier observed smooth E.R. Increasing numbers of ribosomes appear to be concentrated in the perinuclear region attaching to the nuclear envelope and endoplasmic reticulum, and are also observed freely in the cytoplasm in small clusters (Karasaki, 1964).

RNA synthesis, as determined by autoradiographic detection of ^{3}H-cytidine incorporation into RNAase-sensitive fraction of IECs, increases progressively. The increase in RNA synthesis is significantly greater in the dorsal iris relative to the ventral iris (Yamada, 1977). DNA synthesis, as evidenced by autoradiographic detection of ^{3}H-thymidine incorporation into nuclear DNA likewise continues to increase during stage II. According to Eguchi and Shingai (1971) the percentage of IECs possessing ^{3}H-thymidine nuclear labeling in both the dorsal and ventral iris reaches a maximum at day 7 post-lentectomy. The proliferation of IECs, as measured by the number of mitotic cells per epithelium, is also greatest at 7 days post-lentectomy (Yamada and Roesel, 1971).

With the initiation of nucleic acid synthesis in IECs following lentectomy, alterations in phosphate metabolism would be expected.

Alkaline phosphatase activity within the iris epithelium increases transiently during stage I. During stage II a second, more significant increase in alkaline phosphatase can be detected in the dorsal iris between day 4 to 10 post-lentectomy. While in the ventral iris the activity of this enzyme remains at normal (pre-lentectomized) levels (Eguchi and Ishikawa, 1963). The difference in alkaline phosphatase activity between dorsal and ventral iris epithelia may be related to the higher rate of RNA synthesis observed in the dorsal iris relative to the ventral iris during stage II.

The rate of protein synthesis within the iris epithelium increases progressively. By day 8 post-lentectomy the rate of protein synthesis within both dorsal and ventral iris epithelia is eight-fold higher relative to the normal (pre-lentectomized) rate of protein synthesis (Yamada and Takata, 1963). Post-translational glycosylation of proteins, which occurs in the synthesis of glycoproteins or proteoglycans, involves the activity of glycosyltransferase enzymes which function in the assembly of carbohydrate components of various macromolecules. Idoyaga-Vargas et al. (1976) measured the level of galactosyltransferase activity in dorsal iris tissue at various times after lentectomy. Results of this study indicate that galactosyltransferase activity progressively increases during the first 10 days following lentectomy.

2.4 Stage III: 8 to 10 days post-lentectomy

Proliferation and depigmentation of iris epithelial cells continues. This is especially prominent at the internal pupillary margin of the dorsal iris resulting in the appearance of small,

completely depigmented IECs. The presence of completely depigmented IECs at the mid-dorsal pupillary margin characterize the stage III regenerate. Although depigmentation and proliferation of the internal epithelium occurs lateral to the mid-dorsal pupillary margin and within the ventral iris, the onset and intensity of these events lag with respect to the mid-dorsal pupillary margin and therefore IECs are only partially depigmented in the former regions (Dumont & Yamada, 1972). Proliferation and depigmentation results in a decreased cytoplasmic volume, but nuclei remain enlarged. Nucleoli continue to increase in number and a prominent fibrogranular cortex is observed (Karasaki, 1964).

2.5 Stage IV: 9 to 15 days post-lentectomy

Stage IV is marked by the appearance of a definitive lens vesicle at the mid-dorsal pupillary margin of the iris. The appearance of lens specific proteins has been examined using immunofluorescence. Following lentectomy lens specific crystallin proteins are initially detected at stage IV in a small number of completely depigmented IECs located at the internal aspect of the mid-dorsal pupillary margin. These cells are presumptive lens fibers (Takata et al., 1964). Using antiserum specific to the γ class of crystallin proteins, γ crystallins are not detected within the presumptive lens fibers of the stage IV regenerate, suggesting that synthesis is restricted to the α and/or β crystallin classes (Takata et al., 1966). As discussed earlier DNA synthesis and mitotic cell division within the dorsal and ventral regions of the iris reaches a maximum at day 7 post-lentectomy. A second significant increase in ^{3}H-thymidine nuclear labeling of IECs is observed at day 12

post-lentectomy (Eguchi and Shingai,1971) and at day 15 a significant increase in the number of mitotic cells per epithelium is evident (Yamada and Roesel, 1971).

2.6 Stage V: 12 to 15 days post-lentectomy

The internal layer of the lens vesicle (i.e. that which is facing the vitreous humour) has thickened due to continued proliferation and the incorporation of newly depigmented IECs from the adjacent iris epithelium. Depigmenting IECs at the external layer of the lens vesicle (i.e. that which is facing the aqueous humour) appear more cuboidal relative to the elongating columnar cells of the internal layer. Cytoplasmic volume of these cells is greatly reduced and only a thin rim of cytoplasm surrounds the enlarged nuclei of IECs comprising the lens vesicle. Within the internal layer of the lens vesicle staining of lens specific crystalline proteins, as detected by immunofluorescence, increases in intensity relative to that of stage IV regenerates (Takata et al., 1964). Gamma crystallin protein, which was not detectable at stage IV, can now be detected by immunofluorescence in the internal cells of the lens vesicle of the stage V regenerate (Takata et al., 1966). Combining autoradiographic studies of 3H-thymidine incorporation into nuclear DNA and immunofluorescent detection of lens crystallin proteins Yamada (1966) concludes that α and β crystallins can be detected as early as 3 hours after the final S-phase of the cell cycle, but crystallin synthesis is not detected until 1.5 days after the final S-phase of the cell cycle.

Proliferation and depigmentation events persist lateral to the lens vesicle and within the ventral iris epithelium.

2.7 Stage VI: 12 to 16 days post-lentectomy

Stage VI is characterized by the onset of lens fiber differentiation within the internal layer of cells of the lens vesicle. These cells withdraw from the cell cycle (Eisenberg and Yamada, 1966), continue to elongate and their nuclei appear long and ellipsoid in shape. Nucleoli decrease in number by day 15 post-lentectomy and the fibrogranular cortex is no longer a consistent feature. Within the vesicles of the rough endoplasmic reticulum and within the cytosol fine filamentous material, presumably corresponding to lens crystallins, is observed (Eguchi, 1964). From day 8 post-lentectomy onwards protein synthesis within the iris epithelium is eight-fold higher than that of the normal iris epithelium. Within differentiating lens fibers of the lens vesicle protein synthesis increases further, to a level ten-fold greater than that of the normal iris; this probably represents crytallin synthesis that can be detected by immunofluorescence (Takata et al., 1964).

2.8 Stage VII: 15 to 18 days post-lentectomy

Continued lens fiber differentiation results in the formation of a primary lens fiber complex. Within the lens fiber complex mitotic activity is absent, but continues in those layers of the internal vesicle that are peripheral to the fiber complex, in the external layer of the lens vesicle (presumptive lens epithelium) and within the lens vesicle stalk. Within the lens fiber complex the elongated primary lens fibers are in close contact, nuclei are elongate and the nucleoli lack a fibrogranular cortex. In the more centrally located fibers cytoplasmic organelles are sparse, the basophilic character of the cytosol is lost

as the number of free ribosomes declines and filamentous elements (50 A in width) of low electron density comprise the cytoplasmic matrix (Karasaki, 1964). Relative to the immunofluorescent staining of crystallin proteins within the differentiating lens fibers of the stage VI regenerate, fluorescent staining of the stage VII lens fiber complex is significantly more intense and is observed in a greater number of cells (Takata et al., 1964). At the external layer of the lens vesicle cuboidal cells of the presumptive lens epithelium maintain a high level of mitotic activity and remain separated by large intercellular spaces. These cells have large nuclei with prominent nucleoli possessing a fibrogranular cortex (Karasaki,1964) Cells of the lens vesicle stalk maintain a high level of mitotic activity and continue to contribute to the growing lens vesicle (Eisenberg and Yamada,1966).

During the first 10 days after lentectomy galactosyltransferase activity within the dorsal iris increases progressively. The activity of this enzyme within the lens rudiment continues to increase and by day 41 post-lentectomy enzymatic activity within the regenerated lens is fourteen-fold higher than the activity observed in the normal iris epithelium. Relative to the normal lens, enzymatic activity within the regenerating lens is significantly higher and remains so for some time (Idoyaga-Vargas et al., 1976). Idoyaga-Vargas et al. (1976) suggests that elevated galactosyltransferase activity within the lens rudiment may be associated with the formation of specialized cell junctions between newly differentiated lens fibers.

Outside of the lens vesicle region proliferation and depigmentation events within the iris epithelium begin to decrease during stage VII.

Alkaline phosphatase activity within the dorsal iris epithelium increases progressively during the proliferative and depigmentation phase of IEC dedifferentiation and at the beginning of lens fiber differentiation (stage VI). During stage VII the activity of this enzyme within the iris epithelium begins to decrease. Alkaline phosphatase activity is not detected in cells undergoing lens fiber differentiation. Also associated with active depigmentation of the iris epithelium was a progressive increase in N-acetylglucosaminidase (a lysosomal glycosidase) activity. Within the iris epithelium the activity of this enzyme attains a maximum level on day 17 post-lentectomy and then gradually decreases during subsequent stages of lens regeneration (Idoyaga-Vargas and Yamada, 1974).

2.9 Stage VIII: 15 to 19 days post-lentectomy

At the center of the primary lens fiber complex the cell boundaries of primary lens fibers are less distinct, nuclei and cytoplasmic organelles show signs of degeneration and the filamentous material increases in the cytoplasm. At the equatorial region of the lens vesicle, between the primary lens fiber complex and the cuboidal cells of the lens epithelium, the cells which are forming the secondary lens fibers have ceased proliferation and are undergoing elongation. As a consequence these cells surround the primary lens fiber complex (Eguchi, 1964).

Immunofluorescent staining of lens crystallin proteins is further intensified within the stage VIII primary lens fiber complex and moderate staining of secondary lens fibers is observed (Takata et al., 1964). However, when antiserum specific to the gamma crystallin class

is employed, immunofluorescent staining of secondary lens fibers is infrequently observed, suggesting that crystallin synthesis within the secondary lens fibers is primarily restricted to the α and β crystallin classes (Takata et al., 1966).

At the outer surface of the lens vesicle a basement membrane 0.1 to 0.2 um thick is present. This basement membrane is appreciably thicker than that of the normal iris epithelium (0.03 um thick), but is still much thinner that the 1 um thick lens capsule of the regenerated lens (Karasaki, 1963).

2.10 Stage IX: 18 to 20 days post-lentectomy

The lens fiber complex continues to increase in size through growth of individual fibers and the addition of newly differentiating secondary lens fibers (Yamada, 1967). Gamma crystallin protein is now observed in the secondary lens fibers (Takata et al., 1966). In the primary lens fibers cytoplasmic organelles are virtually absent and nuclear degeneration continues (Karasaki, 1964). The lens epithelium now extends more posteriorly forming an epithelium over most of the lens fiber complex. Depigmentation and mitotic activity continue at the lens vesicle stalk, these dedifferentiated cells gradually move into the lens epithelium and subsequently may be converted to secondary lens fibers (Eisenberg and Yamada, 1966).

Outside of the lens rudiment, iris epithelial cells are following the "pathway of retrieval" (i.e. redifferentiating into melanosomes). By 20 days post-lentectomy DNA synthesis and IEC mitosis has decreased significantly in both the dorsal and ventral iris epithelium (Eisenberg

and Yamada, 1966) and melanosome synthesis is evident in these cells (Yamada, 1977).

2.11 Stage X: 18 to 25 days post-lentectomy

The addition of successive layers of elongated secondary lens fibers around the primary lens fiber core has produced a concentric arrangement of lens fibers which resembles the mature lens. Within the fiber complex, fiber differentiation, characterized by nuclear and organellar degeneration and accumulation of filamentous material (presumably crystallin proteins), proceeds from the inner core to the outer concentric layers of secondary fibers (Eguchi, 1964). With the increased size of the fiber complex, the lens epithelium becomes a single cell layer. Within the lens rudiment DNA synthesis is detected only within the lens epithelium and adjacent stalk (Eisenberg and Yamada, 1966).

At stage X immunofluorescent staining of lens crystallin proteins is most intense within the primary lens fiber core and decreases in intensity towards the more peripheral layers of secondary fibers. At this time weak staining of α and β crystallin classes is detected in cells of the lens epithelium which remain mitotically active and contribute further to the secondary lens fiber line. This suggests that DNA synthesis and synthesis of α and β crystallin proteins are not necessarily mutually exclusive. However, γ crystallins are not detected within the lens epithelium at this stage or during subsequent stages of lens regeneration, suggesting that γ crystallin synthesis is restricted to the non-replicating differentiating fiber cells. At no stage of lens regeneration are lens crystallin proteins detected in

cells of the lens vesicle stalk or within cells of the iris epithelium (Takata et al., 1964; Takata et al., 1966).

2.12 Stage XI: 21 to 30 days post-lentectomy

The continued proliferation within the lens epithelium and differentiation of lens fibers at the equatorial region of the lens rudiment contribute to the further growth of the lens regenerate. The stalk connecting lens vesicle to iris is lost and within approximately two months the autonomous lens will have attained a size equal to that of the normal lens (Yamada, 1967).

3. CELL SURFACE ALTERATIONS

Dedifferentiation of IECs during lens regeneration is accompanied by changes in cell morphology. Cell to cell contact decreases along the lateral and apical surfaces of the epithelium and large intercellular spaces are observed (Dumont and Yamada, 1972). Significant convolutions and invaginations of the basal cell surface accompany the process of melanosome discharge. That changes in cell-surface groups would accompany such morphological alterations has been suggested. Zalik and Scott (1972 & 1973) studied changes at the cell surface during lens regeneration by cell electrophoresis. Cell suspensions were prepared from normal and regenerating irises and the electrophoretic mobilities (EPM) of individual cells were measured. They observed that during IEC dedifferentiation, the cell surface charge density, as reflected in EPM, decreased significantly. To determine the nature of cell surface groups responsible for the observed decrease in EPM, the effects of neuraminidase, ribonuclease, chondroitinase ABC and hyaluronidase

treatment on EPM were measured. All four enzymes were observed to decrease the mean EPM of normal IECs. During early dedifferentiation the effect of ribonuclease,, chondroitinase or hyaluronidase on the EPM of cells was no longer evident, suggesting that surface groups sensitive to these enzymes disappear early during IEC dedifferentiation. Negatively charged surface groups sensitive to neuraminidase are detectable during early dedifferentiation, but are no longer evident by day 15 when most of the regenerate cells have completely dedifferentiated.

The effects of neuraminidase and ribonuclease on EPM were additive. This was also true for the effects of neuraminidase and hyaluronidase, suggesting that different groups, sensitive to these enzymes were present at the periphery of iris cells. The effects of hyaluronidase and ribonuclease on the EPM however were not additive suggesting that these two enzymes were affecting similar groups at the cell surface. Similarly the effects of treatment with chondroitinase and RNase were not additive. These results suggest that an RNase-sensitive component may be associated with a mucopolysaccharide molecule at the cell surface, which is present in normal IECs, but disappears by day 5 after lentectomy. Because hyaluronidase and chondroitinase enzyme preparations exhibit low levels of contaminating chondroitinase and hyaluronidase activity respectively it was not possible to determine if these two enzymes are acting at similar or separate groups on the cell surface.

It would appear that several enzyme-sensitive groups can be identified. A ribonuclease-hyaluronidase or chondroitinase-sensitive

group, disappears at the onset of dedifferentiation when expansion of intercellular spaces becomes evident. It has been suggested by Zalik and Scott (1973) that the ribonuclease-mucopolsaccharide surface component may function in stabilizing the differentiated state of IECs. A neuraminidase-sensitive group does not disappear from the cell surface until IECs are completely dedifferentiated. Their gradual disappearance during the depigmentation phase may be due to a preferential loss associated with the cytoplasmic shedding which accompanies the discharge of membrane-bound melanosome complexes.

4. GLYCOSAMINOGLYCAN SYNTHESIS

The disappearance of hyaluronidase and chondroitinase-sensitive surface components of IECs during the early stages of lens regeneration suggests that alterations in glycosaminoglycan (GAG) composition of the extracellular matrix (ECM) may play a role in IEC dedifferentiation. Kulyk and Zalik (1982) have investigated the pattern of incorporation of $^{35}SO_4$ into sulfated GAG within the normal and regenerating newt iris. Newts were injected with [^{35}S] H_2SO_4 at various times after lentectomy. The accumulation of label into sulfated GAG was determined in the normal and the regenerating iris. Compared to the rate of label uptake in normal (non-lentectomized) newt iris, the rate of incorporation of $^{35}SO_4$ into GAGs increased two-fold at early stages of regeneration and was three-fold higher in 15 day regenerates. Following the 15 day peak, the rate of labeling declined slightly by 20 to 30 days, but remained elevated in comparison with the normal iris.

Based on differences in susceptibility to degradation by chondroitinase AC, chondroitinase ABC and nitrous acid, the relative amounts of label incorporated into three separate classes of GAGs were measured. In the normal and regenerating iris 60 to 70% of total GAG-bound radioactivity was due to heparin/heparan sulfate, while 16-29% of label uptake was associated with the chondroitins 4- and 6- sulfate, and 11-22% of total label uptake was accounted for by dermatan sulfate. For all stages examined the relative amounts of label incorporation into dorsal and ventral regions of the iris were nearly equivalent, indicating that elevated rates of label incorporation into GAGs is not topographically restricted to those regions of the iris destined for cell-type conversion (i.e. the dorsal iris). In advanced regenerates separate determinations for the lens rudiment were carried out. Only negligible quantities of labeled GAG precursor are associated with the lens tissue of the 30 days lens rudiment or the mature lens of normal eyes. These investigators suggested that increased incorporation could be due to the increased synthesis or decreased degradation of a large proteoglycan macromolecule possessing a fixed complement of polysaccharide chains. The fact that the dorsal and ventral iris have equivalent incorporations of $^{35}SO_4$ into different GAGs led these authors to suggest that the increased synthesis of sulfated GAG is involved with iris epithelial cell dedifferentiation and entrance into the retrieval pathway.

5. CONTROL OF LENS REGENERATION

Removal of the lens from the ocular chamber is conveniently used to initiate lens regeneration, implying that the lens in some manner inhibits the process of lens regeneration. Repression of lens regeneration by the lens requires that the lens be in a metabolically intact state (Eguchi, 1961) and in close proximity to the dorsal iris epithelium (Eguchi, 1961; Stone, 1963; Williams and Higginbotham, 1975). There are some experiments that suggest that an inhibitor substance is present in lens tissue (Smith, 1965; Moore and Williams, 1977) or in the aqueous humour of intact newt eyes (Stone, 1963). However further characterization of this putative inhibitory substance has not been pursued.

Many experiments have supported the hypothesis that lens regeneration is stimulated by a neurotrophic factor. In situ, normal lens regeneration requires the presence of a metabolically healthy neural retina (Stone and Steinitz, 1953; Stone, 1966). Even in the presence of an intact lens, lens regeneration can be initiated if nervous tissue (Reyer, 1966; Williams and Higginbotham, 1975; Powell and Powers, 1973) or whole newt pituitary gland (Powell and Segil, 1976) is in close proximity to the responding dorsal iris epithelium. Isolated from the lens, lens regeneration in dorsal iris explants in culture (Yamada and McDevitt, 1974) or transplanted into the regenerating limb blastema (Reyer et al., 1973) requires a neurotrophic influence. Newt pituitary gland or thyrotropin preparations stimulate lens fiber differentiation in organ culture of dorsal iris and cultures of dissociated IECs (Cuny and Zalik, 1981). Isolation of a putative retinal

factor has not been accomplished, nor is there evidence to suggest that stimulation by the neural retina specifies IEC cell-type conversion into lens fiber. Rather it is believed that the neurotrophic influence provides a growth-promoting effect, allowing IECs to complete the critical number of cell divisions which are required before IECs can express their intrinsic potential for cell-type conversion (Yamada and McDevitt, 1984).

During the early stages of lens regeneration morphological and biochemical changes can be observed throughout the iris epithelium, however it is only IECs at the mid-dorsal pupillary margin of the iris that subsequently undergo cell-type conversion and become lens fibers. Evidently epithelial cells of the ventral iris are capable of undergoing cell-type conversion under certain conditions. Lens regeneration from the ventral iris can be elicited by exposure to N-methyl-N'-nitro-N-nitrosoguanidine, a potent carcinogen (Eguchi and Watanabe, 1973). Disruption of normal iris epithelial structure increases the potential for ventral IECs to undergo cell-type conversion. For example, ventral iris stripped of it's overlying stromal tissue and cultivated in the presence of frog retinal complex regenerated a lens in 18% of the cases (Yamada and McDevitt, 1974). In cell culture conditions dissociated iris epithelial cells from dorsal and ventral iris are equal in their potential to undergo cell-type conversion and form crystallin-positive lentoid bodies (Horstman and Zalik, 1974; Eguchi et al., 1974). These results suggest that within the iris, topographical control of lens regeneration intrinsically exists within the structural organization of the iris epithelium. Possibly localized differences in molecular

constituents of the epithelial extracellular matrix are responsible for the *in vivo* dorsal-ventral gradient of lens forming potential.

6. THE EXTRACELLULAR MATRIX

Within tissues of the multicellular organism cells reside within a meshwork of extracellular macromolecules that constitute the extracellular matrix (ECM). The protein and polysaccharide molecules making up the matrix are synthesized and secreted locally by cells and assemble into an organized tissue specific matrix forming in some instances highly specialized structures such as basal lamina, corneal stroma, cartilage, tendon and bone. The ECM in addition to maintaining the physical integrity of tissues also plays an active and complex role in regulating the behaviour of constituent cells. The ECM has been implicated in the control of various cellular processes including proliferation, migration, adhesion, cytoskeletal organization and cellular differentiation (Hay, 1981).

Three major classes of macromolecular components comprise the ECM, collagens, glycosaminoglycans (GAGs), which are usually covalently linked to protein to form proteoglycans, and several types of glycoproteins. The GAG and proteoglycan molecules form a hydrated "gel-like" ground substance in which collagen fibers and ECM glycoproteins are embedded. Collagen fibers provide a physical scaffold for the matrix, while the aqueous GAG phase permits and in some instances controls the diffusion of molecules through the matrix (Hay, 1981).

6.1 Collagens

Collagens, the principal component of the ECM, are fibrous proteins characterized by their triple-stranded helical structure. Three polypeptide α-chain types which may vary in amino acid composition as well as degree of glycosylation are organized in a left-handed helix and wind around each other to generate a rope like collagen molecule approximately 300 nm long and 1.5 nm in diameter. The triple-helical conformation requires that glycine be present as every third amino acid residue and therefore the polypeptide sequence which characterizes the helical domain consists of a series of Gly-X-Y triplets in which X and Y can be any amino acid. Frequently proline and hydroxyproline occur at the X and Y sites respectively. At the amino and carboxyl terminal ends, non-helical sequences of the chains are involve in the formation of intra- and inter-molecular crosslinks during collagen fibril formation (Linsenmayer, 1981). At least seven genetically distinct collage chains have been recognized. Of all the possible triple-stranded combinations ten different collagen types, assigned Roman numerals I through X, are currently recognized and have been reviewed recently by Mayne (1984) and Martin et al. (1985).

Type IV collagen appears to be present in all basement membranes. In comparison to the interstitial collagens (types I, II and III) type IV collagen has a higher carbohydrate content and contains higher amounts of hydroxylated amino acids. In addition, as reflected by it's lower glycine content (less that one third of the residues are glycine), frequent interruptions in the triplet Gly-X-Y sequence of the triple-helical domain gives rise to a more flexible molecule. The α chains

of type IV collagen appear to undergo very little processing of the procollagen precursor before incorporation into the basement membrane. Type IV collagen does not form collagen fibrils, but rather forms an interacting network within the basement membrane. At the amino terminus a region referred to as 7S is involved in tetrameric overlap allowing four α chains to interact. Alpha chains also interact with one another at their non-helical carboxyl terminal ends, thus forming a network (Mayne, 1984).

For many cell types, growth in culture is often improved by maintaining the cells on collagen substrata. Binding to collagen is mediated by cell type specific attachment proteins. A preference for specific collagen types further reflects the in vivo specificities of cell matrix interactions. Many cell types including fibroblasts, myoblasts, osteocytes, hepatocytes, certain metastatic tumor cell lines, to mention but a few, are capable of binding to all types of collagen (I through IV), with fibronectin mediating this interaction. Chondrocytes utilize chondronectin attachment protein and prefer type II collagen substrata. Epithelial cells attach preferentially to type IV (basement membrane) collagen and laminin acts as the specific attachment factor (Kleinman et al., 1981).

Binding to collagens is thought to physically stabilize the cells within the ECM. In addition to or as a result of such binding, collagens have been observed to influence the differentiative state of cells. Myoblast fusion to produce multinucleated myotubes is promoted by culture on collagen substrata (Ketley et al., 1976), with fibronectin mediating the myoblast-collagen interaction (Chicquet et al., 1979).

Within the developing chick limb bud (Dessau et al., 1980) or the regenerating salamander limb (Lisenmayer and Smith, 1976) mesenchyme condensation is associated with increased synthesis of type I collagen. During subsequent chondrogenesis the synthesis of type I collagen decreases and synthesis of type II collagen increases.

There is evidence to suggest that epithelial morphology is influenced by it's association with collagen. When corneal epithelium is separated from it's underlying collagenous rich stroma, it undergoes blebbing of the plasmalemma at the basal surface. If cultured on a collagenous substrate or in the presence of soluble collagen (types I to IV), laminin or fibronectin, surface blebs retract and actin filaments reform the basal cortical mat typical of corneal epithelium in vivo (Sugrue and Hay, 1981). This suggests that extracellular molecules are involved in the organization of intracellular cytoskeletal elements. Collagen may also play a role in establishing epithelial polarity. In culture, the epithelium of the thyroid follicle will form hollow spheres in which the apical cell surface is directed towards the medium. The addition of denatured collagen causes cell polarity to revert to it's in vivo morphology, with apical surfaces directed towards the central cavity of the follicle (Mauchamp et al, 1979).

6.2 Laminin

Laminin, a non-collagenous glycoprotein specific for the basement membrane was originally isolated from a murine tumor, the EHS sarcoma, which produces an ECM particularly rich in basement membrane constituents (Timpl et al., 1979). Laminin is composed of three B chains (M_r=200K) and one A chain (M_r=400K) held together by disulfide

bonds (Kleinman et al., 1984). This molecule exists as monomers (850K), dimers (1500K) and larger aggregates (Foidart et al., 1981). Visualized by electron microscopy, rotary shadowed laminin appears as an asymmetric cross with a long arm (75 nm) and three short arms (35 nm) of low flexibility with globular domains at the termini of each arm (Engel et al., 1981).

Distinct domains of the laminin molecule have been shown to interact specifically with type IV collagen (Rao et al., 1982), heparan sulfate and heparin (Sakashita et al., 1980). Laminin also binds to gangliosides (Kennedy et al., 1983) and to a basement membrane heparan sulfate proteoglycan (Woodley et al., 1983). When type IV collagen, laminin and heparan sulfate proteoglycan are combined under appropriate conditions a basement membrane-like gel structure is reconstituted (Kleinman et al., 1984). A cell surface laminin receptor has been identified on breast carcinoma cells (Terranova et al., 1983) and a specific laminin-binding protein has been isolated from murine fibrosarcoma cells (Malinoff and Wicha, 1983).

Using immunofluorescence it has been found that laminin is localized in a variety of basement membranes; Reichert's membrane in the rat parietal yolk sac (Laurie and Leblond, 1983), all basement membranes of the early mouse embryo (Leivo et al., 1980), chick retinal pigmented epithelium (Turksen et al., 1985), epithelia of the optic vesicle and lens placode in developing rat ocular tissue (Parmigiani and McAvoy, 1984) and kidney glomerular and tubular basement membranes (Ekblon et al., 1980) to mention but a few. Studies using immunoelectron microscopy indicate that laminin is present in the lamina rara but

absent in the lamina densa of epidermal, epithelial (Foidart et al., 1980) and glomerular (Madri et al., 1980) basement membranes. In kidney tubular basement membrane, the mesangial matrix and Bowman's capsule, laminin is distributed uniformly throughout the basement membrane (Madri et al., 1980). Teratocarcinoma-derived endoderm cells in culture synthesize a basement membrane-like matrix. Using immunoelectron microscopy laminin is localized within the fibrillar matrix adjacent to the basal cell membrane and in the attachment fibrils which connect the fibrillar matrix to the plasma membrane, while heparan sulfate-containing particles are present at the attachment fibril - fibrillar matrix junction, and along the attachment fibril (Leivo, 1983). A coincident distribution of laminin, heparan sulfate proteoglycan and fibronectin is observed at the surface or normal kidney cells in culture, while virally transformed cells lack such a surface network (Hayman et al., 1982). Tumor metastasis is often accompanied by local dissolution of the basement membrane (Liotta et al., 1984). Using immunofluorescent staining it can be shown that laminin is absent or irregularly distributed around malignant tumor infiltrations (Birembaut et al., 1983).

In culture, epithelial and endothelial cells preferentially attach to type IV collagen substrata, with laminin specifically mediating the interaction. Laminin however does not promote attachment of fibroblasts or mesenchyme cells to collagen substrata (Terranova et al., 1980). Epithelial and endothelial cells in culture synthesize laminin, while fibroblasts and mesenchyme cells do not (Foidart et al., 1980). The *in vitro* adhesion specificity of epithelial and endothelial cells reflects

the specific matrix associations of these cells in vivo. In tissues epithelial and endothelial cells are normally associated with a basement membrane which characteristically contains type IV collagen and laminin.

6.3 Glycosaminoglycans and Proteoglycans

Glycosaminoglycans (GAGs) formerly known as mucopolysaccharides are long unbranched polysaccharide chains composed of repeating disaccharide units. Within the disaccharide repeat one of the sugar residues is always an amino sugar (i.e. N-acetylglucosamine or N-acetylgalactosamine), which typically alternates with residues of uronic acid (D-glucuronic acid or L-iduronic acid). Seven groups of GAGs have been distinguished on the basis of their repeating disaccharide unit composition, type of linkage between residues and the number and location of sulfated residues. They are hyaluronic acid, chondroitin-4-sulfate, chondroitin-6-sulfate, dermatan sulfate, heparan sulfate, heparin and keratan sulfate.

6.3.a Hyaluronic Acid

Hyaluronic acid is not typical of most GAGs. The carbohydrate chain is unusually long, varying in length from 200 to 20,000 sugar residues, and consists of a single repeating disaccharide unit of N-acetyl-D-glucosamine and D-glucuronic acid residues. It is the only GAG type which does not contain any sulfated sugar residues and the carbohydrate polymer is not covalently linked to protein. Hyaluronic acid is present in most connective tissues and it's hydrodynamic properties are important in maintaining tissue turgor and providing a structural resilience to these tissues. By virtue of it's high osmotic potential, hyaluronate mediated changes in tissue volume are thought to accompany a

variety of morphogenic phenomena; opening pathways for cell migration, separation and translocation of mesenchyme cells, and gross anatomical changes in shape during organogenesis (Toole et al., 1984).

The proliferative and migratory events of morphogenesis often take place within a hyaluronate (HA) rich ECM, while the subsequent phase of cytodifferentiation is often accompanied by decreases in HA content. Neural crest cell migration occurs along pathways that are particularly rich in HA, while the condensation of neural crest cells and differentiation into spinal ganglia is accompanied by a localized decrease in HA (Pratt et al., 1975; Derby, 1978; Pintar, 1978). In the sclerotome region of the somite, loss of epithelial organization and cell dispersion is associated with elevated HA synthesis (Solursh et al., 1979). During chick limb bud development condensation of pre-chondrogenic cells is accompanied by a localized decrease in HA (Kosher et al., 1981). Chondrogenesis in chick chondrocyte cultures (Solursh et al., 1980) and somitic cell cultures (Toole, 1973) is inhibited by exogenous HA treatment. During chick corneal development, synthesis and accumulation of HA corresponds temporally to swelling of the primary corneal stroma. Subsequent migration of mesenchyme cells into the HA rich stroma and deposition of the secondary stroma matrix is accompanied by decreased HA synthesis, increased hyaluronidase activity and compaction of the stromal matrix (Toole and Trelstad, 1971). A similar pattern of elevated tissue HA content is observed during the morphogenic processes of gastrulation in chick (Solursh, 1976) and rat (Solursh and Morris, 1977) embryos, during heart formation (Markwald et al., 1978)

and blastema formation in the regenerating adult newt limb (Toole and Gross, 1971).

6.3.b Proteoglycans

Relative to hyaluronic acid the glycosaminoglycan types including, chondroitin sulfate, dermatan sulfate, heparan sulfate, heparin and keratan sulfate normally exist as much shorter carbohydrate chains, usually less than 300 sugar residues per chain. Each GAG type is distinguished by a characteristic repeating disaccharide unit, however substitutions within the repeat formulae do occur, conferring a certain degree of heterogeneity to each GAG type class. Further heterogeneity exists in that sulfate groups, which may be located at several positions on the hexosamine residue, or, less frequently, on the uronic acid residue, are present to a variable extent along the carbohydrate polymer. Except for hyaluronic acid, naturally occurring GAGs are covalently linked to protein to form proteoglycan. Although the major types of GAGs are common to many different tissues and cell types, the protein core to which the GAG is bound often shows cell- and tissue-specific differences (Hassell et al., 1986). Proteoglycans, a diverse group of macromolecules, are present extracellularly in almost all tissues and are especially prominent in connective tissues. They serve a variety of structural, organizational and regulatory functions.

One of the most studied proteoglycans is that present in cartilage. The predominant proteoglycan in cartilage has an estimated Mr=2,500,000, however variations in protein core size and GAG composition are evident. In mature hyaline cartilage two proteoglycans of different size and GAG composition, but similar in immunological determinants, can be isolated.

While in fetal or immature cartilage a single proteoglycan species is detected. A typical cartilage proteoglycan contains approximately 100 chondroitin sulfate chains and 130 keratan sulfate chains of varying length. The amino terminal end of the core protein contains no GAG, most of the N-linked oligosaccharides and separate binding sites which specifically interact with hyaluronic acid and link protein (Hassell et al., 1986). Within the cartilage matrix many proteoglycan monomers assemble onto a hyaluronic acid carbohydrate chain at intervals of 30 nm, to form proteoglycan aggregates of molecular weights in excess of 2×10^8 daltons (Hascall and Hascall, 1981). Due to the net negative charge of the GAG chains these aggregates occupy large hydrodynamic volumes which may vary depending on the proteoglycan concentration and competition for available solvent in the matrix. Therefore local variations in proteoglycan concentration may reflect the structural properties required of the cartilage matrix in specific tissues.

Proteoglycans, stained with various cationic probes (ruthenium red or cationized ferritin), have been shown to be present in a variety of basement membranes. Within the corneal basal lamina (Trelstad et al., 1974) and the glomerular basement membrane (Kanwar and Farquhar, 1979), cation-stained proteoglycan granules are observed within the lamina rara externa and lamina rara interna at regular 60 nm intervals. Heparan sulfate proteoglycans have been isolated from various basement membrane (bm) sources; glomerulus basement membrane (Kanwar et al., 1981; Kobayashi et al., 1983), the basement membrane-producing EHS sarcoma (Hassell et al., 1985), and a mouse parietal yolk sac cell line (Oohira et al., 1982; Oohira et al., 1983). These basement membrane heparan

sulfate proteoglycans vary considerably in terms of size, GAG content and the molecular weight estimates of the protein cores range from 30,000 (glomerulus bm) to 400,000 (EHS sarcoma). However these bm proteoglycans do appear to share common immunological determinants on their core proteins. Antibodies against the EHS bm proteoglycan cross-react with parietal yolk sac bm proteoglycan (Oohira et al., 1982) as well as basement membranes in a wide variety of normal tissues (Hassell et al., 1980). Antibodies to the heparan sulfate proteoglycan of glomerular bm cross-reacts with the EHS sarcoma proteoglycan (Hassell et al., 1986). Chondroitin sulfate proteoglycans are also a constituent of some basement membranes. In the glomerular bm 15% of the extracted proteoglycan is chondroitin sulfate proteoglycan (Kanwar et al., 1981). In the submandibular gland 40% of the GAG within the basal lamina is chondroitin or dermatan sulfate (Cohn et al., 1977). For the glomerular bm it is the heparan sulfate proteoglycan component which imparts selective-charge barrier properties that are necessary to the filtration function of the glomerulus (Kanwar et al., 1980). It seems likely that in other basement membranes the proteoglycan component also serves to sterically and electrostatically regulate the passage of macromolecules to or from the cells which are associated with the basement membrane.

Cell surface proteoglycans have been isolated from a variety of sources; mouse mammary epithelial cells, skin fibroblasts, human melanoma cells, hepatocytes and rat ovarian granulosa cells (Hassell et al., 1986). These cell surface proteoglycans are immunologically distinct from the proteoglycans of the basement membrane (Jalkanen et

al., 1985; Stow et al., 1985). Some exist as integral membrane components while others are peripheral and associate with the cell membrane indirectly. The proteoglycans within this group show a large diversity of structure and core protein size (Hassell et al., 1986), and in some cases have been shown to be immunologically distinct from one another (Stow et al., 1985), suggesting that these proteoglycans are not closely related.

Two forms of heparan sulfate proteoglycan have been isolated from hepatocytes, a periperal non-intercalated form which is thought to be derived from a slightly larger intercalated form (Kjellen et al., 1981). The hepatocyte cell membrane contains a receptor that interacts with heparan sulfate (Kjellen et al., 1980), suggesting that the cell surface heparan sulfate proteoglycan may function in cell-cell adhesion.

Several different proteoglycans have been isolated from cultures of rat ovarian granulosa cells. Two cell surface proteoglycans, one with dermatan sulfate chains and the other with heparan sulfate chains are shown to have core proteins of approximately equal molecular weight (Yanagishita and Hascall, 1984a & 1984b).

Epithelial cells from the mammary gland of the mouse have a cell surface heparan sulfate-rich proteoglycan which is immunologically distinct from the heparan sulfate proteoglycan of the epithelial basal lamina. This cell surface proteoglycan is intercalated into the plasma membrane by a lipophilic domain of it's core protein (Hassell et al., 1986). This proteoglycan binds specifically to type I collagen, but not to type IV collagen. Further evidence shows that this integral membrane proteoglycan interacts with the cytoskeleton of the epithelial cell. It

is proposed that for the mammary gland and analogous lobular epithelial organs, this cell surface proteoglycan by it's specific interaction with interstitial type I collagen, which accumulates at the interlobular clefts and on the stalk, imparts a morphological stability to these cells which is necessary for normal branching morphogenesis (Bernfield et al., 1984).

In addition to the large HA-binding proteoglycans many connective tissues including; cartilage, tendon, bone, skin and cornea also contain smaller proteoglycans. Within this group two immunologically distinct core protein species are recognized and a keratan sulfate proteoglycan appears to be unique to the corneal stroma (Hassell et al., 1986). In some instances these proteoglycans clearly have a structural function. Within the cornea the small proteoglycans can be accommodated between the orthagonal layers of collagen fibrils without distorting the matrix and presumably facilitate and stabilize the orderly packing of fibrils which is required for optical transparency (Hascall and Hascall, 1981).

Proteoglycans constitute a rapidly expanding field of very active research and therefore have only been cursorily reviewed in this thesis. No doubt further proteoglycans will be identified and an understanding of their diverse biological roles will continue to be revealed.

6.4 Fibronectin

Fibronectins is the current term used to describe a class of closely related glycoproteins that have previously been known by a variety of synonyms: cold-insoluble globulin (Morrison et al., 1948), cell attachment factor (Klebe, 1974), cell adhesion factor (CAF) (Pearlstein and Gold, 1978) cell surface protein (Yamada and Weston,

1974) and large, external transformation-sensitive (LETS) protein (Hynes and Bye, 1974).

Although highly similar in structure and function, the plasma and cellular forms of fibronectin (Fn) can be distinguished on the basis of certain physical and biological characteristics. Plasma fibronectin is present at a concentration of approximately 0.3 mg/ml plasma. When analyzed under reducing conditions by polyacrylamide gel electrophoresis, plasma Fn migrates as a closely spaced doublet with an apparent subunit molecular weight of 215 - 220 K. Cellular fibronectin is slightly larger, with an apparent subunit molecular weight of 220-240K and migrates as a single, more diffuse band (Yamada, 1981). A further distinction between plasma and cellular Fn is their solubility properties. Plasma Fn is soluble at neutral pH while cellular Fn requires an alkaline (pH 11) or treatment with strong denaturing agents to remain soluble (Yamada and Olden, 1978). In vitro assessment of biological activity shows the two forms of fibronectin to be indistinguishable in assays involving cell attachment to various substrata, or in opsonic activity for macrophages. However cellular Fn is much more active than plasma Fn in mediating erythrocyte agglutination and in the restoration of normal cell morphology in transformed cell lines (Yamada and Kennedy, 1979).

Fibronectin is a glycoprotein and approximately 5% of it's mass is carbohydrate consisting of the complex oligosaccharide type linked to asparagine residues. Essentially all of the carbohydrate is localized in the collagen-binding and cell-binding regions of the molecule. In the presence of tunicamycin, an inhibitor or glycosylation,

unglycosylated fibronectin is synthesized and secreted by cells at a rate comparable to untreated cells. This unglycosylated fibronectin is similar in it's biological activities to normal, glycosylated fibronectin but experiences a several-fold higher rate of turnover, suggesting that the carbohydrate functions to protect Fn from proteolytic attack by cellular proteases (Olden et al., 1978; 1979).

Fibronectin is composed of two nearly identical, disulfide-linked polypeptides with a combined dimeric molecular weight of approximately 450 K. Physical measurements predict an asymmetric protein in which protease-resistant globular domains are separated by flexible segments of the polypeptide chain (Hynes and Yamada, 1982). Indeed, protease fragmentation of the molecule has identified a number of structural domains possessing specific ligand binding capabilities, arranged in a modular fashion along the polypeptide subunits of fibronectin (see Figure 4) (Ruoslahti et al., 1982a).

Fibronectin binds to fibrin or to fibrinogen at sites in it's amino terminal domain and carboxyl terminal domain, however transglutaminase-mediated cross-linking of Fn to fibrin appears to occur only at the amino terminal binding site. The amino terminal domain of Fn mediates binding to Staphylococci bacteria, actin, and heparin (Hynes and Yamada, 1982).

The collagen binding domain of Fn can be isolated as proteolytic fragments 30,000 - 40,000 daltons in size and can be mapped to the carboxyl terminal side of the amino terminal domain (Ruoslahti et al., 1982a). The rate of Fn binding to collagen is enhanced by heparin by not other GAGs (Johansson and Hook, 1980) and Fn-collagen complexes are

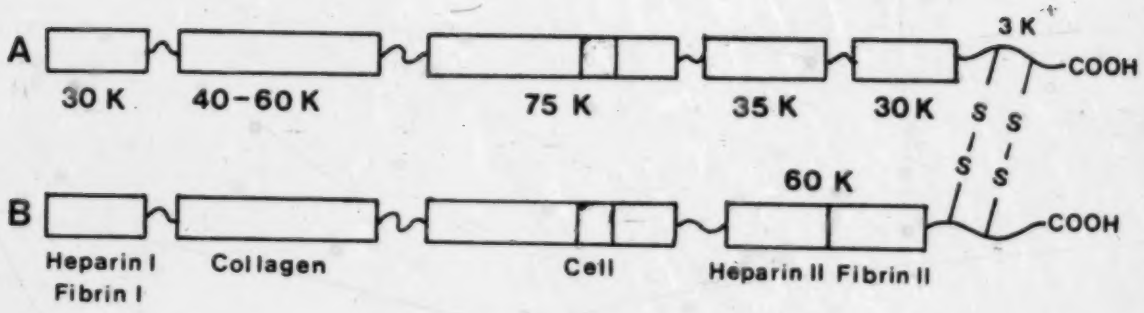

Figure 4.

Schematic diagram of fibronectin illustrating the A and B monomer polypeptide chains that comprise the dimeric glycoprotein. Each monomer consists of protease-resistant domains (represented by boxes) which are separated by protease-sensitive regions (represented by wavy lines). The specific binding characteristics and molecular weights (K = kilodalton) of each domain are indicated (adapted from Yamada, 1983).

apparently stabilized by the presence of heparin, heparan sulfate and hyaluronic acid (Ruoslahti and Engvall, 1980). In addition to interaction at the collagen-binding site, collagen may also be covalently cross-linked to the amino terminal domain of Fn by transglutaminase (Mosher et al., 1980).

The cell-binding domain of Fn can be isolated as peptic fragments and has been mapped to the central region of the Fn molecule, between the collagen binding domain and the carboxyl terminal heparin-binding domain (Hayashi and Yamada, 1983). The entire primary sequence of an 11,500 dalton fragment constituting the cell-binding domain was reproduced into four tandem synthetic peptides and cell attachment activity was confined to the 30 amino acids nearest the carboxyl terminus of the domain (Pierschbacher et al., 1983). This 30 amino acid segment apparently contains the cell-recognition signal sequence of L-arg-gly-asp-ser. A tetrapeptide of arg-gly-asp-ser can competitively inhibit cell attachment to Fn substrates and when such peptides are coupled to solid substrates they will promote cell adhesion.

Several variations in the fourth (ser) position do not appear to alter the activity of the tetrapeptide, and even the reverse sequence (ser-asp-gly-arg) possesses cell recognition activity, suggesting that it is the amino acid side chains of the arg-gly-asp residues, and not their polarity along the peptide backbone, that are critical to recognition by a cell surface receptor (Pierschbacher and Ruoslahti, 1984).

The cell-surface Fn receptor may be an integral membrane glycoprotein of estimated molecular weight 140,000 daltons (Pytela et

al., 1985). Studies employing immunoflouorescent staining show that fibronectin, the putative 140 K Fn receptor and cytoskeletal α-actin co-localize at extracellular contact sites on the ventral surface of cultured fibroblasts. Further, antibodies to the 140 K receptor inhibit attachment and spreading of normal and transformed fibroblasts on fibronectin substratum (Chen et al., 1985). Several other putative cell-surface Fn receptors have been suggested, a 47,000 dalton glycoprotein and certain gangliosides (Yamada et al., 1985). Additionally a glycoprotein IIb/IIIa complex at the surface of thrombin-activated platelets appears to act as a specific Fn receptor (Hynes, 1985a). It is possible that the cell-surface Fn receptor consists of a heterogeneous group of molecules with variable functional properties and cell-type specific distributions.

Fibrin also binds to fibronectin at a site close to the carboxyl terminus of the monomer subunit, but with lower affinity than the amino terminal fibrin-binding site. Binding of heparin within the carboxyl terminus is of higher apparent affinity relative to the heparin-binding site of the amino terminal domain (Hayashi and Yamada, 1982). Fn may interact with sulfated proteoglycans at the cell surface (Perkins et al., 1979). Fibronectin also binds hyaluronic acid at an unknown site, but this latter does not interfere with the binding of heparin to fibronectin (Yamada et al., 1980).

In tissues fibronectin (Fn) can be localized by immunohistochemical and immunofluorescent techniques in connective tissues, a variety of mesenchymal tissues and in many basement membranes. In cell cultures immunofluorescently labeled Fn is initially localized between cells and

at the ventral cell surface in contact with the substratum suggesting an adhesive function for cell surface fibronectin. Later as the cells reach confluency fibronectin appears as a dense pericellular fibrillar network (Yamada and Olden, 1978). Fibronectin has been shown to mediate adhesive events in a variety of cell types. Attachment of normal (Lisenmayer et al., 1978; Grinnell and Feld, 1979) and transformed (Pearlstein, 1976; Pearlstein and Gold, 1978; Yamada et al., 1978) fibroblast cell lines to collagen substrata is mediated by fibronectin. Fibronectin agglutinates fixed sheep erythrocytes and increases aggregation of living dissociated chick embryo and baby hamster kidney (BHK) cells (Yamada et al., 1979). Cells transformed by oncogenic viruses or carcinogens generally lose their cell surface Fn, adopt a rounder morphology and become less adherent. During mitosis of the cell cycle cell-surface fibronectin is reduced although intracellular levels of Fn appear unaltered (Hunt et al., 1975; Stenman et al., 1977). Double immunofluorescent staining of actin and fibronectin have shown that extracellular fibronectin fibrils at the surface of cultured fibroblasts are highly coincident with the actin containing microfilaments of the cytoskeleton, suggesting a transmembrane relationship between fibronectin and the cytoskeleton (Singer, 1979). At sites where cells make close contact with the extracellular matrix transmembrane linkage of extracellular Fn fibrils and intracellular actin microfilament bundles is apparently mediated by the 140 Kd membrane-associated Fn receptor complex (Chen et al., 1985; Duband et al., 1986).

It has been suggested that Fn may be involved in neural crest cell migration in the embryo. Although Fn does not appear to direct neural

crest cell migration by haptotactic (directed migration of cells due to increasing adhesion gradients mediated by insoluble, solid-phase substratum material) (Mayer et al., 1981) or contact guidance (Tosney, 1982) mechanisms, the interaction of neural crest cells with Fn is critical to their migration. Perturbation of this interaction, by injecting a synthetic dectapeptide containing the cell recognition sequence of Fn into the cell-free space of avian embryos drastically inhibits crest cell emigration from the dorsal border of the closing neural tube (Boucaut et al., 1984a). Antibodies against the putative 140 Kd fibronectin receptor reveal that in vivo during neural crest cell migration in quail embryos and in vitro cultures of neural crest cells, this receptor is diffusely organized and highly mobile in the plane of the membrane on the cell surface of motile neural crest cells (Duband et al., 1986). Such an organization would suggest that neural crest cells are capable of reversible, low-affinity interactions with Fn which would be expected for rapid cell motility. Fibronectin is also coincidentally present in the migration pathway utilized by primordial germ cells (Heasman et al., 1981).

In the early chick embryo Fn is primarily localized to the basal lamina of the epiblast and associated interstitial bodies (Critchley et al., 1979; Duband and Thiery, 1982; Sanders, 1982). Like neural crest cells, the mesodermal cells do not appear to synthesize fibronectin nor is fibronectin associated with the cell surface of mesoderm cells (Sanders, 1980 & 1982). It is suggested that following ingression at the primitive streak, the presumptive mesodermal cells utilize the Fn-rich basal lamina of the epiblast as a substratum for their subsequent

lateral migration. The invagination of mesodermal cells during amphibian gastrulation apparently utilizes the Fn-rich ECM, which is present at the inner surface of the blastocoel roof (Boucaut and Darribere, 1983; Darribere et al., 1985), as a substratum for migration. The synthesis and extracellular deposition of fibronectin is temporally and spatially controlled during development such that when gastrulation is initiated Fn is observed only on those surfaces upon which mesoderm will migrate (Lee et al., 1984). Microinjection of anti-fibronectin antibodies (Boucaut et al., 1984b) or a synthetic dectapeptide containing the cell recognition sequence of Fn (Boucaut et al., 1984a) into blastula and early gastrula stage amphibian embryos inhibits the invagination of mesoderm cells into the blastocoel cavity.

Fibronectin is not present in the corneal epithelial basement membrane, however, shortly after wounding (i.e. removal of epithelial cells) fibronectin appears on the denuded corneal surface and apparently provides a substratum for subsequent migration of epithelial cells into the wound site (Fujikawa et al., 1981). In skin wounds on adult newts the migration of epidermal cells into the wound site can be supported on artificially implanted fibronectin or fibrinogen substrates (Donaldson and Mahan, 1983). It has been suggested that fibronectin binding to the fibrin(ogen) clot at a wound site promotes the attachment of fibroblasts during wound healing (Ruoslahti et al., 1982a). Fibronectin as a constituent of the ECM is apparently utilized as a substratum by cells in their morphogenic movements for a variety of developmental processes.

Developmentally regulated patterns of fibronectin distribution are observed during the course of embryonic limb morphogenesis.

Immunofluorescent staining of fibronectin in the developing chick limb bud reveals that fibronectin is uniformly distributed in the mesenchymal tissue of the limb bud, and with continued development Fn persists in the proximal central core where cells are undergoing chondrogenesis, but progressively decreases in peripheral regions undergoing myogenesis (Kosher et al., 1982; Tomasek et al., 1982). Using antibodies against human fibronectin the pattern of fibronectin distribution in the regenerating limb of the adult newt was studied. Following limb amputation differentiated tissues undergo a process of dedifferentiation and give rise to a mesenchymal population (limb blastema) which subsequently redifferentiates into a new limb. Immunofluorescent staining of fibronectin within the regenerating limb show fibronectin to be present in the ECM surrounding the dedifferentiating blastema cells. During blastema growth and the early stages of redifferentiation fluorescent staining for Fn increases. During redifferentiation in the limb blastema chondrogenic and myogenic differentiation is accompanied by a progressive decrease in fluorescent staining for Fn. However after brief treatment with hyaluronidase, Fn could be detected within the developing cartilage matrix, suggesting that Fn does not actually disappear but rather is masked by glycosaminoglycans synthesized by the maturing chondrocytes (Gulati et al., 1983). These results in which anti-human Fn antiserum was used may need to be re-evaluated in that antibodies to amphibian Xenopus fibronectin show a very low cross-reactivity to mammalian fibronectins (Heasman et al., 1981). Results in this thesis also show that antibodies to human fibronectin have a low cross-reactivity to Xenopus or newt fibronectins.

MATERIALS AND METHODS

1. COLLECTION OF XENOPUS PLASMA

Blood from a mixed population of adult male and female specimens of Xenopus laevis was collected by heart puncture. Approximately 5 ml of blood was drawn into a 10 ml syringe containing 1 ml of citrated amphibian plasma saline (0.147 M sodium citrate, 3 mM sodium azide, 0.1 mM phenylmethylsulphonyl fluoride (PMSF), 0.106 M NaCl in 0.02 M sodium phosphate buffer, pH 7.2). Alternatively some animals were decapitated and blood was collected dropwise into citrated amphibian plasma saline at a ratio of 1 ml citrated saline to 10 ml of blood. Approximately 30 mls of non-coagulated Xenopus blood, at a ratio of 1 volume citrated saline to 8 volumes blood, was collected and centrifuged at 900 x g for 10 minutes. The plasma supernatant was removed and centrifuged at 900 x g for 10 minutes and the final plasma supernatant was stored at -70°C in siliconized plastic tubes.

2. ISOLATION OF XENOPUS PLASMA FIBRONECTIN BY AFFINITY CHROMATOGRAPHY

Plasma fibronectin was isolated by modifications of the procedures of Ruoslahti et al. (1982b) and of Hynes (1985b). All glassware, columns and tubing was siliconized overnight and washed extensively in distilled water prior to column assembly. Sepharose 4B (Pharmacia) was washed in several changes of elution buffer (0.106 M NaCl, 0.01 M sodium citrate, 3 mM sodium azide, 0.1 mM PMSF in 0.02 M sodium phosphate buffer pH 7.30. The Sepharose slurry was packed into a column (0.9 cm diameter x 26 cm length) at a flow rate of 14 ml/h. The column was

connected via a peristaltic pump (LKB Microperpex) to a UV monitor with recorder (LKB 2138 Uvicord S and LKB 2210 potentiometric recorder) and a fraction collector (LKB 2111 Multirac). The column was equilibrated with elution buffer until the absorbance (A_{280}) reading of column outflow reached a steady baseline. To preabsorb the plasma and remove components that absorb non-specifically to Sepharose, the citrated blood was applied first to the sepharose 4B column, at a flow rate of 7 ml/h and fractions of a 5 ml volume were collected. Following loading of the sample the column was washed with elution buffer until the absorbance reading of column outflow had returned to a steady baseline. Those fractions with an A_{280} reading greater than baseline were pooled.

Xenopus plasma fibronectin was isolated by affinity chromatography. Gelatin-Sepharose 4B (Pharmacia) was washed in elution buffer and the slurry was packed into a column (0.9 cm diameter x 28 cm length) at a flow rate of 14 ml/h. The gelatin-Sepharose-4B column was equilibrated with elution buffer until the absorbance (A_{280}) reading of column outflow reached a steady baseline. The pooled fractions of plasma which had been preabsorbed on the Sepharose 4B column were applied to the gelatin-Sepharose 4B affinity column at a flow rate of 7 ml/h and fractions of a 5 ml volume were collected. Following loading of the sample the column was washed with elution buffer until the A_{280} reading of column outflow had returned to a steady baseline. Fibronectin was then eluted from the affinity column with a solution of 1.0 M sodium bromide (NaBr), 0.05 M sodium acetate pH 5.0 (Dessau et al., 1978). Fibronectin eluted as a single peak and those fractions with an A_{280} reading greater than baseline were pooled and placed in membrane

dialysis tubing (Spectrapor; mw cut off 6,000 to 8,000) and dialyzed against elution buffer. The fibronectin sample was then concentrated on a bed of solid polyethylene glycol (Fisher Scientific; MW 20,000). Aliquots of the fibronectin sample were removed and used either for protein determination or for sodium dodecyl sulfate-polyacrylamide gel electrophoresis (SDS-PAGE). The remaining sample was stored at -70°C.

3. PROTEIN DETERMINATION AND SODIUM DODECYL SULFATE - POLYACRYLAMIDE GEL ELECTROPHORESIS (SDS-PAGE)

Protein concentration of the fibronectin sample was determined by the method of Bradford (1976) as described in the Bio-Rad laboratory protein determination kit. A series of standards consisting of bovine gamma globulin at concentrations ranging from 0.8 μg/ml to 13 μg/ml were prepared according to the Bio-Rad instruction manual. Standards and fibronectin sample in a total volume of 0.8 ml sample buffer were placed in test tubes, to which 0.2 ml concentrated dye reagent was added. A blank consisted of 0.8 ml sample buffer plus 0.2 ml dye reagent. Each test tube was mixed and absorbance at 595 nm was read in a Beckman DU-8 spectrophotometer. A standard curve of A_{595} against concentration of standards was used to determine the protein concentration of the fibronectin sample.

The molecular weight of the isolated fibronectin sample was determined by SDS-PAGE (Laemmli, 1970). A 7.5% polyacrylamide gel was prepared as follows; 7.3 ml of acrylamide-bis-acrylamide stock solution (60% acrylamide (w/v),1.6% bis-acrylamide (w/v) (Eastman Kodak) in distilled water) was added to 22.7 ml of distilled water and degassed under vacuum for 10 minutes. Then 15 ml of 0.2% ammonium persulfate

(w/v) (Fisher) in an aqueous 0.4% SDS (w/v) (Bio-Rad) solution was added to the acrylamide mixture and finally 15 ml of TEMED solution (0.13% N, N, N', N'-tetramethylethylene diamine (v/v) (Eastman Kodak) in 18.2% Tris (w/v) (Fisher), pH 8.3 in distilled water) is added and the solution was immediately poured into a LKB gel mold assembled as described in the LKB Application Note 306. Polymerization took place overnight at room temperature and the gel slab (dimensions of 120 x 250 x 2 mm) was prepared for horizontal electrophoresis on a LKB 2117 Multiphor Electrophoresis apparatus equipped with a cooling plate. Current was applied with an Ortec:4100 Pulsed/Constant Power supply. A Tris-glycine electrode buffer (0.3% Tris (w/v), 1.4% glycine (w/v) (Fisher), o.1% SDS 9w/v) in distilled water, pH 8.3) was used as a running buffer. Pre-electrophoresis of the gel at 300 volts and 300 pulse per second current was carried out to remove impurities within the gel matrix.

Proteins used as standards for molecular weight consisted of mixtures of proteins of high molecular weight from Bio-Rad which included ovalbumin (MW 45,000), bovine serum albumin (MW 66,2000), phosphorylase B (MW 92,500), B-galactosidase (MW 116,250) and myosin (MW 200,000). A mixture containing proteins of low molecular weight consisted of lysozyme (MW 14,400), soybean trypsin inhibitor (MW 21,500), carbonic anhydrase (MW 31,000), ovalbumin, BSA and phosphorylase B. The protein mixture was diluted with solubilizing buffer (2% SDS (w/v), 5% B-mercaptoethanol (Sigma) (v,v), 8 M urea (Bio-Rad) in 0.05 M Tris) to a concentration of 0.1 µg of each protein

standard per µl of buffer. A drop of 0.5% bromophenol blue (Fisher) was added and the standard mixture was heated at 60°C for 30 minutes.

A sample of affinity purified Xenopus plasma fibronectin was diluted with sample buffer to a final concentration of 0.13 µg protein per ul of buffer; Xenopus plasma was diluted 1:2 with sample buffer and both were heated at 60°C for 30 minutes. The protein standards and samples each at a volume of 15 µl were loaded into slots of the gel and electrophoresis was carried out at a voltage of 150 volts and a pulsed current of 150 pulses per second (pps) until samples were seen to move out of the application slots. The voltage and pulsed current were then increased by 50 volts/50 pps increments at half-hour intervals until a value of 300 volts/300 pps was attained.

Following electrophoresis gels were stained with silver according to the method of Wray et al. (1981). The gel was fixed overnight in an aqueous solution containing 50% methanol (v/v) and 10% acetic acid (v/v), (Fisher reagent grade). The following day the gel was washed in an aqueous solution of 5% methanol (v/v) and 7% acetic acid (v/v) for 1 hour. The gel was then fixed in an aqueous solution of 5% glutaraldehyde (v/v) for 1 hour and then extensively washed in distilled water for 2 hours. The gel was then stained in an ammoniacal silver solution prepared in the following manner: 8 ml of silver nitrate solution (1.6g silver nitrate (Fisher) dissolved in 8 ml distilled water) was added, dropwise, to 42 ml of an aqueous 0.36% sodium hydroxide solution containing 2.8 ml concentrated ammonium hydroxide and the solution was then made up to 200 ml with distilled water. After 15 minutes in the staining solution the gel was washed for 5 minutes in

distilled water. The gel was then incubated in citric acid developer (0.005% citric acid (w/v), 0.019% formaldehyde (w/v) and 5% methanol (v/v) in distilled water) for 4 to 5 minutes or until stained bands began to appear. To stop further development the gel was washed briefly in distilled water, then washed in an aqueous solution of 50% methanol and 10% acetic acid for 30 minutes. Following silver staining some proteins are not stained but appear as clear bands on the gel. Using a silver/coomassie blue double staining technique described by Dzandu et al. (1984), those proteins insensitive to the silver staining technique can be visualized by coomassie blue staining. Following silver staining the gel was washed in distilled water and then incubated in an aqueous solution containing 0.1% coomassie brilliant blue (w/v) (Bio-Rad), 25% methanol (v/v) and 7.5% acetic acid (v/v) for 1 hour. The gel was then destained overnight in an aqueous solution containing 25% methanol (v/v) and 7.5% acetic acid (v/v). After destaining the gel was photographed.

Estimates of molecular weight of the stained protein bands were made from measurement of migration distances of the standard proteins and sample proteins. Mobility (Mr) values for the standards and sample proteins were calculated as follows:

$$Mr = \frac{\text{distance traveled by protein}}{\text{distance traveled by dye}} \times \frac{\text{length of gel before staining}}{\text{length of gel after staining}}$$

Mr values for the protein standards were plotted against their known log MW values to obtain a standard curve. Linear regression analysis of the data was used to determine the molecular weights which correspond to the Mr values of the unknown protein sample bands.

4. PREPARATION OF RABBIT ANTISERUM AGAINST XENOPUS PLASMA FIBRONECTIN

The affinity-purified Xenopus plasma fibronectin was dialyzed against mammalian PBS (0.145 M NaCl in 0.005 M sodium phosphate buffer, pH 7.2) and then concentrated on a bed of solid polyethylene glycol (Fisher, MW 20,000). Protein concentration of this sample was estimated to be 0.344 mg/ml. Approximately 300 μg of fibronectin in 1.4 ml of mammalian PBS was emulsified in 1 ml of Freund's complete adjuvant (Difco Laboratories) and then injected subcutaneously at ten separate sites along the dorsal skin of a four month old, Dutch Belted rabbit. This same rabbit had been bled to obtain samples of preimmune serum, two days previous to the initial immunization. Two weeks after the initial immunization 100 μg of fibronectin in 300 μl of mammalian PBS was emulsified in Freund's incomplete adjuvant and administered subcutaneously. Two weeks later 100 μg of fibronectin in mammalian PBS was injected subcutaneously. One week later 15 ml of blood was collected from the rabbit. The blood was allowed to clot at room temperature and left overnight at 4°C. The following day the serum was decanted and centrifuged at 1000 x g in an IEC Centra-7R refrigerated centrifuge at 4°C for 30 minutes. The antiserum supernatant was removed and aliquoted into appropriate sized aliquots for storage at -70°C. Blood was collected four more times at 10 day intervals and antiserum was prepared as described above.

5. PROTEIN BLOTTING AND IMMUNOBLOTTING

Iris tissue was dissected from normal adult newt eyes and held in Amphibian Ringer solution (0.11 M NaCl, 1.87 mM KCl, 1.08 mM $CaCl_2$, 9.89

mM glucose, 0.406 mM $MgSO_4$ in 0.005 M sodium phosphate buffer, pH 7.6). A total of 60 irises were collected and transferred to a 0.1 ml mini tissue grinder (Jencons Scientific). Tissue was then homogenized with 250 µl of solubilizing buffer (5% SDS (w/v), 5% B-mercaptoethanol (v/v), 8 M urea (Schwartz-Mann) in 0.05 M Tris (Schwartz-Mann)): this gave a ratio of 6 irises per 25 µl of solubilizing buffer. Homogenization was repeated intermittently while the extract was being incubated at 60°C for 30 minutes. The homogenate was then centrifuged at 100,000 x g for 15 minutes in a Beckman airfuge™. The supernatant was removed and stored at -70°C. Samples of newt skin were dissected from eyelid region and placed directly into solubilizing buffer. Tissues were homogenized in mini tissue grinders at 60°C for 30 minutes. The homogenates were centrifuged at 100,000 x g for 20 minutes. The supernatant was removed and centrifuged at 100,000 x g for 20 minutes and the final supernatant was stored at -70°C. Prior to electrophoresis the iris and skin samples were heated again at 60°C for 30 minutes. For some gels, newt plasma was also prepared for electrophoresis. Newt plasma was collected by decapitation of anesthetized newts and collection of small quantities of blood into citrated amphibian plasma saline containing 10^{-3} M PMSF. The non-coagulated blood was centrifuged at 100,000 x g for 15 minutes and the plasma supernatant was then diluted 1:2 with solubilizing buffer.

Affinity purified Xenopus plasma Fn and human plasma Fn (Gibco), both at a concentration of 0.1 ug protein per µl of solubilizing buffer were also used for SDS-PAGE.

When vertical SDS-PAGE was carried out, a Bio-Rad PROTEAN II slab cell electrophoresis apparatus was used. A 6.5% acrylamide gel (1.5 mm

thickness) was prepared as follows: 7.58 ml of 30 % acrylamide stock solution (29.2 g of acrylamide (Bio-Rad) and 0.8 g of bis-acrylamide (Bio-Rad) dissolved in 100 ml of distilled water), 18.15 ml of distilled water, 8.75 ml of 1.5 M Tris (Schwartz-Mann) pH 8.8, and 350 µl of 10% SDS in distilled water were mixed and degassed under vacuum for 15 minutes. To the acrylamide mixture 175 µl of 10% ammonium persulfate (w/v) (Bio-Rad) in distilled water and 17.5 µl of TEMED (Bio-Rad) were added and the mixture was immediately poured into a gel casting sandwich assembled as described in the Bio-Rad instruction manual. A thin layer of water was gently pipetted onto the monomer solution surface and polymerization took place overnight at room temperature. Following polymerization of the 6.5% separating gel a 4.0% stacking gel was casted on the surface of the separating gel. The 4.0% acrylamide gel was prepared as follows: 2.6 ml of 30% acrylamide stock solution, 12.2 ml of distilled water, 5 ml of 0.5 M Tris pH 6.8, and 200 µl of 10% SDS are mixed and degassed under vacuum for 15 minutes. To the acrylamide mixture 100 µl of 10% ammonium persulfate and 20 µl of TEMED were added and the stacking gel monomer solution was poured onto the polymerized 6.5% stacking gel surface. A sample application comb was inserted during the casting of the stacking gel. Once polymerization was complete (40 to 50 minutes) the comb was removed and the sample wells were rinsed with distilled water and then dried with filter paper.

Samples of human fibronectin (Gibco) and Xenopus fibronectin each in a volume of 20 µl (2 ug of protein), as well as samples of extracts of newt iris and newt skin in a volume of 10 µl, and samples of newt plasma in a volume of 15 µl were loaded into individual wells. An

aqueous Tris-glycine-SDS electrode buffer (25 mM Tris, 192 mM glycine (Schwartz-Mann) and 0.5% SDS (w/v), pH 8.3) was used for electrophoresis (Laemmli, 1970). Electrophoresis of samples through the 4% stacking gel was conducted at a constant current of 25 mAmps and once samples had entered the 6.5% separating gel the current was increased to 35 mAmps. During the 2 hour run the voltage increased from 123 volts to 230 volts. Following electrophoresis the gel was equilibrated in transfer buffer (25 mM Tris, 192 mM glycine, pH 8.3) for 15 to 20 minutes.

For protein blotting a modification of the procedure of Towbin (1979) was used. Electrophoretic transfer of proteins to nitrocellulose (0.22 μm) (Bio-Rad) was carried out using a Bio-Rad Trans-Blot cell apparatus. The gel and nitrocellulose were assembled in a gel holder as described in the Bio-Rad instruction manual. Transfer was performed at a constant voltage of 136 volts and during the 2 hour transfer period the current increased from 0.71 amps to between 1.7 and 1.9 amps. Following transfer the nitrocellulose protein blots were rinsed in distilled water and then stored at -20°C. In some instances electrophoresis of was performed on a Bio-Rad mini PROTEAN™ II slab cell apparatus at a constant voltage of 100 volts. Following electrophoresis the gels were electrophorectically transferred to 0.22 μm nitrocellulose as described above.

The nitrocellulose protein blots were probed with anti-Xenopus fibronectin antiserum or with anti-human fibronectin antiserum (Bethesda Research Laboratories, BRL). To reduce non-specific binding of antibody the protein blots were first incubated overnight in a blocking solution of tris buffered saline (TBS) (20 mM Tris-HCl, pH 7.5, 0.5 M NaCl in

distilled water) containing 3% BSA (Sigma; A-7030) and 0.01% thimerosal (Sigma). The blots were then washed in several changes of TTBS (TBS containing 0.05% TWEEN-20 (v/v); Bio-Rad) followed by exhaustive washing in distilled water. Blots were then incubated for 2 hours in rabbit anti-Xenopus fibronectin antiserum diluted 1:2000 in TTBS containing 1% BSA. In order to further verify the immunospecificity of the anti-Xenopus Fn antiserum obtained in this study, a small sample of antiserum raised to Xenopus plasma Fn, which was generously provided by Dr. R. Hynes (Massachusetts Institute of Technology), was used to probe protein blots of newt iris and newt skin and the immunoreactivity of the two antisera were compared. This antiserum was diluted 1:1000 in TTBS containing 1% BSA and 0.01% thimerosal and the blots were incubated overnight. In some instances, instead of using anti-Xenopus Fn antiserum, the blots were incubated overnight in rabbit anti-human Fn antiserum (BRL) diluted 1:300 in TTBS containing 1% BSA and 0.01% thimerosal. Following incubation in primary antiserum, the blots were washed in TTBS and distilled water as described previously. The blots were then incubated for 1 hour in goat-anti-rabbit immunoglobulin coupled to horse radish peroxidase (Bio-Rad) diluted 1:3000 in TTBS containing 1% BSA. The blots were washed in TTBS and distilled water as described previously, and finally in TBS for 1 hour. All incubation and washing steps were carried out at room temperature with gentle rotation.

Immunostaining of the nitrocellulose blots was performed according to Hawkes et al. (1982). Color development solution was prepared as follows: 60 mg of HRP color development reagent (4-chloro-1-naphthol) (Bio-Rad) was dissolved in 20 ml of ice cold methanol (BDH analytic

grade), to this 100 ml of TBS at room temperature plus 60 µl of hydrogen peroxide (Fisher) were added. The prostetic heme group of peroxidase is oxidized by it's primary substrate, hydrogen peroxide. The 4-chloro-1-naphthol acting as an electron donor, regenerates the enzyme to it's reduced state, and is released as a colored oxidation product allowing immunoreactive antigenic sites on the nitrocellulose protein blot to be visualized (Sternberger, 1986). Color development took place within 3 to 15 minutes and development was arrested by rinsing the blot in several changes of distilled water. Blots were photographed shortly after development. The blot was subsequently stained with amido black (0.1% amido black (w/v) (Eastman) in 45% methanol, 10% acetic acid in distilled water) in order to visualize protein standards and protein bands within the samples which do not react with the primary antiserum. The amido black stained nitrocellulose blot was then photographed again. Estimates of molecular weight of immunoreactive protein bands were made using the standard curve obtained from the protein standards and calculated by linear regression.

6.0 LOCALIZATION OF FIBRONECTIN IN THE DORSAL IRIS DURING LENS REGENERATION BY IMMUNOFLUORESCENCE

6.1 Maintenance and Lentectomy of Newts

Adult newts, Notophthalmus viridescens, were purchased from Lee's Newt Farm, Oak Ridge, Tennessee. The animals were maintained in dechlorinated water at 8°C with weekly feedings. When required for lens regeneration the newts were anaesthetized in 0.05% Tricaine (ethyl m-aminobenzoate methanesulfonic acid; Sigma) and then lentectomized by making a horizontal incision across the cornea and gently squeezing the

eyeball to remove the lens. Following lentectomy the animals were held in dechlorinated water at room temperature with weekly feedings until the desired stage of regeneration. Normal irises were removed from newts maintained in aquaria at 8°C.

6.2 Histological Preparation of Newt Iris Tissue

Adult newts prior to lentectomy (normal condition) or at various times after lentectomy (regenerating condition) were anaesthetized in 0.05% Tricaine. A circumferential incision was made just posterior to the scleral-corneal junction and the anterior portion of the eye was excised intact. The orientation of the ciliary and iris epithelium was maintained by virtue of their normal physical connection to the scleral-corneal tissue. These latter could also be used as reference tissues when examining the histology of the iris tissue and lens regenerates. The excised ocular tissue was placed in amphibian Ringer's solution (0.11 M NaCl, 1.87 mM KCl, 1.08 mM $CaCl_2$, 9.89 mM glucose, 0.406 mM $MgSO_4$ in 0.005 M sodium phosphate, pH 7.6) and adhering neural retina tissue and the lens were removed and discarded. The ocular tissue was fixed using the periodate-lysine-paraformaldehyde (PLP) fixative (0.01 M periodate, 0.075 M lysine, 2% paraformaldehyde (w/v), 0.075 M glucose in 0.037 M sodium phosphate buffer, pH 7.4) described by McLean and Nakane (1974) and modified by Pearse (1980). Tissue was fixed for 3 hours at 4°C and then washed in several changes of 2% sucrose (w/v) in phosphate buffered saline (PBS) (0.145 M NaCl in 0.01 M sodium phosphate buffer, pH 7.4) for 15 minutes. Tissue was then placed in O.C.T. Tissue Tek compound (Canlab) overnight at 4°C. Following infiltration of the tissue with embedding compound, the tissue was placed in plastic

embedding molds containing O.C.T. compound and then frozen at -20°C. Cryostat sections 6 μm in thickness were cut on a Histostat cryotome model 855 (American Optical) at -20°C to -25°C. The tissue sections were melted onto microscope slides. The latter had been previously acid cleaned and coated with a thin film of rubber cement (Lepage's) which provided an adhesive substrate for the cryostat sections. Tissue sections attached to microscope slides were stored in microscope slide boxes at -20°C and immunostaining was usually performed on the following day. Tissue sections were not stored longer than two weeks before immunostaining was carried out.

6.3 Immunofluorescent Staining of Newt Iris Tissue

Iris tissue sections were removed from -20°C storage and hydrated in several changes of phosphate buffered saline (PBS) to remove and dissolve the water soluble O.C.T. embedding compound. Rabbit anti-Xenopus plasma fibronectin (Fn) antiserum, rabbit anti-human plasma fibronectin (Fn) antiserum (Bethesda Research Laboratories) and preimmune rabbit serum were diluted 1:100 with PBS containing 0.5% BSA (Sigma A-7030). Goat anti-rabbit immunoglobulin conjugated with fluorescein isothiocyanate (FITC) (Miles Scientific) was diluted 1:25 with PBS containing 0.5% BSA. Antisera as well as immunoglobulin preparations were always centrifuged at 100,000 x g for 15 minutes immediately prior to use. Following centrifugation the upper two-thirds of supernatant fluid was removed and in the case of anti-Xenopus Fn antiserum the supernatant was diluted 1:10 with 0.5% BSA in PBS giving a final working dilution of 1:1000. The anti-human Fn antiserum supernatant was not diluted further and therefore the final working

dilution was 1:100. The FITC conjugated anti-rabbit IgG supernatant was diluted 1:2 with 0.5% BSA in PBS giving a final working dilution of 1:50. Control sera were subjected to the same manipulations and used at the same dilutions as the antisera. In every experiment in which tissue sections were immunostained with a specific antiserum, sister sections were stained with control serum.

Microscope slides were placed horizontally inside a humid chamber. Antiserum preparations consisted of anti-Xenopus Fn antiserum (diluted 1:1000) and anti-human Fn antiserum (diluted 1:100). Corresponding negative controls consisted of preimmune rabbit serum (diluted 1:1000 and 1:100). These preparations were pipetted onto the upper surface of individual microscope slides and 0.5 to 1.0 ml of solution was sufficient to completely cover the 15 to 20 iris tissue sections per slide. Iris tissue sections were incubated for 2 hours at room temperature. Following incubation in control serum or primary antiserum, the iris tissue sections were rinsed briefly in distilled water, washed in cold PBS with gentle shaking for 10 minutes and finally rinsed briefly in distilled water. The slides were returned to the humid chamber and FITC conjugated anti-rabbit IgG (diluted 1:50) was pipetted onto the iris tissue sections and incubated for 20 minutes at room temperature. Following incubation with the second antibody, the slides were washed as described above. To quench some of the autofluorescence of the stromal iridiophores and iris tissue the slides were then submerged in 0.01% Evan's Blue (Sigma) in distilled water for 1 minute and then washed in distilled water on a rotating shaker for 10 minutes. Finally the iris tissue sections were mounted in DABCO

mounting medium (2.5% DABCO (1.4-Diazabicyclo (2,2,2) octane (Sigma), 90% glycerol in PBS) (Johnson et al., 1982).

The fluorescence staining pattern was observed with a Zeiss photomicroscope III adapted for epi-fluorescence and phase contrast optics. A standard fluorescein filter set (Zeiss #487709) consisted of an excitor pass band filter of 450-490 nm and a barrier longwave pass band filter of 520 nm. Photographs were taken on Kodak Ektachrome 200 ASA slide film with the ASA setting of the camera being pushed to 400 ASA or 800 ASA.

RESULTS

1. ISOLATION OF *XENOPUS* PLASMA FIBRONECTIN

The total yield of non-coagulated blood from 13 specimens of *Xenopus laevis* was 30 ml (i.e. 25 ml blood plus 5 ml of citrated amphibian plasma saline). After centrifugation, the final volume of *Xenopus* plasma decreased to 22 ml. The citrated plasma was passed through a column of Sepharose 4B to remove any proteins which could interact non-specifically with the Sepharose polymer. The absorbance at 280 nm of column outflow was monitored and recorded on a print out. Figure 5A is a scaled illustration of the actual printout and shows the elution profile of the citrated plasma filtered through Sepharose 4B. Tubes 4 through 12 had an increased absorbance at 280 nm. These tubes, each containing 5 ml, were pooled giving a total volume of 45 ml of Sepharose pre-absorbed citrated plasma. The pre-absorbed plasma sample was then passed over a gelatin-Sepharose 4B affinity column (Pharmacia) in order to selectively absorb the plasma fibronectin via it's collagen-binding site to the gelatin-Sepharose. The absorbance of column outflow can be seen in Figure 5B. After addition of the NaBr-NaAcetate eluent buffer the fibronectin bound to the affinity column eluted as a single peak in tubes 25 and 26, giving a total volume of 10 ml of eluted Fn sample. The sample of plasma Fn was dialyzed against elution buffer and it's volume increased to 12 ml. The protein concentration of this sample was estimated to be 9.75 μg/ml, giving a total protein yield of 1.17 mg of *Xenopus* plasma fibronectin. The 12 ml sample of Fn in elution buffer was dialyzed against mammalian PBS and then concentrated

Figure 5.

A. Preabsorption of Xenopus plasma on a Sepharose 4B column. Fractions contained in tubes 4 through 12 were pooled and contain Xenopus plasma in which the proteins that interact non-specifically with Sepharose have been removed.

B. Affinity chromatography of Xenopus plasma fibronectin. After addition of the eluent buffer with NaBr-NaAcetate a peak with an increased absorption at 280 nm is observed in tubes 25 and 26. This peak corresponds to the eluted fibronectin.

100
50
0
Tube Number
12
13
14
15
Elution Buffer
Xenopus Plasma sample
1
2
3
A
Absorbance at 280nm

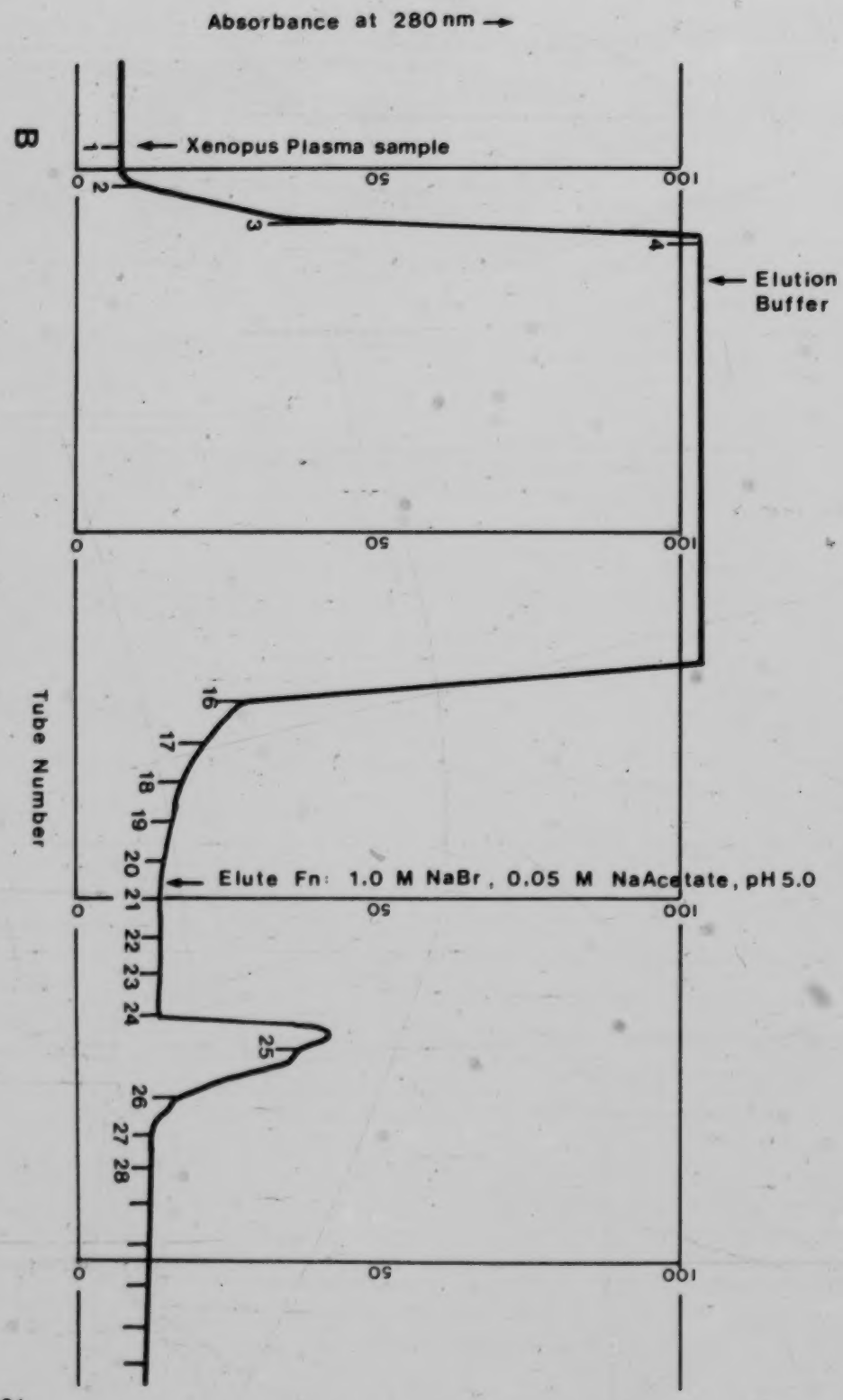
Absorbance at 280 nm
B
Xenopus Plasma sample
Elution Buffer
Tube Number
Elute Fn: 1.0 M NaBr, 0.05 M NaAcetate, pH 5.0
0
50
100
1
2
3
4
16
17
18
19
20
21
22
23
24
25
26
27
28

on a polyethylene glycol bed to a final volume of 2 ml. The protein concentration of the 2 ml sample was estimated to be 344 μg/ml, giving a total protein yield of 0.688 mg of Xenopus plasma fibronectin. From these determinations of protein concentration it appears that not all of the eluted fibronectin is recovered after dialysis steps; this could probably be due to adsorption of fibronectin to the dialysis membrane.

The affinity purified Xenopus plasma fibronectin was examined by SDS-PAGE under reducing conditions. When polyacrylamide gels were double-stained with silver and coomassie blue (Figure 6A) or with coomassie blue (Figure 6B), three protein bands were observed in the affinity purified Xenopus plasma fibronectin sample. The molecular weights of these bands based on linear regression analysis of Bio-Rad protein standards were estimated to be 199,000 ± 11,000 (mean ± SE), 92,000 ± 3000, and 31,000 ± 4000. Other investigators have reported that plasma fibronectin isolated from Xenopus blood shows a doublet on SDS-PAGE which approximately comigrates with fibronectins purified from hamster cells or human plasma (Heasman et al., 1981); these latter range in molecular weight from 215,000 to 220,000 daltons (Yamada, 1981). Plasma fibronectin isolated from the amphibian, Pleurodeles waltlii, shows a doublet on SDS polyacrylamide gels with an approximate molecular weight of 220,000 (Boucaut and Darribere, 1983). Since, in the present experiments the affinity purified Fn gave rise to three protein bands of lower molecular weight, it is possible that proteolysis of Fn took place during collection of the plasma. This is a common problem that occurs during the isolation of fibronectin from plasma (Ruoslahti et al., 1982b and Hynes, 1985b).

Figure 6. SDS-PAGE analysis of affinity purified *Xenopus* plasma fibronectin sample.

A. A polyacrylamide gel double stained with silver and coomassie blue.

B. A polyacrylamide gel stained with coomassie blue.

In these two gels three main protein bands can be identified (indicated by arrows) in the affinity purified Fn sample. As based on linear regression analysis of Bio-Rad protein standard mobilities, the molecular weight estimates of the protein bands in the affinity purified Fn sample are; 199,000 ± 11,000 (mean ± SE), 92,000 ± 3000, and 31,000 ± 4000.

The molecular weights of the standards are shown to the left as follows: 1 = Myosin 200,000, 2 = B-Galactosidase 116,250, 3 = Phosphorylase B 92,500, 4 = BSA 66,200 and 5 = Ovalbumin 45,000. The uneven vertical line in gel A is due to breakage of the gel during staining.

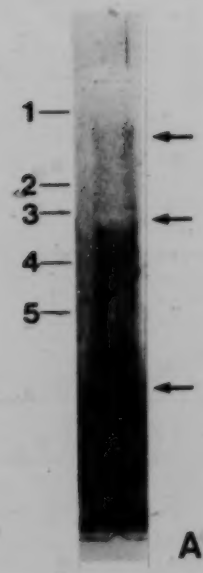
1
2
3
4
5
A

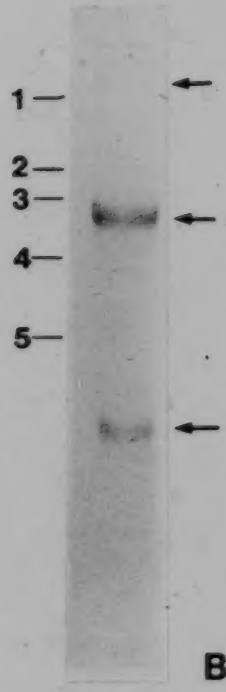
1
2
3
4
5
B

Analysis of mammalian fibronectins has shown that each polypeptide monomer contains a series of protease-sensitive regions (Ruoslahti et al., 1982a). Mammalian plasma fibronectin is highly susceptible to proteolysis and is cleaved by plasmin to yield cleavage products, which, when analyzed by SDS-PAGE range in molecular weight from 190,000 to 27,000 daltons (Jilek and Hormann, 1977). With limited plasmin digestion of Fn only three protein bands are identified; 200,000, 190,000 and 30,000 of which only the higher molecular weight fragments possess collagen-binding activity (Balian et al., 1979). When fibronectin is cleaved by different proteolytic enzymes, fragments of this molecule are generated which retain collagen-binding activity; these fragments vary in size. Thermolysin generates a 40,000 dalton collagen-binding fragment (Sekiguchi and Hakomori, 1980). Cathepsin D yields a 72,000 dalton collagen-binding fragment and subsequent plasmin digestion of this fragment gives rise to a 42,000 dalton collagen-binding fragment (Balin et al., 1979). Trypsin digestion of Fn generates collagen-binding fragments of 70,000 and 30,000 daltons (Ruoslahti et al., 1979).

In light of these findings it is probable that the three protein bands evident in the affinity-purified Fn sample represent cleavage products of Fn that retain the collagen binding site. This indicates that the isolation conditions used in this study (i.e. collecting blood dropwise into citrated saline containing 10^{-4} M PMSF as protease inhibitor did not completely inhibit proteolytic cleavage of fibronectin by the plasma proteases present in the Xenopus blood. Cleavage products of fibronectin of low molecular weight are also present in preparations

of affinity purified fibronectin reported from another laboratory (Lee et al., 1984).

2. IMMUNOBLOT ANALYSIS

Having obtained an antiserum against the preparation of Xenopus fibronectin it was important to determine the components in tissue extracts to which the antiserum reacted. For this purpose tissue extracts were prepared from newt iris and eyelid skin tissues and subjected to SDS-PAGE, then transferred to nitrocellulose, and subjected to immunoblot analysis as described in the materials and methods.

Results from the immunoblotting experiments revealed that antiserum raised against the affinity purified Xenopus plasma fibronectin sample reacted with four protein bands in extracts of newt iris and skin (Figure 7A). As determined from three separate immunoblots of newt iris tissue proteins, the antiserum reacted with 4 bands of approximate molecular weights of 232,000 ± 6000 (mean ± SE), 220,000 ± 6000, 186,000 ± 2600 and 144,000 ± 400. Extracts from newt eyelid when reacted with the antiserum gave rise to 4 protein bands of approximate molecular weight of 240,000 ± 9000, 224,000 ± 10,500, 187,000 ± 2500 and 143,000 ± 3000. In these samples two higher molecular weight bands approximately fall into the molecular weight range reported for cellular fibronectin, which is 220 to 240 Kd (Yamada, 1981). When analyzed by SDS-PAGE, plasma fibronectin isolated from the amphibian, Pleurodeles waltlii, shows a doublet with a reported molecular weight equal to 220,000 (Boucaut and Darribere, 1983). It is probable that in the experiments reported here, the bands of lower molecular weight represent proteolytic

Figure 7A.

Nitrocellulose protein blots of solubilized proteins from newt iris tissue (I) and newt eyelid tissue (E) were probed with antiserum raised to the affinity purified Xenopus plasma fibronectin. Four immunoreactive protein bands (indicated by arrows) were detected in each of the newt tissue samples.

Amido black staining of the immunoblot revealed Bio-Rad protein standards (S). The molecular weights of the Bio-Rad proteins are indicated. In each newt tissue sample protein bands not reactive with the antiserum are stained with Amido black. Based on linear regression analysis of the Bio-Rad protein standard mobilities, the molecular weight estimates of immunoreactive protein bands were determined for three separate immunoblots. For the iris tissue sample immunoreactive protein bands were an estimated molecular weight of, 232,000 $\pm$ 6000 (mean $\pm$ SE), 220,000 $\pm$ 6000, 186,000 $\pm$ 2600 and 144,000 $\pm$ 400. And for the eyelid tissue sample, 240,000 $\pm$ 9000, 224,000 $\pm$ 10,500, 187,000 $\pm$ 2500 and 143,000 $\pm$ 3000.

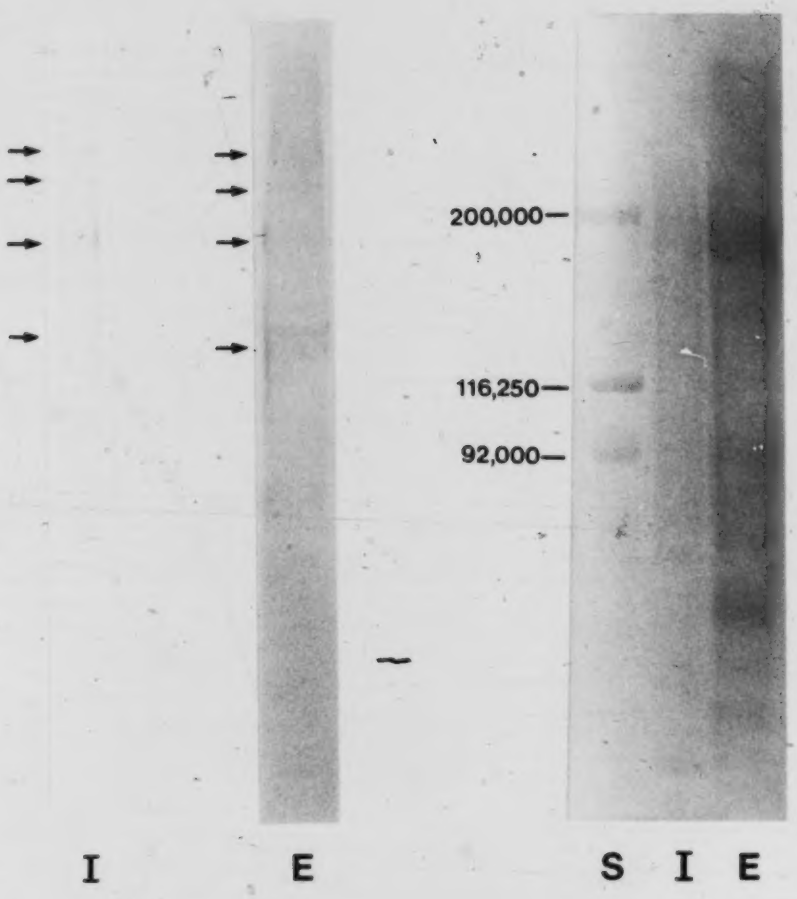

7A.

fragments of fibronectin. Fibronectin is very sensitive to proteases and because a protease inhibitor was not present during the dissection and collection of these tissues, it is possible that endogenous protease activity within the tissue resulted in cleavage at specific, highly protease-sensitive regions of the fibronectin molecule. To verify that our antiserum reacted with fibronectin, a sample of antiserum raised to Xenopus plasma fibronectin, which was generously provided by Dr. R. Hynes, was used to probe protein blots of newt tissue samples. This antiserum reportedly reacts specifically with Xenopus plasma or cellular fibronectin, but has lower reactivity with mammalian fibronectins (Heasman et al., 1981). This antiserum when reacted against protein blots of newt iris or newt eyelid skin also gave rise to four protein bands (Figure 7B) which approximately correspond in molecular weight to the protein bands recognized by the anti-Xenopus Fn antiserum used in these studies (see Figure 7A). Taken from a single immunoblotting experiment, the molecular weight estimates of protein bands reactive with the antiserum obtained from Dr. Hynes were approximately 249,000, 235,000, 192,000 and 145,000 for solubilized newt iris tissue proteins. And for newt eyelid tissue reactive protein bands were an approximate molecular weight of 240,000, 224,000, 187,000 and 143,000.

When protein blots prepared from commercial human fibronectin were reacted with our anti-Xenopus Fn antiserum under the same conditions used for protein blots of newt tissue proteins, no protein bands were detected. This indicates that the antiserum used in this study had little to no affinity to human fibronectin.

Figure 7B.

An immunoblot which was a replicate of that presented in Figure 7A (i.e. a protein blot prepared from the same SDS polyacrylamide gel) was reacted with the anti-Xenopus Fn antiserum obtained from Dr. R. Hynes. Solubilized protein from newt iris (I) and newt eyelid tissue (E) showed 4 immunoreactive protein bands (indicated by arrows), which approximately correspond in molecular weight to the 4 immunoreactive protein bands detected by the anti-Xenopus Fn antiserum used in this study (see Figure 7A).

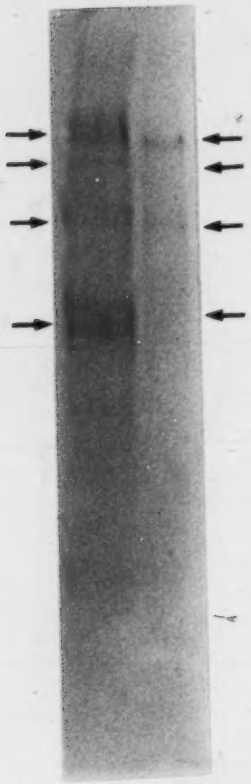

7B.

Commercial anti-human Fn antiserum could react with bands on blots of newt tissue extracts. However the antiserum had to be prepared at higher concentrations than that used for the anti-Xenopus Fn antiserum (i.e. a 1:300 dilution as compared to 1:2000 dilution for anti-Xenopus Fn antiserum). And further the incubation time was longer for the anti-human Fn antiserum (16 h compared to 2h for anti-Xenopus Fn antiserum). Under these conditions a single immunoreactive protein band of estimated molecular weight 230,000 was observed in protein blots of solubilized newt plasma proteins (see Figure 8A). The iris tissue immunoblot showed several immunoreactive protein bands (see Figure 8B). Immunoreactivity, as detected by staining intensity, was highest at a band of estimated molecular weight 198,000. Two protein bands of estimated molecular weights of 105,000 and 61,000 reacted faintly with this antiserum. The reaction at the two lower molecular weight bands also suggests that proteolytic cleavage of fibronectin takes place during the preparation of newt iris tissue samples. Relative to the anti-Xenopus Fn antiserum the anti-human Fn antiserum is less reactive with newt fibronectin. As a consequence this antiserum was not as sensitive a probe to detect changes in the fibronectin distribution in the newt iris during lens regeneration. This is supported by results presented later in this thesis.

3. IMMUNOFLUORESCENT LOCALIZATION OF FIBRONECTIN WITHIN THE NORMAL AND LENS REGENERATING NEWT IRIS

Following lentectomy the newt iris epithelium undergoes a sequence of cellular events that ultimately result in the regeneration of a new

Figure 8.

A. Immunoblots of solubilized newt plasma protein (NP) were probed with commercial anti-human plasma fibronectin antiserum. Based on linear regression analysis of amido black stained Bio-Rad protein standards (S) mobilities, the molecular weight of the single immunoreactive protein band (indicated by arrow) was estimated to be 230,000. Amido black staining of the immunoblot (AB-NP) reveals protein bands which do not react with the antiserum.

B. Immunoblots of solubilized newt iris tissue protein (I) was probed with commercial anti-human plasma Fn antiserum. Based on linear regression analysis of amido black stained Bio-Rad protein standard (S) mobilities, the molecular weight of the main immunoreactive protein band was estimated to be 198,000. Other bands of molecular weights 105,000 and 61,000 also reacted with this antiserum. Amido black staining of the immunoblot (AB-I) reveals protein bands which do not react with the antiserum.

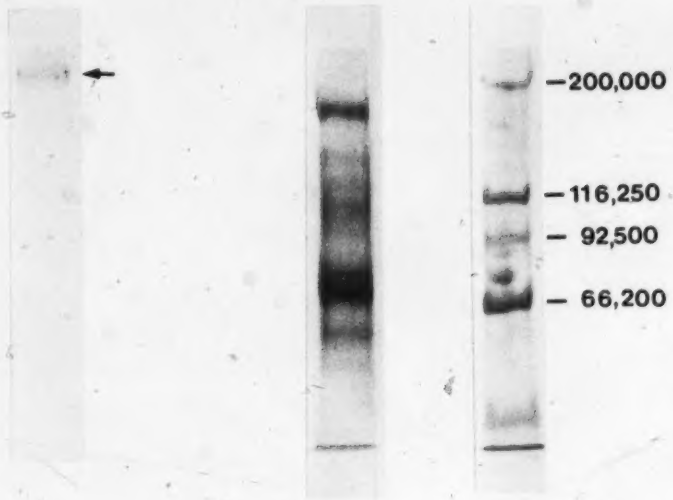
200,000
116,250
92,500
66,200
NP
AB-NP
S

8A.

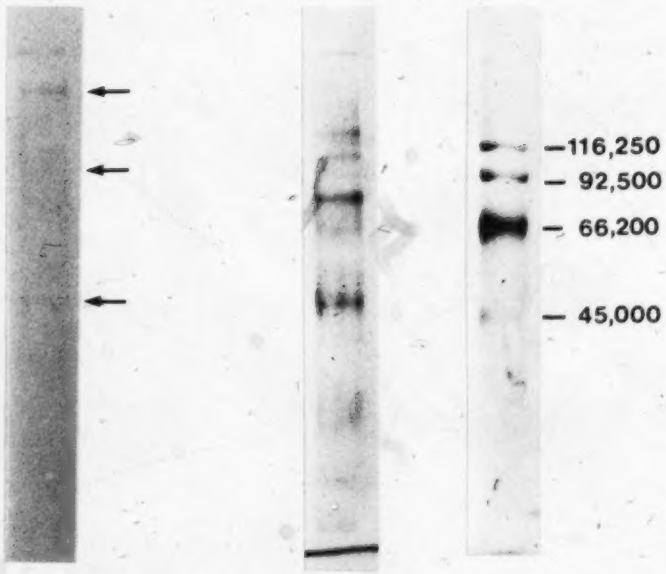
116,250
92,500
66,200
45,000
I
AB-I
S

8B.

lens. The rate at which these events proceed is dependent on various environmental factors. Yamada (1977) established a staging system which correlates morphological stages described by Sato (1940) for lens regeneration in Triturus pyrrhogaster to "days after lentectomy" for Notophthalmus viridescens reared at 21°C under conditions of optimal feeding and constant illumination. Relative to the time course proposed by Yamada, the rate of lens regeneration for the newt population used in this study was somewhat slower, especially during the later stages (V-X) when growth and differentiation of the lens vesicle occurs. In this study lentectomized newts were reared at room temperature with weekly feedings. Illumination was not continuous, and during the winter months the animals would have been exposed to a day length cycle of 7-8 hours. This shorter illumination period may account for the slower rate of lens regeneration. It has been shown that lens regeneration can be greatly retarded by keeping the newt post-operatively in total darkness (Borsuk and Popov, 1968; as cited by Reyer, 1977). Regardless of rate, lens regeneration within this newt population did take place via the ordered progression of morphological and cellular events associated with IEC dedifferentiation and lens fiber redifferentiation.

The staging system proposed by Sato (1940) and adapted by Yamada (1977) divides the process of lens regeneration into ten distinct stages. Because successive stages are not actually discrete from one another and considerable overlap between stages exists, I have organized my results into three broad categories. Stage 0 represents the normal condition of the iris. Stage I through III represent mostly pigmented iris cells engaged in activation and progressive dedifferentiation. In

stages IV through X, regenerates represent cell populations involved in redifferentiation; some of these cells follow the retrieval pathway into pigmented IECs, while other cells located mainly at the dorsal iris margin undergo differentiation into lens fibers. Lens fiber redifferentiation includes the establishment, growth and maturation of the lens vesicle.

A series of experiments were conducted to determine the conditions under which maximal antigenic reactivity could be maintained in the iris tissue sections associated with a minimum level of non-specific staining. Irises were subjected to a variety of fixation procedures in combination with different embedding techniques, and in each of these cases parallel sections were stained with control non-immune serum. It was found that similar results were obtained when tissues were fixed with alcohol or with paraformaldehyde-lysine-periodate (McLean and Nakane, 1974). Since PLP fixation provided a better preservation of tissue morphology, this was the fixative of choice. In addition, a better immunoreactivity was found in tissues frozen in O.C.T. immediately after fixation, as compared with those subjected to paraffin embedding (Sainte-Marie, 1961). Therefore, most experiments and observations were performed in cryostat sections of irises embedded in O.C.T. Most of the observations reported here were done on median saggital sections of irises or regenerates.

Initially immunofluorescent labeling of Fn was performed with a commercial antiserum against human plasma fibronectin. This was done because several studies had employed antiserum raised to mammalian fibronectins in order to study fibronectin distribution in the

regenerating newt limb of Notophthalmus viridescens (Repesh et al., 1981, Repesh et al., 1982 and Gulati et al., 1983). Although even in these studies it was found that plasma fibronectin isolated from the mud puppy, a close phylogenetic relative of the newt, showed a lower cross-reactivity with antibody to human fibronectin when compared to fibronectin from human plasma (Repesh et al., 1981). Further, antiserum raised to Xenopus plasma fibronectin shows a low immunoreactivity with mammalian fibronectins (Heasman et al., 1981). These results suggested that immunological cross-reactivity between mammalian and amphibian fibronectins is weak. Since there was a concern that antiserum raised to human fibronectin may not be a sensitive enough probe to detect changes in newt fibronectin within the iris during lens regeneration, it was decided to obtain antibodies against Xenopus fibronectin. As shown by immunoblotting experiments or immunofluorescent labeling of Fn in iris tissue sections, the antiserum raised to Xenopus Fn was significantly more reactive with newt Fn when compared with antiserum raised to human Fn. Therefore the majority of the results presented in the body of this thesis represent those obtained using, as a probe, anti-Xenopus Fn antiserum. Some of the results obtained with anti-human Fn antiserum are reported at the end of this section.

An indirect immunofluorescent labeling technique was employed to examine Fn distribution within the newt iris. To demonstrate that immunofluorescent labeling of iris tissue Fn was immunospecific, controls, in which the primary antiserum was replaced with preimmune rabbit serum at dilutions equal to that of the primary antiserum, were

carried out in each experiment. Control sections did
immunofluorescent staining of iris or stromal tissues (see Figu

3.1 Anti-Xenopus Fibronectin Antiserum

3.1.a Stage 0: Normal Iris Epithelium

The iris is composed of an external and internal epitheli
is continuous at the pupillary margin, and the epithelia are
apposed to one another along their apical surfaces. The basa
of the external and internal epitheli face the stroma and
chamber respectively. Ultrastructurally, the pigmented, cubo
epithelial cells (IECs) have been reported to be tightly appos
their lateral cell surfaces while at the basal cell surface they
a basal lamina (Karasaki, 1964).

Figures 10 and 11 show representative sections of the norma
iris. In figure 10 Fn staining is observed at the basal surfac
internal and pupillary iris epithelium. Presumably this repre
located with the matrix of the basal lamina. Although not il
in figure 10 or 11 Fn staining at the basal cell surface
underpigmented, internal ciliary epithelium is significant
pronounced and appears more diffuse relative to Fn staining at t
surface of the internal iris epithelium. At the pupillary margi
iris as well as the internal epithelium, Fn appears to also be l
intracellularly. Within the stroma the connective tissue
basement membranes of the capillary endothelium show int
staining. The basal surface of the external iris epitheliu
contact with an acellular layer which is distinguishable from t

Figure 9. Control: Dorsal iris of stage II regenerate

Antiserum (anti-Xenopus Fn antiserum) was replaced with preimmune serum diluted 1:2000 with 0.5% BSA in PBS. No fibronectin (Fn) staining is detected in the iris or stromal tissues. Nuclei and stroma are stained a dull yellow which is apparently due to the Evan's Blue counterstaining. This yellow fluorescence was not due to autofluorescence because unstained sections did not appear yellow under the fluorescence microscope. (Bar = 25 um) Note: The corresponding phase contrast micrograph is shown below the fluorescent micrograph.

THE QUALITY OF THIS MICROFICHE IS HEAVILY DEPENDENT UPON THE QUALITY OF THE THESIS SUBMITTED FOR MICROFILMING.

UNFORTUNATELY THE COLOURED ILLUSTRATIONS OF THIS THESIS CAN ONLY YIELD DIFFERENT TONES OF GREY.

LA QUALITE DE CETTE MICROFICHE DEPEND GRANDEMENT DE LA QUALITE DE LA THESES SOUMISE AU MICROFILMAGE.

MALHEUREUSEMENT, LES DIFFERENTES ILLUSTRATIONS EN COULEURS DE CETTE THESES NE PEUVENT DONNER QUE DES TEINTES DE GRIS.

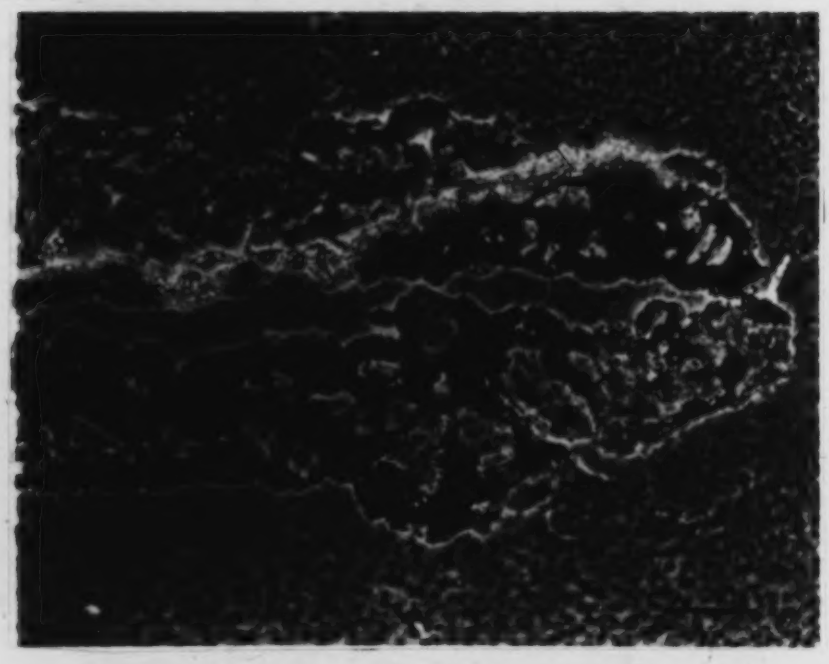

Figure 10. Stage 0: Normal dorsal iris

The external stroma (S) stains intensely for fibronectin. The external pigmented iris epithelium (EIE) is in direct contact with the stromal tissue and faces the aqueous humour. The internal pigmented iris epithelium (IIE) faces the posterior chamber and at the pupillary margin the continuous iris epithelium faces the lens (removed in this section). In the internal iris epithelium (IIE) fibronectin (Fn) immunostaining is localized in the basal lamina (arrow) and is also observed intracellularly. (Bar = 50 um) Note: The corresponding phase contrast micrograph is shown below the fluorescent micrograph.

EIE
S
IIE

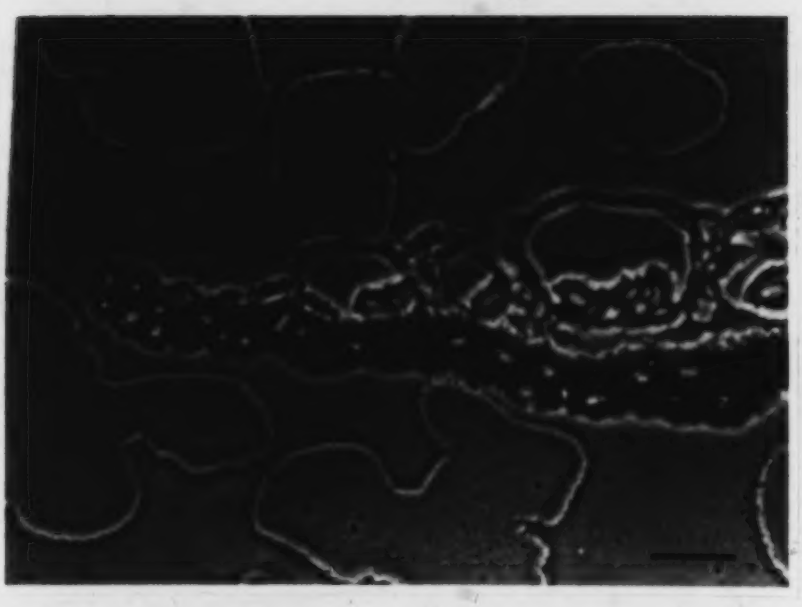

Figure 11. Stage 0: Normal dorsal iris

Fibronectin immunostaining of the basal lamina of the external iris epithelium is observed (arrow). The stroma band (SB with arrow) is counterstained a dull-orange color and Fn immunostaining is less intense within the SB, compared to the intense Fn staining observed in the stroma (S with arrow) connective tissue. Although Fn staining is evident in the basal lamina of the internal iris epithelium, it is not is clear focus in this photograph (* with arrow). (Bar = 10 um) Note: The corresponding phase contrast micrograph is shown below the fluorescent micrograph.

S
SB
*

connective tissue of the stroma by virtue of it's more compact appearance (see Figure 11). This layer is herein referred to as the "stroma band". In the normal iris the stroma band shows Fn staining which varies in intensity between individual specimens. Variations in staining intensity of the stroma band was also observed between regenerates at the same stage. Immunofluorescent staining within the stroma band often obscures the Fn staining of the basal lamina of the external epithelium. Figure 11 shows a higher magnification of a normal dorsal iris and illustrates Fn staining of the basal lamina of the external iris epithelium. The stroma band in this iris does not exhibit significant Fn staining, but rather appears a dull orange color, probably due to the Evan's blue counter-stain.

With regards to their morphology and pattern of Fn staining the normal dorsal and ventral regions of the iris exhibit a great deal of similarity. However the stroma band of the ventral iris appears to be relatively wider than the stroma band associated with the dorsal iris. Measurements made from eleven individual normal irises gives an average width of the stroma of 5 um and 10 um for the dorsal and ventral irises respectively.

3.1.b Stages I through III: Iris Epithelial Cell Dedifferentiation

The activation of iris epithelial cells and the initiation of DNA synthesis in stage I is accompanied by a significant increase in nuclear volume. As revealed by the electron microscope, apical cell contact between the external and internal epithelium decreases (Dumont and Yamada, 1972). However the separation is not distinguishable at the light microscope level, but Fn staining is occasionally observed at the

apposing apical interface. Figure 12 represents a stage I (5 day) regenerate. Fibronectin staining is observed at the apical and lateral cell surfaces of the activated, cuboidal iris epithelial cells. Note also the intense cell surface staining of two IECs. Examination of this section under phase contrast (Figure 12) suggests that both of these cells are slightly above the plane of the section. Perhaps these two cells were dislodged out of the epithelial framework, as a result of localized stress and fracturing along cell boundaries within the epithelium during cryostat sectioning. Therefore these two cells would have a relatively large cell surface area available to the antibody and Fn staining would be very intense. While cells in the plane of the section remain within the epithelial framework and therefore relatively less of the cell surface is represented and Fn staining is of lower intensity.

During stage II and III activated IECs at the pupillary margin and internal epithelium are observed to undergo morphological changes that are associated with the process of dedifferentiation. Cells increase in size and become elongated along their apicobasal axis. At the lateral and apical surfaces of IECs contact decreases and intercellular spaces progressively increase. The process of depigmentation is accomplished by the discharge of melanosome complexes, which are phagocytized by infiltrating macrophages. Mitotic proliferation is most prominent at the pupillary margin and eventually small, depigmented cell comprise the pupillary margin of the dorsal iris (Karasaki, 1964; Dumont and Yamada, 1972).

Figure 12. Stage I Regenerate: Dorsal iris (5 days post-lentectomy)

An increase in the nuclear volume of the pigmented iris epithelial cells is evident. The nuclei (0 with arrow) are counterstained a dull-orange color. Fibronectin is now evident at the apical interface between internal and external iris epithelium (* with arrow). Fibronectin is now also localized at the lateral surfaces of some iris cells (arrow). The basal surface of the internal iris epithelium, not in clear focus in this photograph, also stains for Fn. At the pupillary margin two IECs which appear to be above the plane of focus are observed to display intense Fn staining at their surfaces. (Bar = 25 um) Note: The corresponding phase contrast micrograph is shown below the fluorescent micrograph.

Figure 13 shows two representative stage II regenerates. The Fn distribution observed in these regenerates is typical of the iris during the early stages of dedifferentiation. Fibronectin staining is conspicuous at the lateral cell boundaries of elongated IECs, and in some cells apical staining is also evident. IECs of the external epithelium remain cuboidal and lateral staining is not observed. Fibronectin staining is observed at the basal cell surface of cells located at the external and internal epithelial layers of the pupillary margin. The basal lamina, observed to be present at the basal cell surface in electron microscope studies, can not be resolved within the limits of resolution of the light or fluorescence microscope used here. However it is presumed that at least a portion of the Fn staining observed at the basal cell surface corresponds to Fn located within the basal lamina. Note that in both these stage II regenerates Fn staining at the basal cell surface appears to be thicker relative to the observable staining at the basal cell surface of the normal iris epithelium. Although not substantiated by quantitative measurements it is this author's impression that in the majority of the stage II to III regenerates examined, staining at the basal surface of the pupillary margin and internal epithelium of the iris is thicker relative to the normal, stage 0, iris.

Figures 14 through 16 represent different regenerates at stage III and illustrate the salient features of the dedifferentiating iris epithelium. Cells which are presumed to be macrophages can be identified within the stroma and at the basal surface of the internal iris epithelium (Figure 14). With progressive apical separation of the

Figure 13. Stage II Regenerates: A = Dorsal iris, B = Ventral iris (Both specimens are 10 days post-lentectomy)

Cells at the pupillary margin and internal iris epithelium have increased in size and apicobasal cell elongation is evident. Fn staining is observed at the lateral surfaces of elongated iris epithelial cell (arrow), and in some cells apical staining is observed (* with arrow). Fn staining of the basal lamina is observed at the pupillary margin. The basal lamina (BL) of the internal iris epithelium stains intensely for Fn and relative to the normal epithelium, basal staining appears to be thicker and more diffuse. The activation events appear to be similar in dorsal and ventral regions of the iris. In the dorsal iris the stroma (S) appears reduced. (Bar = 25 um) Note: The corresponding phase contrast micrographs are shown below each fluorescent micrograph.

A
S
BL

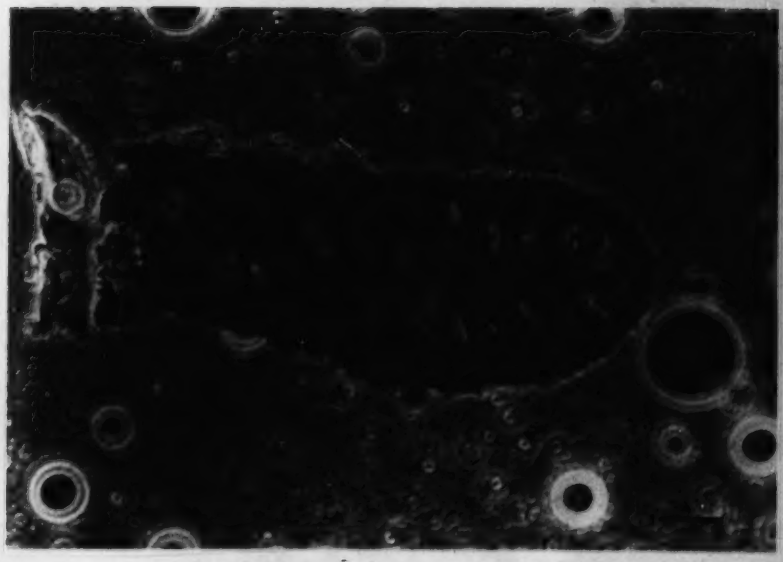

B
S
BL

Figure 14. Stage III Regenerate: Dorsal iris (15 days post-lentectomy)

This figure illustrates a photograph in which the internal epithelium proximal to the pupillary margin is in clear focus. At the pupillary margin, although slightly out of focus, Fn staining of the basal lamina is present. Macrophages (M with arrow), identified by their round cell shape and intense Fn staining of the cell surface are present within the stroma and within the epithelial framework of the internal iris epithelium. Iris epithelial cells adjacent to the interdigitated macrophages have their nuclei positioned in the apical region of the cell and Fn immunostaining of the attenuated baso-lateral cell surface is observed (arrow). Note that the stroma band (SB) has detached from the external epithelium. (Bar = 25 um) Note: The corresponding phase contrast micrograph is shown below the fluorescent micrograph.

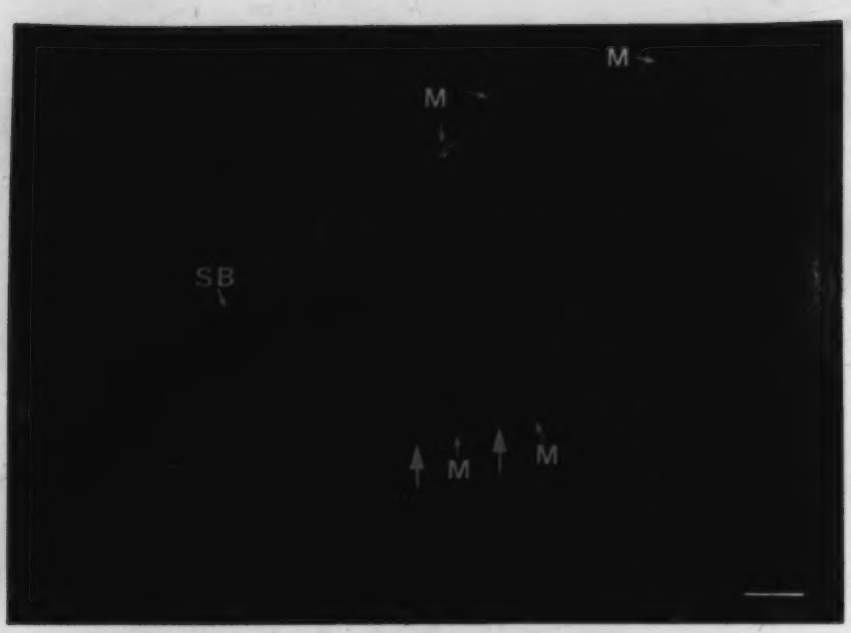
M
M
SB
M
M

Figure 15. Stage III Regenerate: Dorsal iris (15 days post-lentectomy)

With cell division at the pupillary margin of the dorsal iris, the epithelium is no longer a single cell layer, but consists of small depigmenting IECs. Several completely depigmented IECs show intense, homogeneous Fn immunostaining of their cell surface (* with arrow) Partially depigmented IECs display Fn staining at the basolateral cell surface (arrow). A macrophage (M) is observed between the external and internal epithelia. Note that although the stroma (S) is present the stroma band at the pupillary margin is greatly reduced relative to the normal iris. (Bar = 25 um) Note: The corresponding phase contrast micrograph is shown below the fluorescent micrograph.

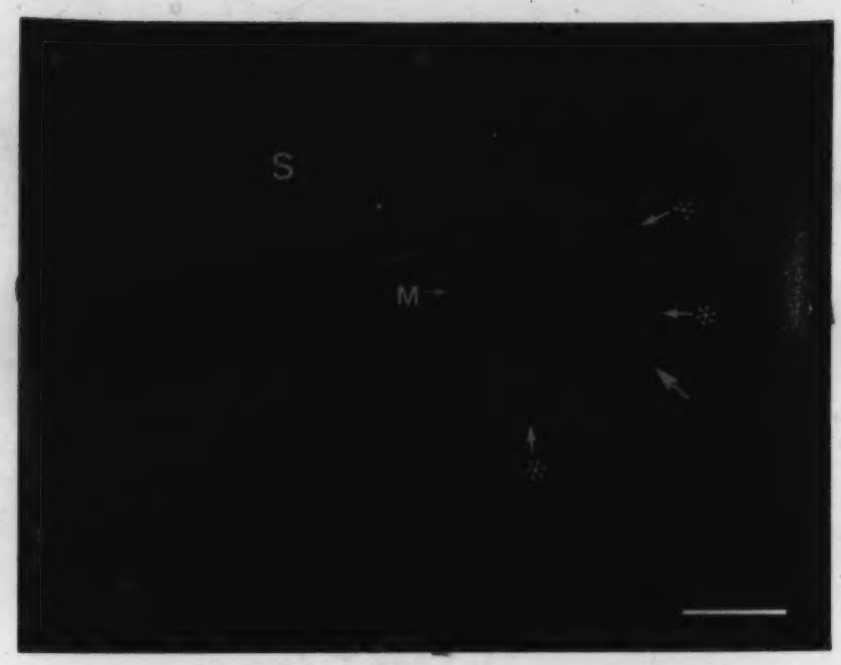
S
M

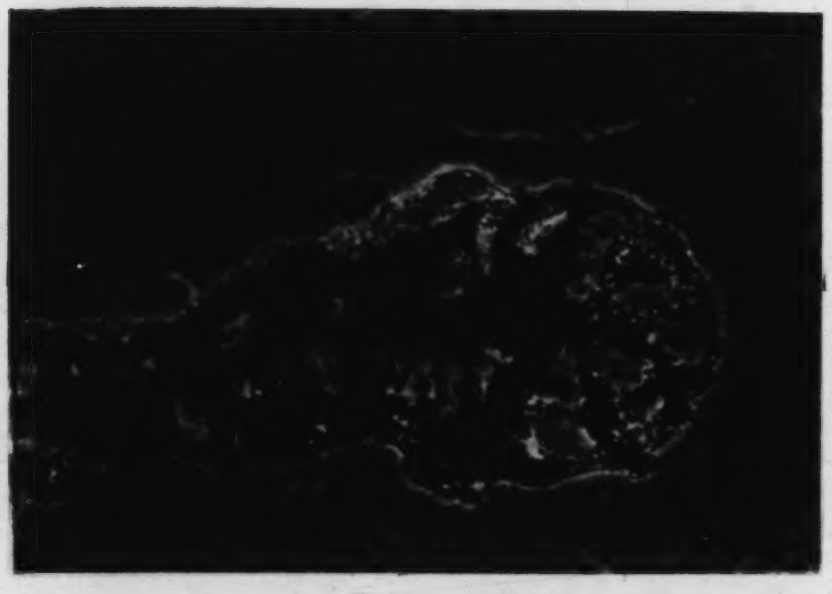

Figure 16. Late Stage III Regenerates: A= Dorsal iris, B = Dorsal iris (Both specimens are 18 days post-lentectomy)

The pupillary margin in both these regenerates consists of small depigmenting IECs which display a random distribution of Fn staining at their cell surfaces. At the pupillary margin separation of external and internal epithelia is observed and Fn staining is evident at the apical cell surface (* with arrow) In photograph A, a cell presumed to be a macrophage (M) is observed within the interlaminar space. Proximal to the pupillary margin the internal epithelium shows reticulate Fn staining of the convoluted basolateral cell surfaces of IECs (arrow). In photograph A, portions of the basal lamina of the internal epithelium are relatively thick and possess intense Fn staining (BL with arrow). Note in photograph A that Fn staining material which adheres to the internal epithelium and pupillary margin (D with arrow) is debris probably derived from the vitreous humour matrix. In the phase contrast picture of photograph B stroma band material is indicated (SB with arrow). Note that cells (P with arrow) in contact with the stroma are not completely depigmented. While adjacent cells (DP with arrow) which do not contact stroma band material are completely depigmented. (Bar = 25 um) Note: The corresponding phase contrast micrographs are shown below each fluorescent micrograph.

A
D
M
BL
BL
D

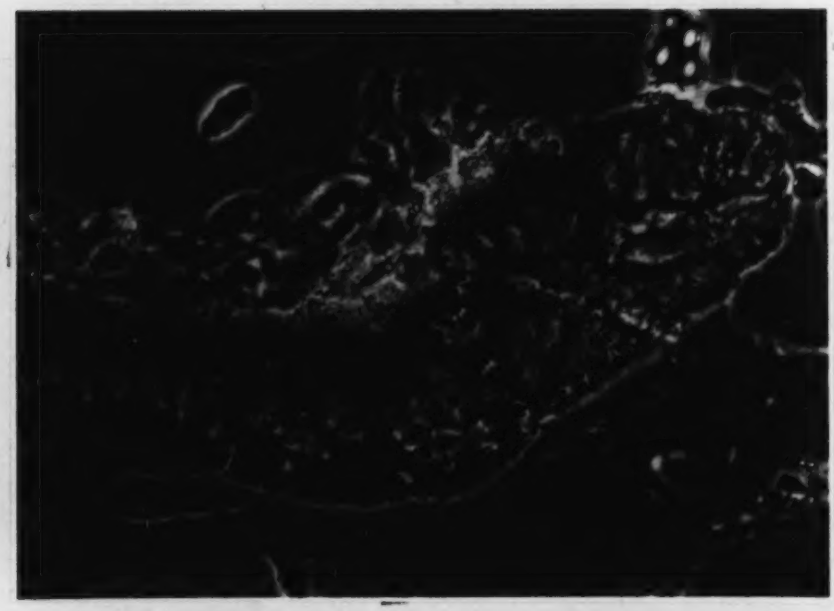

B

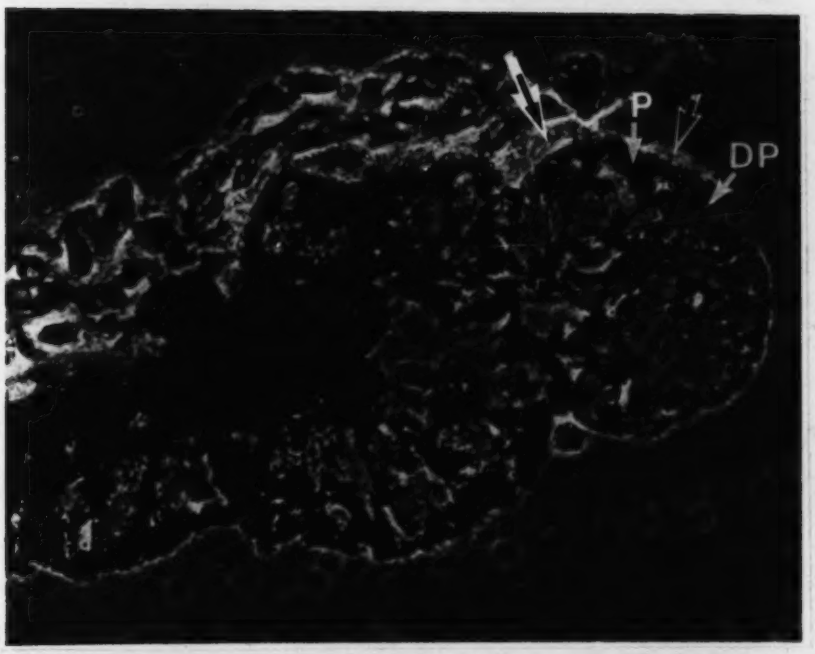
P
DP

external and internal epithelium macrophages are often observed within the interlaminar space (Figures 15 and 16A). The macrophage cell surface stains very intensely for Fn. By stage III intracellular pigment occupies most of the macrophage cell cytoplasm, attesting to their role in depigmentation, and Fn staining is associated with the phagocytized pigment (Figures 14, 15 and 16A).

In figure 14 the microscope was focused on the iris epithelium proximal to the pupillary margin in order to observe several relatively round cells which exhibit intense Fn staining at their surfaces. These cells are interpreted to be macrophages which have interdigitated into the epithelial framework. The epithelial cells immediately adjacent to the putative macrophages have their nuclei located in the apical region and the pigment is localized in the attenuated basal portion of the cell. The IECs show decreased cell contact along their basolateral surfaces and Fn staining of the basolateral cell surface is observed.

Between stage II to III mitotic proliferation progressively increases and is most prevalent at the pupillary margin of the dorsal iris where the epithelium eventually looses it's single celled character. In figure 15 the dorsal pupillary margin of an early stage III (15 day) regenerate is illustrated. External and internal epithelia have separated from one another and what is presumed to be a melanosome-containing macrophage is present within the inter-laminar space. Several completely depigmented IECs display intense, homogeneous Fn staining of their cell surfaces. Incompletely depigmented cells retain a basolateral distribution of Fn staining.

Cell division coupled with depigmentation results in a reduction of cell volume and, by late stage III, the pupillary margin consists of several layers of small, depigmenting IECs. Along the internal epithelium cell division is not as frequent and depigmentation is primarily responsible for the decrease in cell volume. In Figure 16 two individual regenerates at late stage III (18 day) are shown. At the pupillary margin small, depigmented IECs display homogeneous cell surface staining. Fn staining is observed along the apical surface of the separated pupillary epithelia and investing macrophages display intense cell surface staining. Depigmentation continues along the internal epithelium. Elongated cells express staining of lateral cell surfaces and at the convoluted basolateral surface reticulate Fn staining is observed.

During the course of this study many normal and regenerating irises were examined: approximately 25 individual specimens of normal iris tissue, 20 individual specimens of stage I - II regenerates, 25 individual specimens of stage III regenerates and 30 individual specimens of regenerates ranging from stage IV to stage IX. Although quantitative measurements of stroma band width were not made, it is this author's subjective opinion that in the majority of stage II and stage III regenerates examined the stroma band is thinner and receded from the pupillary margin relative to the normal condition of the stroma band. Figures 13, 15 and 16 illustrate the variable but overall reduced character of the stroma band in stage II and III regenerates. In some instances the stroma band has detached from the external epithelium, as illustrated in Figure 14. It is not known if detachment of the stroma

band actually takes place in vivo. Possibly a reduced adhesiveness between the epithelium and the stroma band does exist in vivo, but the detachment, observed in prepared tissue sections, actually takes place during the preparation of the tissue. Further, comparing dorsal and ventral regions of the iris, a reduced and/or detached stroma band is more often observed in the dorsal iris. At the external pupillary margin of the late stage III regenerate a correlation between the level of IEC depigmentation and stroma band contact appears to exist. In many stage II - III regenerates it was observed that IECs which remained pigmented were in contact with stroma band material at their basal surface. While adjacent IECs which had undergone depigmentation were devoid of stroma band material at their basal surfaces. An example of this is illustrated in figure 16B.

3.1.c Stages IV-IX: Redifferentiation and Establishment of the Lens Vesicle

At the dorsal pupillary margin of a stage IV regenerate a definitive lens vesicle consists of small, completely depigmented IECs which will subsequently redifferentiate into lens fibers. Dedifferentiation continues within the internal epithelium and dedifferentiated cells adjacent to the lens vesicle contribute to it's further growth.

Figure 17 is a representative stage IV - V (20 day) regenerate. At the pupillary margin completely depigmented IECs display an orange staining probably induced by the counter-stain. Within the lens vesicle Fn immunostaining at the surface of the presumptive lens fibers is not observed. Although not in focus in this photograph, a basal lamina that stains for Fn was observed at the free border of the lens vesicle. A

Figure 17. Stage IV to V Regenerate: Lens vesicle (20 days post-lentectomy)

By stage IV IECs of the dorsal pupillary margin of the iris constitute a definitive lens vesicle (LV) which is counterstained a dull-red color which appears orange in this photograph. The completely depigmented IECs of the lens vesicle do not display Fn immunostaining. However at the free border of the lens vesicle a continuous basal lamina stains for Fn (arrow), although it is not in clear focus in this photograph. What is believed to be a melanosome-containing macrophage is present at the pupillary margin (* with arrow). Intracellular Fn staining is observed within a partially depigmented IEC at the internal layer of the lens vesicle (0 with arrow). Depigmentation events continue at the internal epithelium proximal to the lens vesicle. Note that stroma band material and stroma connective tissue has apparently detached from the external epithelium. (Bar = 25 um) Note: The corresponding phase contrast micrograph is shown below the fluorescent micrograph.

LV

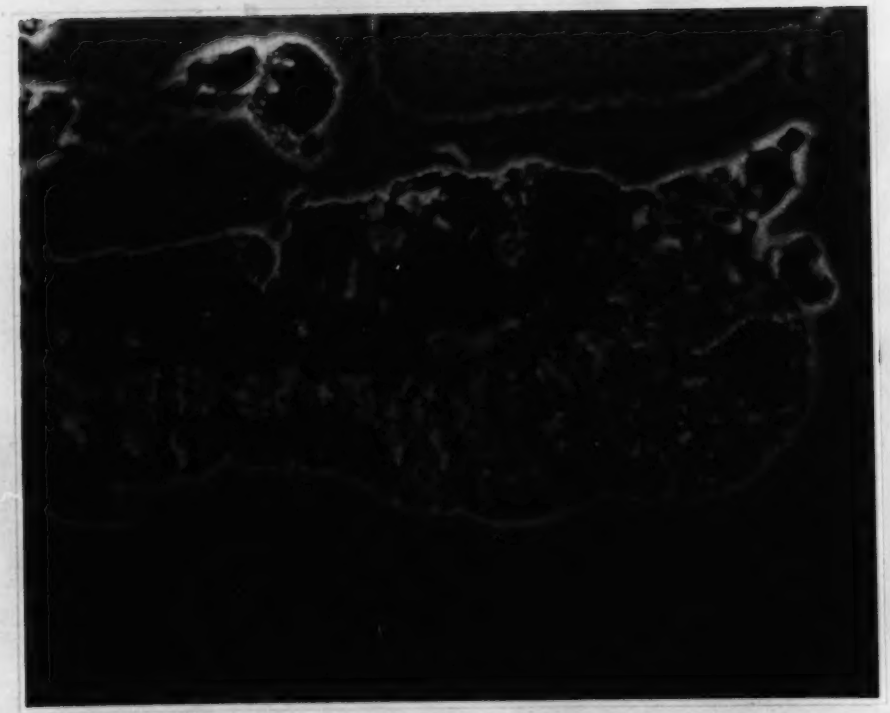

residual melanosome-containing macrophage is present within the vesicle. And an elongated, incompletely depigmented IEC is apparent at the internal layer of this vesicle. Along the internal epithelium elongated IECs display Fn staining at basal and lateral surfaces. Several smaller IECs, displaying homogeneous Fn staini their cell surfaces, are also observed. The external epithelium b the lens vesicle consists of several layers of pigmented IECs w except for two cells immediately adjacent to the lens vesicle, d express Fn staining of their cell surfaces. Figure 18 shows a h magnification of the iris epithelium proximal to the pupillary marg two stage IV regenerates. Both these figures clearly show the pre of Fn staining of the lateral and basal cell surfaces. Decr contact at basolateral cell surfaces is obvious and Fn sta demonstrates the convoluted basolateral surface topography whic typical of the dedifferentiating internal iris epithelium. The ext and internal epithelia are not separated at their apical interfac staining of the apical IEC surface is not observed. The elongated of the internal epithelium display a polarized distribution of nu and melanosome components. The nucleus is located in the apical r of the cell while the melanosomes are concentrated in the basal reg

During stage V cell proliferation results in a thickening of internal layer of the lens vesicle. Stage VI is marked by lens f differentiation in mitotically arrested, elongated cells located wi

Figure 18. Stage IV Regenerates: A = Dorsal iris, B = Ventral iris (Both specimens are 20 days post-lentectomy)

These two photographs illustrate the iris epithelium proximal to the lens vesicle in A and the pupillary margin in B. The external epithelium (EIE) consists of small, cuboidal pigmented IECs. Nuclear volume has not increased in the external IECs. Iris epithelial cells of the internal epithelium are elongate. The enlarged nucleus is localized in the apical portion of the cell and pigment is localized in the basal region of the cell. The external and internal epithelial are not separated from one another and Fn staining is not observed at the apical cell surface. Elongated IECs of the internal epithelium show reticulate Fn staining at their basolateral cell surfaces (arrow). The basolateral cell surface appears convoluted, this is especially evident in photograph A (* with arrow) Lateral staining is also evident in many of these cells. In photograph B the stroma band (Sb with arrow) stains a dull-orange color, probably due to the Evan's blue counterstain. This distinguishes it from the more external connective tissue of the stroma which stains intensely for Fn. A macrophage (M) is present at the basal surface of the internal epithelium. (Bar = 10 um) Note: The corresponding phase contrast micrograph is shown below each fluorescent micrograph.

A
EIE

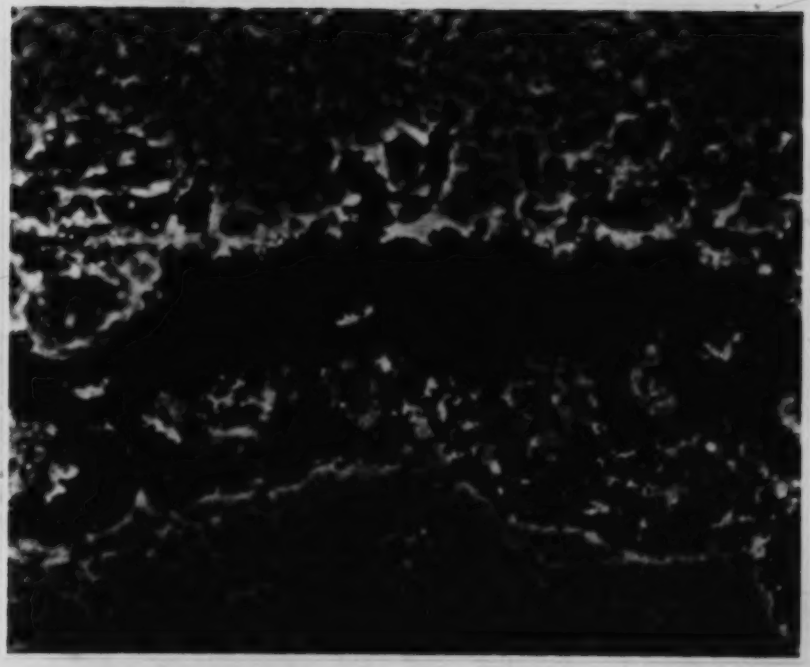

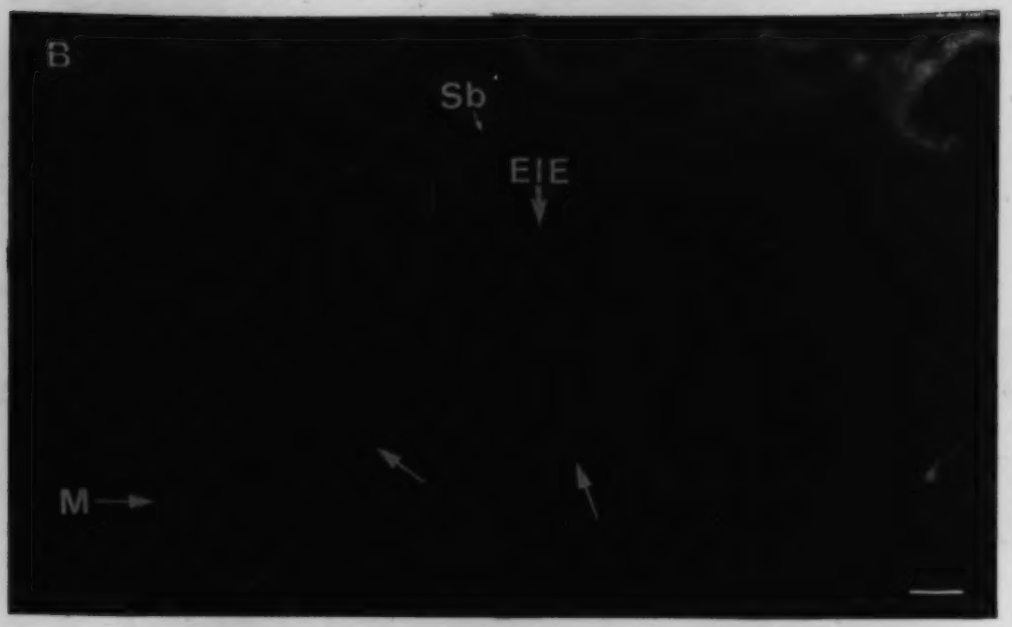
B
Sb
EIE
M

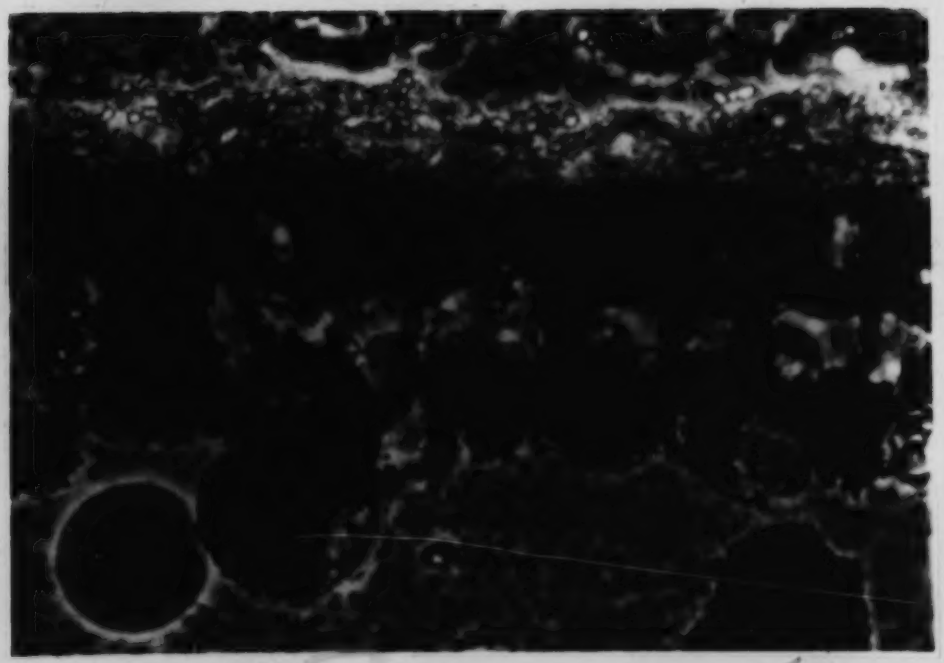

the internal layer of the lens vesicle. Figure 19 shows a representative stage VI (30 day) regenerate. Cells of the external layer of the lens vesicle and the internal iris epithelium proximal to the vesicle display a homogeneous and generalized staining for Fn at their cell surfaces. Relative to the external layer, the cells within the internal layer of the lens vesicle display a reduced level of cell surface Fn staining. At the surface (free border) of the lens vesicle and at the apical surface of the internal layer of the lens stalk a basal lamina that stains for Fn is apparent. Fibronectin staining at the basal surface of the internal and external iris epithelium is relatively thinner as compared to that observed at the surface of the lens vesicle.

During stage VII a primary lens fiber core is established within the internal layer of the lens vesicle. Figure 20 shows a representative stage VII (36 day) regenerate. Within the lens fiber core the elongated primary lens fibers are closely apposed to one another and in some areas Fn staining at the cell surface has decreased to very low levels. At the anterior surface of the fiber core, facing the external lens epithelium, intense Fn staining is observed. Cells peripheral to the fiber core display discontinuous Fn staining of their cell surfaces, presumably corresponding to areas of intercellular separation. Likewise, cells of the presumptive lens epithelium display discontinuous Fn staining at their lateral cell surfaces. Fn staining is observed at the free border of the lens vesicle and at the basal surface of the external and internal iris epithelia.

Figure 19. Stage V to VI: Lens vesicle (30 days post-lentectomy)

Within the thickened posterior layer of the lens vesicle Fn immunostaining is reduced relative to earlier stages (* with arrow). Cells of the external layer of the vesicle (presumptive lens epithelium) and along the internal iris epithelium display Fn staining of their cell surfaces. At the surface (free border) of the lens vesicle a continuous basal lamina stains for Fn (arrow). (Bar = 25 um) Note: The corresponding phase contrast micrograph is shown below the fluorescent micrograph.

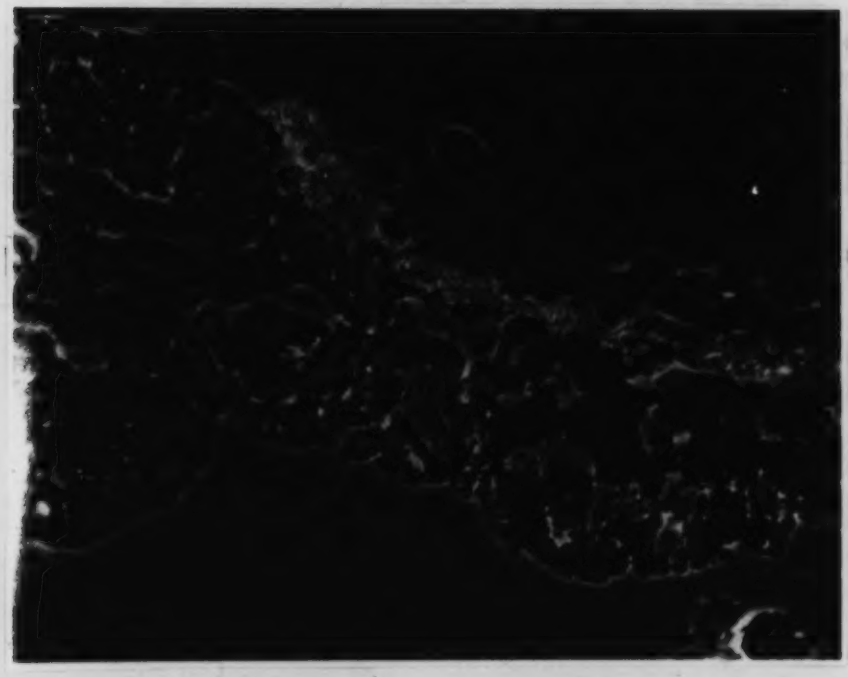

Figure 20. Stage VII: Lens rudiment (36 days post-lentectomy)

Lens fiber differentiation is occurring within the primary lens fiber core (LFC with arrow). Cells have withdrawn from the cell cycle, become more elongate and closely appose one another along their cell boundaries. Within the LFC fibronectin staining is greatly reduced, but along it's anterior margin facing the external lens epithelium (LE) intense Fn staining is observed (* with arrow). Outside the LFC zone Fn staining of the cell surface (arrow) presumably represents areas of intercellular separation. This is also observed in the presumptive LE (arrow). A continuous basal lamina which show Fn staining is present at the surface of the lens vesicle (o with arrow). (Bar = 25 um) Note: The corresponding phase contrast micrograph is shown below the fluorescent micrograph.

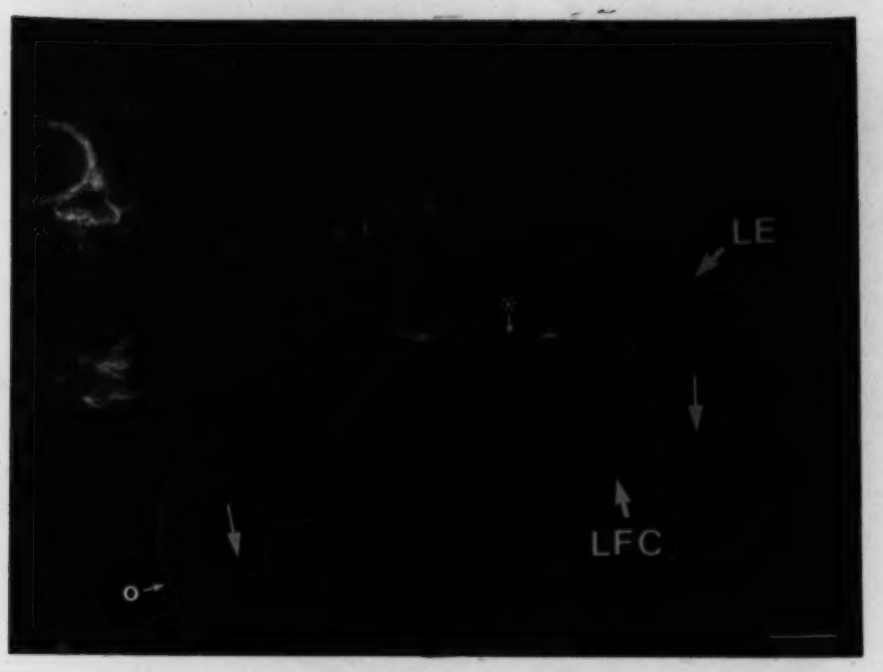
LE
LFC

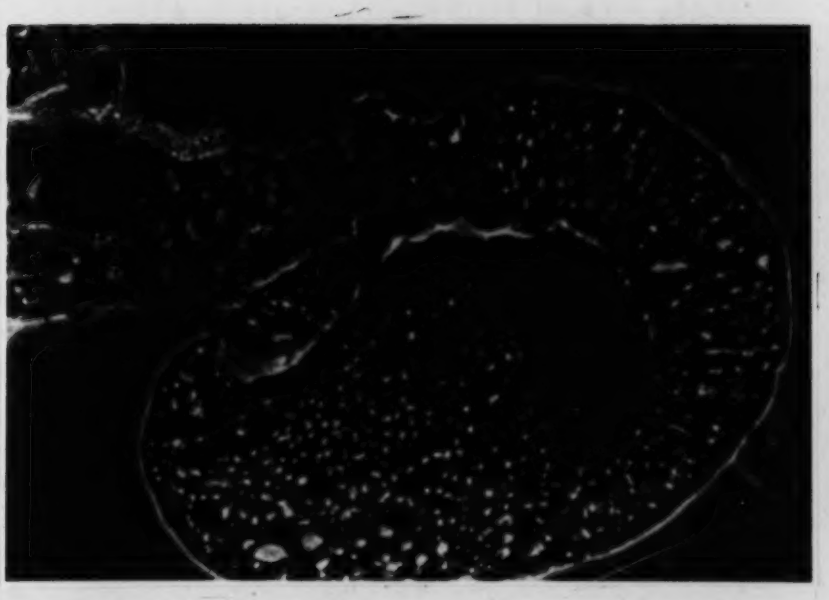

During stage VIII secondary lens fiber differentiation is initiated at the equatorial region of the lens vesicle, between the primary lens fiber core and the lens epithelium. Figure 21A illustrates a stage VIII (40 day) regenerate. Fibronectin staining is not observed within the lens fiber core, but intense Fn staining is observed at the margins of the fiber core delineating it from the peripheral regions of the lens vesicle. Secondary lens fibers located posterior to the lens epithelium and anterior to the fiber core do not display Fn staining of their cell surfaces. However, presumptive secondary lens fibers located peripherally to the fiber core display Fn staining of their cell surface at areas of intercellular separation. Within the lens epithelium Fn staining of lateral cell surfaces is no longer evident. At the surface of the lens rudiment the nascent lens capsule, a product of the lens epithelium, stains very intensely for Fn. Fibronectin staining of the nascent lens capsule is very similar in appearance to the adult lens capsule which is illustrated in figure 21B. Note that in this stage VIII regenerate the lens epithelium and it's associated lens capsule does not extend to the posterior margin of the lens rudiment. This is also true for the adult lens. The internal lens vesicle stalk of the stage VIII regenerate consists of multilayered, depigmented IECs which possess cell surface Fn staining.

Behind the lens vesicle stalk IECs of the internal epithelium are following the pathway of retrieval. Cell division has ceased and partially depigmented IECs begin to resynthesize melanosomes (Yamada, 1977). The dorsal iris proximal to the lens vesicle of stage VIII (40 day) regenerate is illustrated in Figure 22. Epithelial cells

Figure 21. Stage VIII to IX Regenerate: A = Lens rudiment (40 days post-lentectomy). B = Mature lens of an adult, normal Newt eye

Photograph A illustrates the regenerated lens 40 days after lentectomy. The surface of the primary lens fiber core (LFC) displays Fn staining, which appears to delineate it from the peripheral regions of the lens rudiment. Secondary lens fibers located posterior to the lens epithelium and anterior to the fiber core do not display Fn staining of their cell surface (* with arrow). Presumptive secondary lens fibers located lateral to the fiber core display Fn staining in areas which probably represent regions of intercellular separation (arrow). Within the lens epithelium (LE) Fn staining of lateral cell surfaces is no longer evident. Fn staining at the surface of the lens rudiment has increased relative to earlier stages, and presumably represents the nascent lens capsule (o with arrow). In photograph B Fn staining of the lens capsule of an adult lens is observed (arrow) and the lens epithelium is indicated (LE). (Bar = 25 um) Note: For photograph A the corresponding phase contrast micrograph is shown below the fluorescent micrograph.

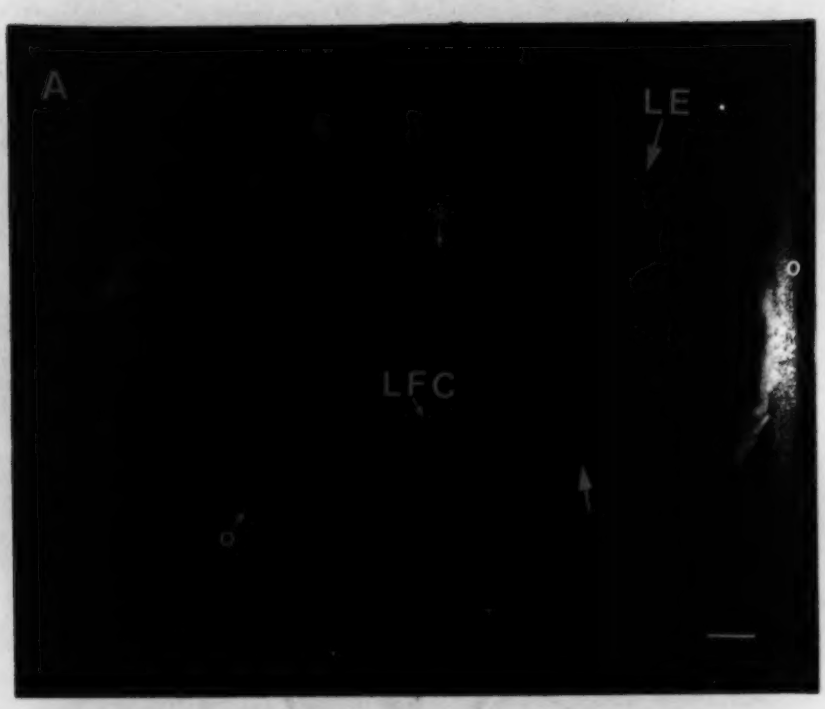
A
LE
LFC

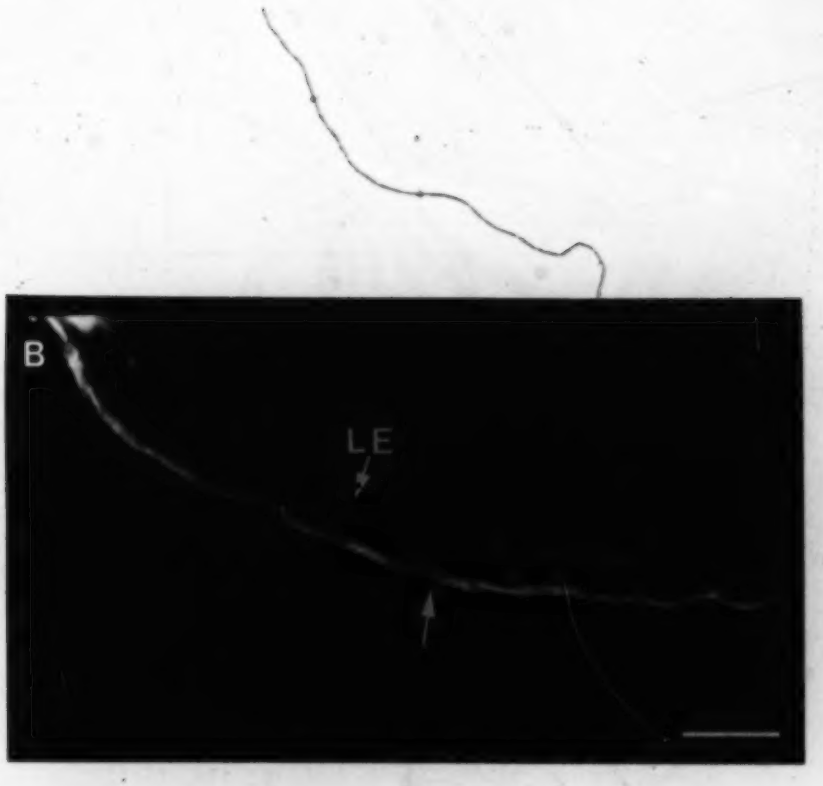
B
LE

Figure 22. Stage VIII to IX Regenerate: Dorsal iris lateral to lens rudiment (40 days post-lentectomy)

In a stage VIII to IX regenerate the internal iris epithelium proximal to the lens rudiment is undergoing retrieval. Fibronectin is localized at basolateral cell surfaces and thickened regions of the basal lamina stain very intensely for Fn (arrow). (Bar = 25 um) Note: The corresponding phase contrast micrograph is shown below the fluorescent micrograph.

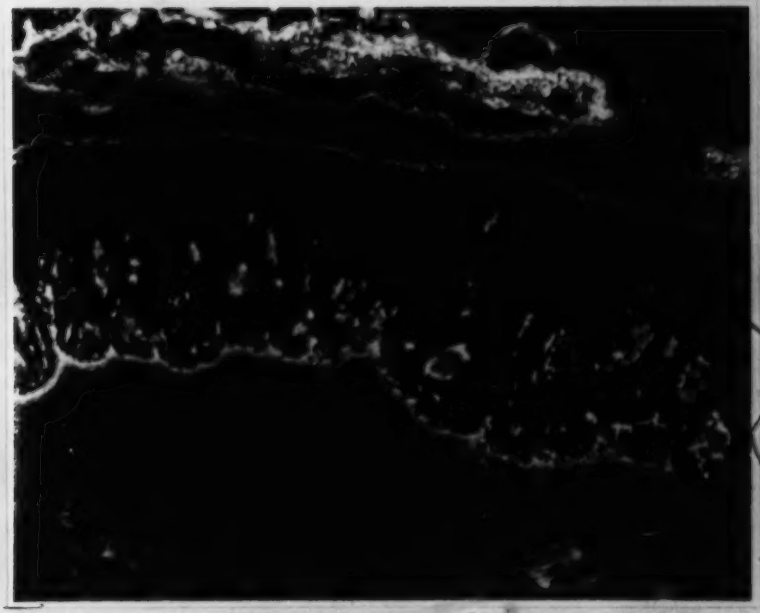

are elongated and intense staining of the lateral cell surface is observed. Fn staining reveals a highly convoluted basolateral cell surface. Thick, diffuse staining is observed at the basal epithelial surface and a reticulate staining pattern is evident at the basolateral aspect of many cells.

Normally lens regeneration does not take place at the pupillary margin of the ventral iris. However the cellular events associated with dedifferentiation that are observed at the dorsal iris epithelium are also evident in the ventral iris epithelium. The onset and rate at which dedifferentiation proceeds appears to be somewhat slower in the ventral iris. For the majority of stage I - III regenerates observed in this study the dorsal and ventral regions of the iris appeared similar in terms of cell morphology and distribution of Fn staining. However, cell proliferation and depigmentation events are most prominent at the dorsal pupillary margin. The ventral iris retains it's early stage III characteristics until the onset of IEC repigmentation sometime during stage VII. Figure 23 shows a section of a ventral iris corresponding to a dorsal iris regenerate at stage VIII (40 day). Relative to the internal epithelium of the dorsal iris (Figure 22) ventral IECs are not conspicuously convoluted at their basolateral surface, and Fn staining of lateral cell surfaces is less prominent. Fn staining of the basal cell surface is not as diffuse or convoluted suggesting closer basolateral apposition between adjacent IECs. The ventral pupillary margin consists of a continuous single layered epithelium of closely apposed, elongated IECs which stain for Fn only at their basal surface.

Figure 23. Ventral Iris (40 days post-lentectomy)

The corresponding dorsal iris of this section was a stage VIII to IX regenerate. Iris epithelial cells at the pupillary margin of this ventral iris and at the internal epithelium remain elongated and possess enlarged, ellipsoid nuclei. Fibronectin staining of lateral cell surfaces is greatly reduced relative to earlier stages, but Fn staining of the basal lamina of the iris epithelium is observed (arrow). (Bar = 25 um) Note: The corresponding phase contrast micrograph is shown below the fluorescent micrograph.

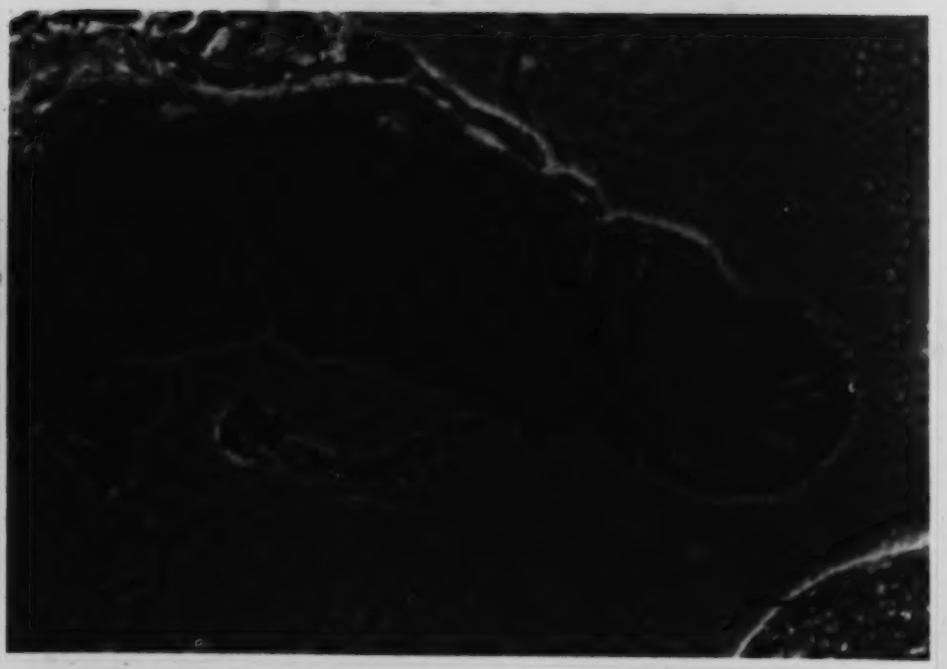

3.2 Anti-Human Fibronectin Antiserum

As demonstrated by immunoblotting techniques (see section 2 of Results) anti-human Fn antiserum does not react as well with newt fibronectin when compared to anti-*Xenopus* Fn antiserum. Immunofluorescent staining of fibronectin in numerous normal irises and lens regenerates were carried out using anti-human Fn antiserum. Comparing the normal iris to stage I, II and III regenerates, anti-human Fn antiserum does not detect the localization of cell surface fibronectin in the normal, pigmented iris cell; moreover changes in the distribution of this molecule during the early stages of lens regeneration remain undetectable. Fibronectin can only be detected in the basal lamina of the capillary endothelium and the basal lamina associated with the iris epithelium. The intensity of immunofluorescence in the capillary endothelium did not vary significantly between individual tissue samples or between regenerates. However the staining intensity of the basal lamina of the iris epithelium was not consistent between sections of the different irises at the same stage of regeneration. No changes in Fn distribution within the iris during lens regeneration were detected with this antiserum. Figure 24A shows a stage I regenerate and figure 24B shows a stage II regenerate. Immunofluorescent staining of Fn within the capillary endothelial basal lamina and within the stroma connective tissue is comparable, while the immunofluorescent staining of the iris epithelial basal lamina is significantly more intense in the stage I relative to the stage II regenerate iris.

Figure 24. Immunostaining with anti-human Fn antiserum:
A = Stage I Regenerate: Dorsal iris (5 days post-lentectomy)
B = Stage II Regenerate: Dorsal iris (10 days post-lentectomy)

Immunofluorescent Fn staining of the endothelial basal lamina of stroma capillaries is consistently observed with anti-human Fn antiserum (* with arrow). However Fn staining of the iris epithelial basal lamina is not consistent. In photograph A the basal lamina does show Fn staining, while in photograph B staining of the iris epithelial basal lamina is of very low intensity (o with arrow). A punctate pattern of Fn staining is observed in the stroma (arrow). (Bar = 10 um) Note: For photograph B the corresponding phase contrast micrograph is shown below the flourescent micrograph.

A

B

During the later stages of lens regeneration, immunofluorescent staining of Fn within the basal lamina associated with the lens vesicle (precursor to the lens capsule) was consistently observed. Compared to the staining intensity observed for the basal lamina of the iris epithelium, an increased staining intensity in the precursor of the lens capsule was observed. This is illustrated in figures 25A and 25B which show stage VI and stage VII lens regenerates respectively. Immunofluorescent staining of the lateral or apical iris epithelial cell surface was not observed using anti-human Fn antiserum as a probe, nor did this antiserum show intracellular Fn staining of IECs.

Figure 25. Immunostaining with anti-human Fn antiserum.
A = Stage VI: Lens vesicle (30 days post-lentectomy)
B = Stage VII to VIII: Lens rudiment (40 days post-lentectomy)

Immunofluorescent Fn staining of the nascent lens capsule is observed in both these regenerates (arrow). In photograph A fibronectin staining of the iris epithelial basal lamina is observed (* with arrow), but IECs do not show Fn staining at their lateral cell surfaces. In photograph B Fn staining of the basal lamina is observed at the stalk of the lens vesicle (VS). Stroma connective tissue shows punctate Fn staining and endothelial vascular elements stain specifically for Fn. (Bar = 25 um) Note: The corresponding phase contrast micrographs are shown below each fluorescent micrograph.

A

B
VS

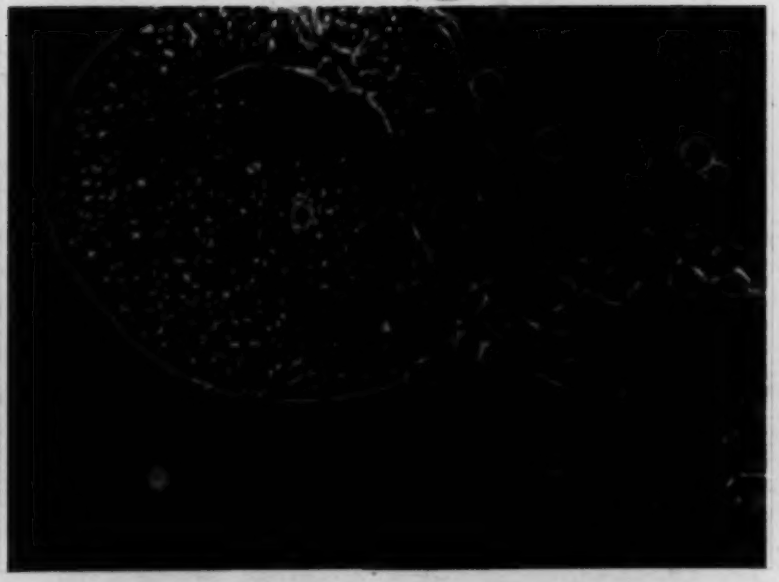

DISCUSSION

The purpose of this study was to examine the distribution of fibronectin within the iris during the process of lens regeneration in the adult newt, Notophthalmus viridescens. And further, to correlate any changes in Fn distribution as they may relate to the morphological and cellular-biochemical changes which accompany the cellular processes of dedifferentiation and redifferentiation.

An indirect immunofluorescent labeling technique was employed to localize fibronectin within iris tissue sections. My results and those of others indicate that antiserum raised to mammalian fibronectins are less reactive with amphibian fibronectin when compared to mammalian fibronectins (Repesh et al., 1981) and likewise antiserum raised to amphibian fibronectins show a low cross-reactivity with mammalian fibronectins (Heasman et al., 1981). Therefore in order to obtain an immunological probe that was sufficiently sensitive with newt fibronectin, plasma fibronectin was isolated from a phylogenetically related species, Xenopus, and antiserum was raised against the Xenopus plasma fibronectin. SDS-PAGE analysis of the affinity-purified Fn sample showed protein bands of molecular weights considerably lower that the expected 200 Kd. As discussed in the Results these lower molecular weight bands presumably represented proteolytic cleavage products of fibronectin. Therefore it was important to show that the antiserum raised to the affinity-purified Fn sample was specifically reactive only with fibronectin. As demonstrated by immunoblotting experiments the antiserum was reactive with four protein bands present in protein blots of proteins solubilized from newt tissues. Two of these protein bands

were within the molecular weight range expected for cellular fibronectin. Reaction at two protein bands of molecular weights lower than that expected for fibronectin were interpreted to represent proteolytic cleavage products of fibronectin. This interpretation is supported by the fact that a sample of anti-Xenopus Fn antiserum from other sources recognized similar protein bands in extracts of newt iris and newt eyelid skin. In addition, in extracts of newt iris tissue, commercial anti-human Fn antiserum, at higher concentrations and longer incubation times, was shown to detect a protein band with a molecular weight similar to that of Fn as well as several bands of lower molecular weight which are regarded as proteolytic fragments of Fn. These results strongly suggest that the anti-Xenopus Fn antiserum used in this study contains predominantly antibodies against sites in Xenopus fibronectin which are also present in newt fibronectin. Therefore the immunofluorescent staining that is observed in the iris and lens regenerates using this antiserum represents the location of fibronectin in these tissues.

As detected by immunofluorescent labeling, the distribution of fibronectin within the iris epithelium is altered during the process of lens regeneration. In the normal iris epithelium Fn staining of the cell surface was restricted to the basal surface of the pigmented iris epithelial cell. Shortly after lentectomy Fn staining was now also evident at lateral and apical cell surfaces. As shown by electron microscopy adjacent cells within the normal iris epithelium are tightly apposed to one another along their lateral cell surfaces and the external and internal lamina are tightly apposed along their apical

interface. Following lentectomy intercellular spaces become eviden between cells (Dumont and Yamada, 1972). The inception of Fn staini at lateral and apical surfaces of activated IECs can be interpreted i several ways. Close cell contact along cell boundaries may physicall impede diffusion of the antibody to antigenic sites. The increase i intercellular spaces which accompanies IEC activation would allow bette access to antigenic sites located at the lateral and apical cel surfaces. It can also be speculated that immunological reactivity of F is affected by it's interaction with other extracellular matri components. Perhaps in the normal iris epithelium fibronectin matri associations affect it's configuration in such a way that immunoreactiv epitopes are unavailable to the antibody. The increased Fn stainin displayed during IEC dedifferentiation may then correspond t modifications in the association of fibronectin with other components o the extracellular matrix. For example, fibronectin within chondrogeni regions of the regenerating newt limb is not detectable b immunofluorescence until after hyaluronidase treatment (Gulati et al. 1983). This implies that hyaluronate within the extracellular matrix i responsible for immunologically masking the fibronectin. Unmasking o fibronectin does not appear to be the main cause of the increased F staining, since preliminary experiments in which normal iris tissue wa pre-treated with hyaluronidase prior to staining did not result in F staining at the lateral and apical cell surfaces of normal iri epithelial cells.

As shown by immunoblotting, the anti-Xenopus Fn antiserum used i this study was very reactive with newt fibronectin, since it reacte

with this molecule at high dilutions. Even if the availability of fibronectin immunoreactive sites was somewhat reduced in the normal iris epithelium a low level of immunofluorescent labeling would have been expected with this antiserum, if fibronectin was present at the lateral and apical cell surfaces. Therefore, it is likely that in the normal iris, the lack of immunofluorescent staining at the lateral and apical cell surface of the pigmented IEC is due to an absence of this molecule in these regions of the quiescent IEC. The formation of intercellular spaces which is observed during the early stages of dedifferentiation, by electron microscopy, is probably accompanied by the deposition of fibronectin at the lateral and apical cell surfaces of the activated IECs. Further work is needed to determine whether the increased immunofluorescent staining of fibronectin reflect actual de novo synthesis of this molecule during dedifferentiation.

As iris epithelial cell dedifferentiation proceeds, basolateral cell separation becomes evident and Fn staining of these surfaces often appeared as a reticulate pattern. Relative to the normal epithelium Fn staining at the basal surfaces of many dedifferentiating IECs appeared to be thicker and more diffuse. At the dorsal pupillary margin, where cell proliferation and depigmentation is most pronounced, the small, completely depigmented cells displayed Fn staining around their entire cell surface. During IEC dedifferentiation the morphological events associated with depigmentation include significant alterations in cell surface ultrastructure (Dumont and Yamada, 1972). Iris epithelial cells become highly pleomorphic with long pseudopod-like extensions branching into thin cytoplasmic strands containing dense populations of

melanosomes. Invading macrophages are often observed within the basolateral intercellular spaces and macrophage cell processes circumscribe and engulf the melanosome-containing IEC pseudopodial extensions. Drawing inference from these ultrastructural observations of the dedifferentiation IEC, the reticulate Fn staining pattern observed at basolateral cell surfaces may be interpreted to correspond to Fn located at the cell surface of the numerous cellular processes of the highly pleomorphic IEC. Ultrastructurally a continuous basal lamina is observed at the plasmalemma surface of those cell processes that extend from the basolateral cell surface. External to this basal lamina amorphous material is irregularly distributed. This amorphous material is not observed in micrographs showing the basal cell surface of normal iris epithelial cells (Dumont and Yamada, 1972). Therefore within the limits of resolution of the light microscope the Fn staining observed at the basolateral cell surface can not be interpreted to correspond only to fibronectin located within the basal lamina, but may also represent fibronectin located within the amorphous material which is observed, at the ultrastructural level, external to the basal lamina. Perhaps the thick, diffuse staining observed at the basolateral and basal cell surface of some dedifferentiating cells corresponds to a significant accumulation of amorphous, extracellular material which contains fibronectin.

To summarize it would appear that during IEC dedifferentiation fibronectin deposition at lateral and apical cell surfaces occurs concomitantly with the formation of intercellular spaces. As depigmenting IECs adopt a highly pleomorphic shape, extracellular

fibronectin accumulates at the surface of the basolateral cell surface projections. And in the completely dedifferentiated IEC fibronectin is distributed around the entire cell surface.

During IEC dedifferentiation the rate of protein synthesis increases (Yamada and Takata, 1963). Part of this increase may be attributed to the synthesis of fibronectin, which is subsequently deposited extracellularly. Perhaps the deposition of fibronectin facilitates the formation of intercellular spaces. Fibronectin may also be involved in the control of iris epithelial cell shape. When IEC depigmentation is observed in vitro cellular projections are observed to be dynamic structures of a highly mobile cell surface. The formation of these projections is dependent on microfilaments and can be suppressed by cytochalasin B, a drug which inhibits actin polymerization (Ortiz as cited by Dumont and Yamada, 1972). Fibronectin interacts with the actin microfilaments of the cytoskeleton and the transmembrane linkage is apparently mediated by a 140 Kd membrane bound Fn receptor complex (Chen et al., 1985; Duband et al., 1986). It is possible that the formation and stability of the cell processes that contain actin microfilaments is dependent on a transmembrane interaction with extracellular fibronectin. Cell surface fibronectin may also play a significant role in the depigmentation process. Plasma fibronectin acting as a circulating opsin is believed to mediate reticulendothelial or macrophage clearance of particulates such as fibrin microaggregates collagenous debris, antibody aggregates of fragments of cells lysed by complement or perhaps even bacteria (Saba and Jaffe, 1980; van-de Water II et al., 1981). Perhaps fibronectin associated with the IEC surface acts as an opsin and

promotes the engulfment and phagocytosis of the melanosome-containing cell processes of the IEC as well as the membrane-bound melanosome complexes discharged by the IECs. More significantly the deposition of fibronectin at the IEC surface and it's possible interactions with other extracellular components may modify the extracellular micro-environment in such a way that the process of cyto-dedifferentiation and cell division can occur. In other developmental systems high levels of extracellular fibronectin can be correlated with a relatively undifferentiated cell state. During limb regeneration in the adult newt fibronectin is synthesized and deposited in the extracellular matrix surrounding the dedifferentiating blastema cells (Repesh et al., 1982; Gulati et al., 1983). In the developing chick limb bud fibronectin is a prominent component of the the extracellular matrix which surrounds the undifferentiated mesenchymal cells of the apical ectodermal ridge (Tomasek et al., 1980).

Glycosaminoglycans, which are also components of the extracellular matrix, show an increased level of synthesis during IEC dedifferentiation (Kulyk and Zalik, 1982). While the synthesis of certain GAG types is equal in dorsal and ventral regions of the iris, the synthesis of hyaluronate shows a much more significant increase in the dorsal iris, especially during the period of most pronounced IEC dedifferentiation (Kulyk et al., in press). In many developmental systems hyaluronate appears to maintain or in some instances induce an undifferentiated state in mesenchymal cell populations (Derby, 1978; Pintar, 1978; Solursh et al., 1979; Markwald et al., 1978 and Kosher et

al., 1981). In the regenerating newt limb hyaluronate synthesis is highest within the dedifferentiating blastema (Toole and Goss, 1971). Within the lens regenerating iris epithelium the deposition of fibronectin at the cell surface and the concomitant increase in GAG synthesis, particularly hyaluronate, coincide temporally with dedifferentiation suggesting that such alterations in the extracellular matrix are instrumental in or conducive to the dedifferentiative process.

Dedifferentiated cells populating the dorsal pupillary margin of the iris subsequently undergo cell-type conversion and redifferentiate into lens fiber cells which withdraw from the cell cycle and adopt an elongate morphology. As observed by the electron microscope, adjacent cells within the primary fiber core are tightly apposed to one another (Karasaki, 1964). The distribution of Fn staining observed within the developing lens rudiment suggested that lens fiber differentiation is accompanied by a decrease and subsequent loss of cell surface Fn. Fibronectin staining was not observed within the primary fiber core. While cells outside the fiber core, which remain mitotically active and are separated from adjacent cells by intercellular spaces, retain fibronectin staining at their cell surfaces. The Fn staining pattern observed in regions of the iris undergoing retrieval showed that melanocyte redifferentiation is also accompanied by the loss of fibronectin from lateral cell surfaces. In other developmental systems cell differentiation is also accompanied by a loss of fibronectin from the cell surface. During myogenesis cell surface fibronectin is lost as myoblast cells undergo fusion (Chen, 1977; Kosher et al., 1982; Tomasek

et al., 1982; Repesh et al., 1982 and Gulati et al., 1983). Also, myoblast fusion *in vitro* is inhibited by exogenous fibronectin (Podleski et al., 1979). Chondrogenesis *in vitro* is associated with a decrease in fibronectin synthesis (Lewis et al., 1978) and exogenous fibronectin will inhibit chondrocyte differentiation (Pennypacker et al., 1979; West et al., 1979).

It would appear that the absence of Fn staining within the primary fiber core and the decrease in lateral staining during melanocyte redifferentiation can be interpreted in two ways. Just as the deposition of fibronectin at the IEC surface may facilitate the formation of intercellular spaces, perhaps it's removal from the cell surface is necessary to bring about a decrease in intercellular spaces as the primary lens fibers become closely apposed to one another. Similarly as melanocytes redifferentiate, the removal of fibronectin from lateral cell surfaces may be necessary in order for cells to re-establish the close cell-to-cell apposition which is characteristic of the normal iris epithelium. More significantly, cell surface fibronectin may have a negative influence on lens fiber differentiation or melanocyte redifferentiation and therefore it's removal from the extracellular environment represents a mechanism by which cytodifferentiation is promoted. It is also possible that Fn is present in the extracellular matrix which surrounds the redifferentiating cells, but becomes complexed with other ECM components and is not detected by immunofluorescent means. Further studies in which tissues are subjected to pre-treatment with hyaluronidase prior to Fn staining, would be necessary to clarify this point.

Lens regeneration is an efficient mechanism of organ replacement and the process of cellular metaplasia appears to take place in a controlled manner. This is in contrast to pathological instances of cellular neoplasia in which cell proliferation occurs at an apparently uncontrolled rate. Metastasizing tumors are often characterized by dissolution or disorganization of their associated basement membranes (Liotta et al., 1984). However, studies using the electron microscope indicate that the integrity of the basal lamina of the iris epithelium is maintained throughout the process of lens regeneration (Dumont and Yamada, 1972). As detected by immunofluorescent staining fibronectin was present at the basal cell surface through out the regenerative process. Perhaps the presence of an intact basal lamina provides a controlling influence over this process thereby limiting the extent of the metaplasic event while allowing an ordered conversion in cell type. This may be especially significant in cellular regions located outside the lens vesicle, where partially dedifferentiated cells redifferentiate and re-establish their former epithelial morphology.

It has also been suggested that the iris stroma plays a repressive role in the process of transformation of iris into lens (Lopashov, 1977). Directly adjacent to the basal surface of the external iris epithelium, a relatively compact acellular layer was distinguishable from the looser connective tissue of the stroma. This layer was referred to as the stroma band. During lens regeneration regressive changes in stroma band character were most often observed at the dorsal pupillary margin. It is possible that the stroma band suppresses dedifferentiation, and at the dorsal pupillary margin enzymatic

dissolution of adhesive contacts with the stroma band allows cells at the margin to undergo precocious dedifferentiation. Within the stroma band fibronectin staining often appeared in a punctate pattern. It would be of interest to characterize the GAG composition of the stroma band, in particular hyaluronate. Endogenous hyaluronidase activity in iris tissue extracts remains constant during lens regeneration, but activity is approximately two fold higher in dorsal iris extracts relative to ventral iris extracts (Kulyk et al., in press). Perhaps within different regions of the intact iris some mechanism exists whereby hyaluronidase activity is temporally controlled during lens regeneration. The higher enzymatic potential of the dorsal iris may be associated with dissolution of the stroma band at the dorsal pupillary margin and thus result in precocious IEC dedifferentiation.

In conclusion it would appear that the distribution of fibronectin within the iris is altered during the process of lens regeneration. Fibronectin is apparently redistributed and deposited at the surface of the dedifferentiating iris epithelial cell. And at later stages lens fiber differentiation and melanocyte redifferentiation is associated not only with a decrease in cell surface fibronectin, but also a localized distribution of this molecule at the cell surface. The developmental significance of these changes can only be speculated on.

Fibronectin only represents one component of the extracellular matrix. Clearly it would be of interest to study the distribution of other extracellular matrix components within the iris during the process of lens regeneration. Immunoelectron microscopic localization of fibronectin within the iris epithelium could provide a more detailed

description of fibronectin's extracellular organization. In addition lectin-conjugate labeling of specific GAG components at the ultrastructural level could also be carried out, providing a more comprehensive examination of the extracellular matrix which supports or facilitates the cellular processes of dedifferentiation and redifferentiation.

REFERENCES

Balin, G., Click, E.M., Crouch, E., Davidson, J.M. and Bornstein, P. (1979) Isolation of a collagen-binding fragment from fibronectin and cold-insoluble globulin. J. Biol. Chem. 254: 1429-1432.

Bernfield, M., Banerjee, S.D., Koda, J.E. and Rapraeger, A.C. (1984) Remodelling of the basement membrane: morphogenesis and maturation. In Basement membranes and cell movement (Ciba Foundation Symposium 108), pp. 179-196. Pitman, London.

Birembaut, P., Caron, Y., Van Cauwenberge, D. and Foidart, J. (1983) Distribution of laminin, a basement membrane glycoprotein in epithelial proliferations. Collagen Rel. Res. 3: 25-31.

Boucaut, J.C. and Darribere, T. (1983) Fibronectin in early amphibian embryos: migrating mesodermal cells contact fibronectin established prior to gastrulation. Cell Tiss. Res. 234: 135-145.

Boucaut, J.C., Darribere, T., Poole, T.J., Aoyama, H., Yamada, K.M. and Thiery, J.P. (1984a) Biologically active synthetic peptides as probes of embryonic development: a competitive peptide inhibitor of fibronectin function inhibits gastrulation in amphibian embryos and neural crest cell migration in avian embryos. J. Cell Biol. 99: 1822-1830.

Boucaut, J.C., Darribere, T., Boulekbache, H. and Thiery, J.P. (1984b) Prevention of gastrulation but not neurulation by antibodies to fibronectin in amphibian embryos. Nature 307: 364-366.

Bradford, M.M. (1976) A rapid and sensitive method for the quantitation of microgram quantities of protein utilizing the principle of protein-dye binding. Anal. Biochem. 72: 248-254.

Chen, L.B. (1977) Alterations in cell surface LETS protein during myogenesis. Cell 10: 393-400.

Chen, W., Hasegawa, E., Hasegawa, T., Weinstock, C. and Yamada, K.M. (1985) Development of cell surface linkage complexes in cultured fibroblasts. J. Cell Biol. 100: 1103-1114.

Chiquet, M., Puri, E.C. and Turner, D.C. (1979) Fibronectin mediates attachment of chicken myoblasts to gelatin-coated substratum. J. Biol. Chem. 254: 5475-5482.

Chylack, L.T. and Bellows, A.R. (1978) Molecular sieving in suprachoroidal fluid formation in man. Invest. Ophthalmol. Visual Sci. 17: 420-427.

Cohn, R.H., Banerjee, S.D. and Bernfield, M.R. (1977) The basal lamina of embryonic salivary epithelia: nature of glycosaminoglycan and organization of extracellular materials. J. Cell Biol. 73: 464-478.

Collins, J.M. (1972) Amplification of ribosomal ribonucleic acid cistrons in the regenerating lens of Triturus. Biochemistry 11: 1259-1263.

Collins, J.M. (1974) Structural changes in deoxyribonucleic acid during early stages of lens regeneration in Triturus. J. Biol. Chem. 249: 1839-1847.

Critchley, D.R., England, M.A., Wakely, J. and Hynes, R.O. (1979) Distribution of fibronectin in the ectoderm of gastrulating chick embryos. Nature 280: 498-500.

Cuny, R. and Zalik, S.E. (1981) Effect of bovine pituitary hormone preparations on newt lens regeneration in vitro: stimulation of thyrotropin. Dev. Biol. 81: 23-35.

Darribere, T., Boulekbache, H., Shi, D.L. and Boucaut, J.P. (1985) Immuno-electron-microscopic study of fibronectin in gastrulating amphibian embryos. Cell Tiss. Res. 239: 75-80.

Derby, M.A. (1978) Analysis of glycosaminoglycans within the extracellular environments encountered by migrating neural crest cells. Dev. Biol. 66: 321-336.

Dessau, W., Jilek, F. and Adelmann, B.C. et al. (1978) Similarity of antigelatin factor and cold insoluble globulin. Biochim. Biophys. Acta. 533: 227-237.

Dessau, W., Von der Mark, H., Von der Mark, K. and Fischer, S. (1980) Changes in the patterns of collagens and fibronectin during limb-bud chondrogenesis. J. Embryol. Exp. Morphol. 57: 51-60.

Donaldson, D.J. and Mahan, J.T. (1983) Fibrinogen and fibronectin as substrates for epidermal cell migration during wound closure. J. Cell Sci. 62: 117-127.

Duband, J.L. and Thiery, J.P. (1982) Appearance and distribution of fibronectin during chick embryo gastrulation and neurulation. Dev. Biol. 94: 337-350.

Duband, J., Rocher, S., Chen, W., Yamada, K.M. and Thiery, J.P. (1986) Cell adhesion and migration in the early vertebrate embryo: location and possible role of the putative fibronectin receptor complex. J. Cell Biol. 102: 160-178.

Dumont, J.N., Yamada, T. and Cone, V.M. (1970) Alteration of nucleolar ultrastructure in iris epithelial cells during initiation of Wolffian lens regeneration. J. Exp. Zool. 174: 187-204.

Dumont, J.N. and Yamada, T. (1972) Dedifferentiation of iris epithelial cells. Dev. Biol. 29: 385-401.

Dzandu, J.K., Den, M.E., Barratt, D.L. and Wise, G.E. (1984) Detection of erythrocyte membrane proteins, sialo glycoproteins, and lipids in the same polyacrylamide gel using a double-staining technique. Proc. Natl. Acad. Sci. USA 81: 1733-1737.

Eisenberg, S. and Yamada, T. (1966) A study of DNA synthesis during the transformation of the iris into lens in the lentectomized newt. J. Exp. Zool. 162: 353-368.

Eguchi, G. (1961) The inhibitory effect of the injured and displaced lens on the lens-formation in Triturus larvae. Embryologia 6: 13-35.

Eguchi, G. and Ishikawa, M. (1963) Alkaline phosphatase in the dorsal and the ventral halves of the iris during early stages of lens regeneration in the newt. Embryologia 7: 295-305.

Eguchi, G. (1963) Electron microscopic studies on lens regeneration. I. Mechanisms of depigmentation of the iris. Embryologia 8: 45-62.

Eguchi, G. and Shingai, R. (1971) Cellular analysis on localization of lens-forming potency in the newt iris epithelium. Develop. Growth Differentiation 13: 337-349.

Eguchi, G. and Watanabe, K. (1973) Elicitation of lens from the ventral iris epithelium of the newt by a carcinogen, N-methyl-N'-nitro-N-nitrosoguanidine. J. Embryol. Exp. Morphol. 30: 63-71.

Eguchi, G., Abe, S.I. and Watanabe, K. (1974) Differentiation of lens-like structures from newt iris epithelial cells in vitro. Proc. Natl. Acad. Sci. USA 71: 5052-5056.

Ekblom, P., Alitalo, K., Vaheri, A., Timpl, R. and Saxen, L. (1980) Induction of a basement membrane glycoprotein in embryonic kidney: possible role of laminin in morphogenesis. Proc. Natl. Acad. Sci. USA 77: 485-489.

Engel, J., Odermatt, E., Engel, A., Madri, J.A., Furthmayer, H., Rohde, H. and Timpl, R. (1981) Domain organizations and flexibility of laminin and fibronectin, two multifunctional proteins of the extracellular matrix. J. Mol. Biol. 150: 97-120.

Fine, B.S. and Yanoff, M. (1979) Ocular histology: a text and atlas (2nd edition). Harper and Row, Hagerstown.

Foidart, J.M., Bere, E.W., Yaar, M., Rennard, S.I., Gullino, M., Martin, G.R. and Katz, S.I. (1980) Distribution and immunoelectron microscopic localization of laminin, a noncollagenous basement membrane glycoprotein. Laboratory Invest. 42: 336-342.

Foidart, J.M., Timpl, R., Furthmayer, H. and Martin, G.R. (1981) Laminin, a glycoprotein from basement membranes. In Immunocytochemistry of the extracellular matrix, Vol. I, (H. Furthmayer ed.). CRC Press, pp. 126-133. Boca Raton, Florida.

Fujikawa, L.S., Foster, S.C., Harrist, T.J., Lanigan, J.M. and Colvin, R.B. (1981) Fibronectin in healing rabbit corneal wounds. Laboratory Invest. 45: 120-129.

Grinnell, F. and Feld, M.K. (1979) Initial adhesion of human fibroblasts in serum-free medium: possible role of secreted fibronectin. Cell 17: 117-129.

Gulati, A.K., Zalewski, A.A. and Reddi, A.H. (1983) An immunofluorescent study of the distribution of fibronectin and laminin during limb regeneration in the adult newt. Dev. Biol. 96: 355-365.

Hascall, V.C. and Hascall, G.K. (1981) Proteoglycans. In Cell biology of extracellular matrix (E.D. Hay, ed.), pp. 39-63. Plenum Press, New York.

Hassell, J.R., Robey, P.G., Barrach, H.J., Wilczek, J., Rennard, S.I. and Martin, G.R. (1980) Isolation of a heparan sulfate-containing proteoglycan from basement membrane. Proc. Natl. Acad. Sci. USA 77: 4494-4498.

Hassell, J.R., Leyshon, W.C., Ledbetter, S.R., Tyree, B. and Suzuki, S., et al. (1985) Isolation of two forms of basement membrane proteoglycans. J. Biol. Chem. 260: 8098-8105.

Hassell, J.R., Kimura, J.H. and Hascall, V.C. (1986) Proteoglycan core protein families. Ann. Rev. Biochem. 55: 539-567.

Hawkes, R., Niday, E. and Gordon, J. (1982) A dot-immuno-binding assay for monoclonal and other antibodies. Anal. Biochem. 119: 142-147.

Hay, E.D. (1981) Introductory remarks. In Cell biology of extracellular matrix (E.D. Hay, ed.), pp. 1-4. Plenum Press, New York.

Hayashi, M. and Yamada, K.M. (1982) Divalent cation modulation of fibronectin binding to heparin and to DNA. J. Biol. Chem. 257: 5263-5267.

Hayashi, M. and Yamada, K.M. (1983) Domain structure of the carboxyl-terminal half of human plasma fibronectin. J. Biol. Chem. 258: 3332-3340.

Hayman, E.G., Oldberg, A., Martin, G.R. and Ruoslahti, E. (1982) Codistribution of heparan sulfate proteoglycan, laminin and fibronectin in the extracellular matrix of normal rat kidney cells and their coordinate absence in transformed cells. J. of Cell. Biol. 94: 28-35.

Heasman, J., Hynes, R.O., Swan, A.P., Thomas, V. and Wylie, C.C. (1981) Primordial germ cells of xenopus embryos: the role of fibronectin in their adhesion during migration. Cell 27: 437-447.

Horstman, L.P. and Zalik, S.E. (1974) Growth of newt iris epithelial cells in vitro: A study of the cell cycle. Exp. Cell Res. 84: 1-14.

Hunt, R.C., Gold, E. and Brown, J.C. (1975) Cell cycle dependant exposure of a high molecular weight protein on the surface of mouse L cells. Biochim. Biophys. Acta. 413: 453-458.

Hynes, R.O. and Bye, J.M. (1974) Density and cell cycle dependance of cell surface proteins in hamster fibroblasts. Cell 3: 113-120.

Hynes, R.O. and Yamada, K.M. (1982) Fibronectins: multifunctional glycoproteins. J. Cell Biol. 95: 369-377.

Hynes, R.O. (1985a) Molecular biology of fibronectin. Annual Rev. of Cell Biol. 1: 67-90.

Hynes, R.O. (1985b) Personal communication.

Idoyaga-Vargas, V. and Yamada, T. (1974) Glucosaminidase and dedifferentiation of newt iris epithelium. Differentiation 2: 91-98.

Idoyaga-Vargas, V., Yamada, T. and Michel, C. (1976) Cell type conversion and galactosyltransferase in lens regeneration. Dev. Biol. 49: 563-568.

Jalkanen, M., Nguyen, H., Rapraeger, A., Kurn, N. and Bernfield, M. (1985) Heparan sulfate proteoglycans from mouse mammary epithelial cells: localization on the cell surface with a monoclonal antibody. J. Cell Biol. 101: 976-984.

Jilek, F. and Hormann, H. (1977) Cold-insoluble globulin, II. Plasminolysis of cold-insoluble globulin. Hoppe-Seyler's Z. Physiol. Chem. 358: 133-136.

Johansson, S. and Hook, M. (1980) Heparin enhances the rate of binding of fibronectin to collagen. Biochem. J. 187: 521-524.

Johnson, G.D., Davidson, R.S., McNamee, K.C., Goodwin, R.D. and Holborow, E.J. (1982) Fading in immunofluorescence during microscopy: a study of the phenomenon and its remedy. J. of Immuno. Meth. 55: 231-242.

Kanwar, Y.S. and Farquhar, M.G. (1979) Presence of heparan sulfate in the glomerular basement membrane. Proc. Natl. Acad. Sci. USA 76: 1303-1307.

Kanwar, Y.S., Linker, A. and Farquhar, M.G. (1980) Increased permeability of the glomerular basement membrane to ferritin after removal of glycosaminoglycans (heparan sulfate) by enzyme digestion. J. Cell Biol. 86: 688-693.

Karasaki, S. (1964) An electron microscopic study of Wolffian lens regeneration in the adult newt. J. Ultrastruct. Res. 11: 246-273.

Kennedy, D.W., Rohrbach, D.H., Martin, G.R., Momoi, T. and Yamada, K.M. (1983) The adhesive glycoprotein laminin is an agglutinin. J. Cell Physiol. 114: 257-262.

Ketley, J.N., Orkin, R.W. and Martin, G.R. (1976) Collagen in developing chick muscle in vivo and in vitro. Exp. Cell Res. 99: 261-268.

Kjellen, L., Oldberg, A. and Hook, M. (1980) Cell surface heparan sulfate: mechanism of proteoglycan cell association. J. Biol. Chem. 255: 407-413.

Kjellen, L., Pettersson, I. and Hook, M. (1981) Cell-surface heparan sulfate: an intercalated membrane proteoglycan. Proc. Natl. Acad. Sci. USA 78: 5371-5375.

Klebe, R.J. (1974) Isolation of a collagen-dependant cell attachment factor. Nature 250: 248-251.

Kleinman, H.K., Klebe, R.J. and Martin, G.R. (1981) Role of collagenous matrices in the adhesion and growth of cells. J. Cell Biol. 88: 473-485.

Kleinman, H.K., McGarvey, M.L., Hassell, J.R., Martin, G.R., Baron van Evercooren, A. and Dubois-Dalcq, M. (1984) The role of laminin in basement membranes and in the growth, adhesion and differentiation of cells. In The role of extracellular matrix in development (R.L. Trelstad, ed.), pp. 123-143. Alan R. Liss, Inc., New York.

Kobayashi, S., Oguri, K., Kobayashi, K. and Okayama, M. (1983) Isolation and characterization of proteoheparan sulfate synthesized in vitro by rat glomeruli. J. Biol. Chem. 258: 12051-57.

Kosher, R.A., Savage, M.P. and Walker, K.H. (1981) A gradation of hyaluronate accumulation along the proximodistal axis of the embryonic chick limb bud. J. Embryol. Exp. Morphol. 63: 85-98.

Kosher, R.A., Walker, K.H. and Ledger, P.W. (1982) Temporal and spatial distribution of fibronectin during development of the embryonic chick limb bud. Cell Differentiation 11: 217-228.

Kulyk, W.M. and Zalik, S.E. (1982) Synthesis of sulfated glycosaminoglycan in newt iris during lens regeneration. Differentiation 23: 29-35.

Kulyk, W.M., Zalik, S.E. and Dimitrov, E. (1987) Hyaluronic acid production and hyaluronidase activity in the newt iris during lens regeneration. Exp. Cell. Res (in press).

Laemmli, U.K. (1970) Cleavage of structural proteins during the assembly of the head of bacteriophage T4. Nature 227: 680-685.

Laurie, G.W. and Leblond, C.P. (1983) What is known of the production of basement membrane components. J. Histochem. Cytochem. 31: 159-163.

Lee, G., Hynes, R. and Kirscher, M. (1984) Temporal and spatial regulation of fibronectin in early Xenopus development. Cell 36: 729-740.

Leivo, I., Vaheri, A., Timpl, R. and Wartiovaara, J. (1980) Appearance and distribution of collagens and laminin in the early mouse embryo. Dev. Biol. 76: 100-114.

Leivo, I. (1983) Basement membrane-like matrix of teratocarcinoma-derived endoderm cells: presence of laminin and heparan sulfate in the matrix at points of attachment to cells. J. Histochem. Cytochem. 31: 35-45.

Lewis, C.A., Pratt, R.M., Pennypacker, J.P. and Hassel, J.R. (1978) Inhibition of limb chondrogenesis in vitro by vitamin A: alterations in cell surface characteristics. Dev. Biol. 64: 31-47.

Linsenmayer, T.F. and Smith, G.N. (1976) The biosynthesis of cartilage type collagen during regeneration in the larval salamander. Dev. Biol. 52: 19-30.

Linsenmayer, T.F. (1981) Collagen. In cell biology of extracellular matrix (E.D. Hay, ed.), pp. 5-32. Plenum Press, New York.

Linsenmayer, T.F., Gibney, E., Toole, B.P. and Gross, J. (1978) Cellular adhesion to collagen. Exp. Cell Res. 116: 470-474.

Liotta, L.A., Rao, N.C., Barsky, S.H. and Bryant, G. (1984) The laminin receptor and basement membrane dissolution: role in tumor metastasis. In Basement membranes and cell movement. (Ciba Foundation Symposium 108), pp. 146-162. Pitman, London.

Lopashov, G.V. (1977) Levels in stabilization of cell differentiation and its experimental transformation. Differentiation 9: 131-137.

Madri, J.A., Roll, J., Furthmayer, H. and Foidart, J.M. (1980) Ultrastructural localization of fibronectin and laminin in basement membranes of the murine kidney. J. Cell Biol. 86: 682-687.

Malinoff, H.L. and Wicha, M.S. (1983) Isolation of a cell surface receptor protein for laminin from murine fibrosarcoma cells. J. Cell Biol. 96: 1475-1479.

Markwald, R.R., Fitzharris, T.P., Bank, H. and Bernanke, D.H. (1978) Structural analysis on the matrical organization of glycosaminoglycans in developing endocardial cushions. Dev. Biol. 62: 292-316.

Martin, G.R., Timpl, R., Muller, P.K. and Kuhn, K. (1985) The genetically distinct collagens. Trends in Biochem. Sci. (TIBS) 10: 285-287.

Mauchamp, J., Margotat, A., Chambard, M., Charrier, B., Remy, L. and Michel-Bechet, M. (1979) Polarity of three-dimensional structures derived from isolated hog thyroid cells in primary culture. Cell Tiss. Res. 204: 417-430.

Mayer, B.W., Hay, E.D. and Hynes, R.O. (1981) Immunocytochemical localization of fibronectin in embryonic chick trunk and area vasculosa. Dev. Biol. 82: 267-286.

Mayne, R. (1984) The different types of collagen and collagenous peptides. In the role of extracellular matrix in development (R.L. Trelstad, ed.), pp. 33-42. Alan R. Liss, Inc., New York.

McLean, I.W. and Nakane, P.K. (1974) Periodate-lysine-paraformaldehyde fixative: a new fixative for immunoelectron microscopy. J. Histochem. Cytochem. 22: 1077-1084.

Moore, M.D. and Williams, L.A. (1977) The effect of lens components on Wolffian lens regeneration in Notophthalmus. Am. Zool. 17: 95.

Morrison, P.R., Edsall, J.T. and Miller, S.G. (1948) Preparation and properties of serum and plasma proteins XIII. The separation of purified fibrinogen from fraction I of human plasma. J. Am. Chem. Soc. 70: 3103-3108.

Mosher, D.F., Schad, P.E. and Vann, J.M. (1980) Cross-linking of collagen and fibronectin by factor XIIIa: localization of participating glytaminyl residues to a trypic fragment of fibronectin. J. Biol. Chem. 255: 1181-1188.

Olden, K., Pratt, R.M. and Yamada, K.M. (1978) Role of carbohydrates in protein secretion and turnover: effects of tunica mycin on the major cell surface glycoprotein of chick embryo fibroblasts. Cell 13: 461-473.

Olden, K., Pratt, R.M. and Yamada, K.M. (1979) The role of carbohydrate in biological function of the adhesive protein fibronectin. Proc. Natl. Acad. Sci. 76: 3343-3347.

Oohira, A., Wight, T.N., McPherson, J. and Bornstein, P. (1982) Biochemical and ultrastructural studies of proteoheparan sulfates synthesized by PYS-2, a basement membrane-producing cell line. J. Cell Biol. 92: 357-367.

Oohira, A., Wight, T.N. and Bornstein, P. (1983) Sulfated proteoglycans synthesized by vascular endothelial cells in culture. J. Biol. Chem. 258: 2014-2021.

Ortiz, J.R., Yamada, T. and Hsie, A.W. (1973) Induction of the stellate configuration in cultured iris epithelial cells by adenosine and compounds related to adenosine 3', 5'-cyclic monophosphate. Proc. Natl. Acad. Sci. USA 70: 2286-2290.

Parmigiani, C. and McAvoy, J. (1984) Localization of laminin and fibronectin during rat lens morphogenesis. Differentiation 28: 53-61.

Pearlstein, E. (1976) Plasma membrane glycoprotein which mediates adhesion of fibroblasts to collagen. Nature 262: 497-499.

Pearlstein, E. and Gold, L.I. (1978) High-molecular-weight glycoprotein as a mediator of cellular adhesion. Ann. N.Y. Acad. Sci. 312: 278-292.

Pearse, E. (1980) Histochemistry: theoretical and applied. Vol. 1 (4th Edition), pp. 151-152. Churchill Livingstone, New York.

Pennypacker, J.P., Hassell, J.R., Yamada, K.M. and Pratt, R.M. (1979) The influence of an adhesive cell surface protein on chondrogenic expression in vitro. Exp. Cell Res. 121: 411-415.

Perkins, M.E., Ji, T.H. and Hynes, R.O. (1979) Cross-linking of fibronectin to sulfated proteoglycans at the cell surface. Cell 16: 941-952.

Pierschbacher, M., Hayman, E.G. and Ruoslahti, E. (1983) Synthetic peptide with cell attachment activity of fibronectin. Proc. Natl. Acad. Sci. 80: 1224-1227.

Pierschbacher, M.D. and Ruoslahti, E. (1984) Variants of the cell recognition site of fibronectin that retain attachment-promoting activity. Proc. Natl. Acad. Sci. USA 81: 5985- 5988.

Pintar, J.E. (1978) Distribution and synthesis of glycosaminoglycans during quail neural crest morphogenesis. Dev. Biol. 67: 444-464.

Podleski, T.R., Greenberg, I., Schlessinger, J. and Yamada, K. (1979) Fibronectin delays the fusion of L_6 myoblasts. Exp. Cell Res. 122: 317-326.

Powell, J.A. and Powers, C. (1973) Effect on lens regeneration of implantation of spinal ganglia into the eyes of the newt, Notophthalmus. J. Exp. Zool. 183: 95-114.

Powell, J.A. and Segil, N. (1976) Secondary lens formation caused by implantation of pituitary into the eyes of the newt, Notophthalmus. Dev. Biol. 52: 128-140.

Pratt, R.M., Larsen, M.A. and Johnston, M.C. (1975) Migration of cranial neural crest cells in a cell-free hyaluronate-rich matrix. Dev. Biol. 44: 298-305.

Pytela, R., Pierschbacher, M.D. and Ruoslahti, E. (1985) Identification and isolation of a 140 Kd cell surface glycoprotein with properties expected of a fibronectin receptor. Cell 40: 191-198.

Rao, C.N., Margulies, I.M., Tralka, T.S., Terranova, V.P., Madri, J.A. and Liotta, L.A. (1982) Isolation of a subunit of laminin and it's role in molecular structure and tumor cell attachment. J. Biol. Chem. 257: 9740-9744.

Reese, D.H., Puccia, E. and Yamada, T. (1969) Activation of ribosomal RNA synthesis in inhibition of Wolffian lens regeneration. J. Exp. Zool. 170: 259-268.

Reese, D.H. (1973) In vitro initiation in the newt iris of some early molecular events of lens regeneration. Exp. Eye Res. 17: 435-444.

Repesh, L.A., Furcht, L.T. and Smith, D. (1981) Immunocytochemical localization of fibronectin in limb tissues of the adult newt, Notophthalmus viridescens. J. Histochem. Cytochem. 29: 937-945.

Repesh, L.A., Fitzgerald, T.J. and Furcht, L.T. (1982) Changes in the distribution of fibronectin during limb regeneration in newts using immunocytochemistry. Differentiation 22: 125-131.

Reyer, R.W. (1966) The influence of neural retina and lens on lens regeneration from dorsal implants in Triturus viridescens larvae. Dev. Biol. 14: 214-245.

Reyer, R.W., Woolfitt, R.A. and Withersty, L.T. (1973) Stimulation of lens regeneration from the newt dorsal iris when implanted into the blastema of the regenerating limb. Dev. Biol. 32: 258-279.

Reyer, R.W. (1977) The amphibian eye: development and regeneration. In Handbook of sensory physiology, vol. 7(5) (F. Crescitelli, ed.), pp. 309-390. Springer Verlag, Berlin.

Ruoslahti, E., Hayman, E.G., Kuusela, P., Shively, J.E. and Engvall, E. (1979) Isolation of a tryptic fragment containing the collagen-binding site of plasma fibronectin. J. Biol. Chem. 254: 6054-6059.

Ruoslahti, E. and Engvall, E. (1980) Complexing of fibronectin, glycosaminoglycans and collagen. Biochim. Biophys. Acta. 631: 350-358.

Ruoslahti, E., Pierschbacher, M., Hayman, E.G. and Engvall, E. (1982a) Fibronectin: a molecule with remarkable structural and functional diversity. TIBS May 1982, 188-190.

Ruoslahti, E., Hayman, E.G., Pierschbacher, M. and Engvall, E. (1982b) Fibronectin: purification, immunochemical properties and biological activities. Methods in Enzymology 82: 803-830.

Saba, T.M. and Jaffe, E. (1980) Plasma fibronectin (opsonic glycoprotein): Its synthesis by vascular endothelial cells and role in cardiopulmonary integrity after trauma as related to reticuloendothelial function. Am. J. Med. 68: 577-594.

Sainte-Marie, G. (1962) A paraffin embedding techniques for studies employing immunofluorescence. J. Histochem. Cytochem. 10: 250-256.

Sakashita, S., Engvall, E. and Ruoslahti, E. (1980) Basement membrane glycoprotein laminin binds to heparin. FEBS LEH. 116: 243-246.

Sanders, E.J. (1980) The effect of fibronectin and substratum-attached material on the spreading of chick embryo mesoderm cells in vitro. J. Cell Sci. 44: 225-242.

Sanders, E.J. (1982) Ultrastructural immunocytochemical localization of fibronectin in the early chick embryo. J. Embryol. Exp. Morphol. 71: 155-170.

Sekiguchi, K. and Hakomori, S. (1980) Functional domain structure of fibronectin. Proc. Natl. Acad. Sci. USA 77: 2661-2665.

Singer, I.I. (1979) The fibronexus: a transmembrane association of fibronectin-containing fibers and bundles of 5 nm microfilaments in hamster and human fibroblasts. Cell 16: 675-685.

Smith, S.D. (1965) The effects of electrophoretically separated lens proteins on lens regeneration in Diemyctylus viridescens. J. Exp. Zool. 159: 149-166.

Solursh, M. (1976) Glycosaminoglycan synthesis in the chick gastrula. Dev. Biol. 50: 525-530.

Solursh, M. and Morriss, G.M. (1977) Glycosaminoglycan synthesis in rat embryos during the formation of the primary mesenchyme and neural folds. Dev. Biol. 57: 75-86.

Solursh, M., Fisher, M., Meier, S. and Singley, C.T. (1979) The role of extracellular matrix in the formation of the sclerotome. J. Embryol. Exp. Morphol. 54: 75-98.

Solursh, M., Hardingham, T.E., Hascall, V.C. and Kimura, J.H. (1980) Separate effects of exogenous hyaluronic acid on proteoglycan synthesis and deposition in pericellular matrix by cultured chick embryo limb chondrocytes. Dev. Biol. 75: 121-129.

Stenman, S., Wårtiovaara, J. and Vaheri, A. (1977) Changes in the distribution of a major fibroblast protein, fibronectin, during mitosis and interphase. J. Cell Biol. 74: 453-467.

Sternberger, L.A. (1986) Immunocytochemistry, Third Edition, pp. 56-63. John Wiley & Sons, Toronto.

Stone, L.S. and Steinitz, H. (1953) The regeneration of lenes in eyes with intact and regenerating retina in adult Triturus v. viridescens. J. Exp. Zool. 124: 435-468.

Stone, L.S. (1963) Experiments dealing with the role played by the aqueous humor and retina in lens regeneration of adult newts. J. Exp. Zool. 153: 197-210.

Stone, L.S. (1966) Experiments dealing with the inhibition and release of lens regeneration in eyes of adult newts. J. Exp. Zool. 161: 83-94.

Stow, J.L., Kjellen, L., Unger, E., Hook, M. and Farquhar, M.G. (1985) Heparan sulfate proteoglycans are concentrated on the sinusoidal plasmalemmal domain and in intracellular organelles of hepatocytes. J. Cell Biol. 100: 975-980.

Sugrue, S.P. and Hay, E.D. (1981) Response of basal epithelial cell surface and cytoskeleton to solubilized extracellular matrix molecules. J. Cell Biol. 91: 45-54.

Sugrue, S.P. and Hay, E.D. (1982) Interaction of embryonic corneal epithelium with exogenous collagen, laminin and fibronectin: role of endogenous protein synthesis. Dev. Biol. 92: 97-106.

Takata, C., Albright, J.F. and Yamada, T. (1964) Lens antigens in a lens-regenerating system studies by the immunofluorescent technique. Dev. Biol. 9: 385-397.

Takata, C., Albright, J.F. and Yamada, T. (1966) Gamma crystallins in Wolffian lens regeneration demonstrated by immunofluorescence. Dev. Biol. 14: 382-400.

Terranova, V.P., Rohrbach, D.H., Martin, G.R. (1980) Role of laminin in the attachment of PAM 212 (epithelial) cells to basement membrane collagen. Cell 22: 719-726.

Terranova, V.P., Rao, C.N., Kalebic, T., Marguilies, M. and Liotta, L.A. (1983) Laminin receptor on human joreast carcinoma cells. Proc. Natl. Acad. Sci. USA 80: 444-448.

Thorpe, C.W., Bond, J.S. and Collins, J.M. (1974) Early events in lens regeneration: changes in cyclic AMP concentrations during initiation of RNA and DNA synthesis. Biochim. Biophys. Acta. 340: 413-418.

Timple, R. and Rohde, H. (1979) Laminin - a glycoprotein from basement membranes. J. Biol. Chem. 254: 9933-9937.

Tomasek, J.J., Mazurkiewicz, J.E. and Newman, S.A. (1982) Nonuniform distribution of fibronectin during avian limb development. Dev. Biol. 90: 118-126.

Toole, B.P. and Trelstad, R.L. (1971) Hyaluronate production and removal during corneal development in the chick. Dev. Biol. 26: 28-35.

Toole, B.P. and Gross, J. (1971) The extracellular matrix of the regenerating newt limb: synthesis and removal of hyaluronate prior to differentiation. Dev. Biol. 25: 57-77.

Toole, B.P. (1973) Hyaluronate and hyaluronidase in morphogenesis and differentiation. Am. Zool. 13: 1061-1065.

Toole, B.P., Goldberg, R.L., Chi-Rosso, G., Underhill, C.B. and Orkin, R.N. (1984) In The role of extracellular matrix in development (R.L. Trelstad, ed.), pp. 43-66. Alan R. Liss, Inc., New York.

Tosney, K.W. (1982) The segregation and early migration of cranial neural crest cells in the avian embryo. Dev. Biol. 89: 13-24.

Towbin, H., Staehelin, T. and Gordon, J. (1979) Electrophoretic transfer of proteins from polyacrylamide gels to nitrocellulose sheets: procedure and some applications. Proc. Natl. Acad. Sci. USA 76: 4350-4354.

Trelstad, R.L., Hayashi, K. and Toole, B.P. (1974) Epithelial collagens and glycosaminoglycans in the embryonic cornea: macromolecular order and morphogenesis in the basement membrane. J. Cell Biol. 62: 815-830.

Turksen, K., Aubin, J.E., Sodek, J. and Kalnins, V.I. (1985) Localization of laminin, type IV collagen, fibronectin and haparan sulfate proteoglycan in chick retinal pigment epithelium basement membrane during embryonic development. J. Histochem. Cytochem. 33: 665-671.

Van der Water III, L., Schroeder, S., Crenshaw III, B.E. and Hynes, R.O. (1981) Phagocytosis of gelatin-latex particles by a murine macrophage line is dependant on fibronectin and heparin. J. Cell Biol. 90: 32-39.

West, C.M., Lanza, R., Rosenbloom, J., Lowe, M. and Holtzer, H. (1979) Fibronectin alters the phenotypic properties of cultured chick embryo chondroblasts. Cell 17: 491-501.

Williams, L.A. and Higginbotham, L.T. (1975) The role of a normal lens in Wolffian lens regeneration. J. Exp. Zool. 191: 233-252.

Woodley, D.T., Rao, C.N., Hassell, J.R., Liotta, L.A., Martin, G.R. and Kleinman, H.K. (1983) Interactions of basement membrane components. Biochim. Biophys. Acta. 761: 278-283.

Wray, W., Boulikas, T., Wray, V.P. and Hancock, R. (1981) Silver staining of proteins in polyacrylamide gels. Anal. Biochem. 118: 197-203.

Yamada, K.M. and Weston, J.A. (1974) Isolation of a major cell surface glycoprotein from fibroblasts. Proc. Natl. Acad. Sci. USA 71: 3492-3496.

Yamada, K.M., Olden, K. and Pastan, I. (1978) Transformation-sensitive cell surface protein: Isolation, characterization and role in cellular morphology and adhesion. Ann. N.Y. Acad. Sci. 312: 256-277.

Yamada, K.M. and Olden, K. (1978) Fibronectins - adhesive glycoproteins of cell surface and blood. Nature 275: 179-184.

Yamada, K.M. and Kennedy, D.W. (1979) Fibroblast cellular and plasma fibronectins are similar but not identical. J. Cell Biol. 80: 492-498.

Yamada, K.M., Kennedy, D.W., Kimata, K. and Pratt, R.M. (1980) Characterization of fibronectin interactions with glycosaminoglycans and identification of active proteolytic fragments. J. Biol. Chem. 255: 6055-6063.

Yamada, K.M. (1981) Fibronectin and other structural proteins. In: Cell biology of extracellular matrix. (E.D. Hay, ed.), pp. 95-114. Plenum Press, New York.

Yamada, K.M. (1983) Cell surface interactions with extracellular materials. Ann. Rev. Biochem. 52: 761-99.

Yamada, K.M., Akiyama, S.K., Hasegawa, T., Hasegawa, E., Humphries, M.J., Kennedy, D.W., Nagata, K., Urushihara, H., Olden, K. and Chen, W. (1985) Recent advances in research on fibronectin and other cell attachment proteins. J. Cellular Biochem. 28: 79-97.

Yamada, T. and Takata, C. (1963) An autoradiographic study of protein synthesis in regenerative tissue transformation of iris into lens in the newt. Dev. Biol. 8: 358-369.

Yamada, T. and Karasaki, S. (1963) Nuclear RNA synthesis in newt iris cells engaged in regenerative transformation into lens cells. Dev. Biol. 7: 595-604.

Yamada, T. (1966) Control of tissue specificity: the pattern of cellular synthetic activities in transformation. Am. Zool. 6: 21-31.

Yamada, T. (1967) Cellular and subcellular events in Wolffian lens regeneration. In: current topics in developmental biology, vol. 2 (A.A. Moscona and Monroy, A., eds.), pp. 247-283. Academic Press, New York.

Yamada, T. and Roesel, M.E. (1969) Activation of DNA replication in the iris epithelium by lens removal. J. Exp. Zool. 171: 425-432.

Yamada, T. and Roesel, M. (1971) Control of mitotic activity in Wolffian lens regeneration. J. Exp. Zool. 177: 119-128.

Yamada, T. and McDevitt, D.S. (1974) Direct evidence for transformation of differentiated iris epithelial cells into lens cells. Dev. Biol. 38: 104-118.

Yamada, T. (1977) Control mechanisms in cell-type conversion in newt lens regeneration. In: Monographs in developmental biology, vol. 13 (A. Wolsky, ed.). S. Karger, Basel.

Yamada, T., Dumont, J.N., Moret, R. and Brun, J.P. (1978) Autophagy in dedifferentiating newt iris epithelial cells in vitro. Differentiation 11: 133-147.

Yamada, T. and McDevitt, D.S. (1984) Conversion of iris epithelial cells as a model of differentiation control. Differentiation 27: 1-12.

Yanagishita, M. and Hascall, V.C. (1984a) Proteoglycans synthesized by rat ovarian granulosa cells in culture. J. Biol. Chem. 259: 10260-10269.

Yanagishita, M. and Hascall, V.C. (1984b) Metabolism of proteoglycans in rat ovarian granulosa cell cultures. J. Biol. Chem. 259: 10270-10283.

Zalik, S.E. and Scott, V. (1972) Cell surface changes during dedifferentiation in the metaplastic transformation of iris into lens. J. Cell Biol. 55: 134-146.

Zalik, S.E. and Scott, V. (1973) Sequential disappearance of cell surface components during dedifferentiation in lens regeneration. Nature New Biol. 244: 212-214.